Effect Of Mucin On Hydrodynamic Diameter And Zeta Potential Of
Polymeric Nanospheres

By

Victoria Goldenshtein

B.S., Brooklyn College, CUNY, 2011

Thesis

Submitted in partial fulfillment of the requirements for the Degree of Master
of Science in the Department of Molecular Pharmacology, Physiology and
Biotechnology, and the Center of Biomedical Engineering at Brown
University

PROVIDENCE, RHODE ISLAND

MAY 2017

AUTHORIZATION TO LEND AND REPRODUCE THIS THESIS

As the sole author of this thesis, I authorize Brown University to lend it to other institutions or individuals for the purpose of scholarly research.

Date: _____ Signature: _____

Victoria Goldenshtein, Author

I further authorize Brown University to reproduce this thesis by photocopying or other means, in total or in part, at the request of other institutions or individuals for the purpose of scholarly research.

Date: _____ Signature: _____

Victoria Goldenshtein, Author

This thesis by Victoria Goldenshtein is accepted in its present form by the Department of Molecular Pharmacology, Physiology, and Biotechnology, and the Center of Biomedical Engineering as satisfying the thesis requirements for the degree of Master of Science.

Date: _____ Signature: _____

Dr. Edith Mathiowitz, Adviser

Date: _____ Signature: _____

Dr. Eric Darling, Reader

Date: _____ Signature: _____

Dr. Anubhav Tripathi, Reader

Approved by the Graduate Council

Date: _____ Signature: _____

Andrew G. Campbell, Ph.D., Dean of the Graduate School

Vita

<div align="center">

VICTORIA GOLDENSHTEIN

</div>

Education

2017   BROWN UNIVERSITY. PROVIDENCE, RI.
            Master of Science in Biomedical Engineering, May 2017 (anticipated)

2011   BROOKLYN COLLEGE, CUNY. Brooklyn, NY.
            Bachelor of Science in Chemistry, minor in Biochemistry.
            SUMMA CUM LAUDE, May 2011.

Research Experience

2015-17   *Research Assistant*, Mathiowitz Lab. Department of Molecular
            Pharmacology, Physiology and Biotechnology. Brown University.
            Providence, RI.

2010-11   *Research Assistant*, Gibney Lab. Department of Chemistry. Brooklyn
            College, CUNY. Brooklyn, NY.

Honors and Awards

SUMMA CUM LAUDE
Dean's List for 2007, 2008, 2009, 2010 and 2011
Recipient of 2010-2011 STARR Foundation Scholarship
Recipient of 2010-2011 Dr. Franklin H Epstein Scholarship
Recipient of 2011 Donald D Wright Memorial Award in Chemistry
Recipient of Best Poster Session Award at 6th Annual BioMedical
Engineering and Biotechnology Graduate Program Retreat, Brown
University

Teaching and Work Experience

2016   *Teaching Assistant*, Brown University, Providence, RI.
            BIOL2110: Drug and Gene Delivery.

2012-13   *Sr. Laboratory Assistant*, Cellular Therapy Lab, New York Blood Center.

Posters and Presentations

V. Goldenshtein. *Effect of Mucin on Hydrodynamic Diameter and Zeta Potential of Polymeric Nanospheres*. Master Thesis Defence Presentation, Brown University, Providence, RI. April 2017.

A. Azagury, J.Perez-Rogers, **V. Goldenshtein**, D. Calvao, E. Steranka, C.M. Baker, E. Mathiowitz. *Is It All About Mucin?* Non-Invasive Delivery of Macromolecules Conference. Calrsbad, CA. February 2017.

V. Goldenshtein, A. Azagury, E. Mathiowitz. *Effect of Mucous Fluid on Hydrodynamic Diameter and Zeta Potential of Various Polymeric Nanospheres.* Biomedical Engineering and Biotechnology Seminar, Brown University, Providence, RI. November 2016.

V. Goldenshtein, A. Azagury, E. Mathiowitz. *Effect of Mucous Fluid on Hydrodynamic Diameter and Zeta Potential of Various Polymeric Nanospheres*. 6th Annual Biomedical Engineering and Biotechnology Graduate Program Retreat, Brown University, Providence, RI. September 2016.

S. Hojsak, S. Rege, **V. Goldenshtein**, A. Azagury, E. Mathiowitz. *Quantifying Bulk Mechanical Properties of Polymers and Their Relation to Diffusion Properties as Microparticles*. Honor thesis Defense Poster Session. Brown University, Providence, RI. May 2016.

V. Goldenshtein, A. Azagury, E. Mathiowitz. *The Effect of Mucosa on Effective Size and Charge of Polymeric Nanoparticles*. Biomedical Engineering and Biotechnology Seminar, Brown University, Providence, RI. April 2016.

Acknowledgments

First and foremost, I would like to thank my family for never-ending support and encouragement throughout my academic career. I am fortunate to have a husband, who believes in me more that I believe in myself. And I am especially grateful for my two little girls, who were patient, understanding, and allowed me to immerse in science.

I am greatly indebted to my amazing mentor prof. Edith Mathiowitz for her continuous guidance during my time at Brown University. I thank her for providing working environment, that allowed me to excel professionally, all the while taking care of my family. I was honored to work under leadership of Aharon Azagury, who challenged me to think deeper and to work harder. I thank him for being excellent instructor and for always finding time to answer my questions.

I am grateful to all Mathiowitz lab members, who helped creating collaborative environment and made my time in the lab a rewarding experience: Elaine Steranka, Dom Calvao, Christopher Baker, Stacia Furtado, Katarina Veszeleiova, Wing Lam Ho, James Perez-Rogers, Cameron Babtista, Ve Leandre, and others. Special thanks to Stephanie Hojsak and Soham Rege for their bioadhesion study; Dom Calvao and Chris Baker for assistance with SEM, Natalie Lam Ho for helping out with DLS measurements and PIN productions; and Vera Fonseca from Darling lab for AFM measurements.

Finally, I would like to acknowledge the entire MPPB department as well as faculty at Biomedical Engineering program at Brown University, who made my success possible.

Table of Contents

List of Figures

List of Tables

Abstract

The degree of interaction between nanoencapsulated material and gastrointestinal mucin can be an important determinant in efficiency of absorption of orally delivered therapeutics. Mucus lining of gastrointestinal tract successfully entraps and eliminates the majority of nanoparticles, making it hard to achieve therapeutically relevant levels of drugs systemically. Although numerous studies have tackled the problem of poor mucosal permeability, little is known about the effect of physicochemical particles' properties such as size, composition, charge, and surface chemistry on their interaction with mucin. This study utilized changes in DLS measurements of hydrodynamic diameter and zeta potential of polymeric nanospheres in purified mucin from porcine stomach to predict their affinity to mucin fibers. An array of polymeric nanospheres with different physicochemical characteristics were used. While non-adhesive PEG-PLGA did not show significant change, highly bioadhesive PBMAD and polystyrene (PS) nanospheres exhibited biggest increase in effective size in mucin compared to water. These findings highlight the correlation between bioadhesion and degree of interaction with mucin. All tested polymers illustrated significant reduction in negative zeta potential in mucin compared to water. Calculation of surface charge concentration revealed that while all tested polymers experienced 80-90% of charge masking by mucin, PS samples had 96-99% reduction of original charge in water, compared to 47-71% surface charge reduction for PEG-PLGA samples. High degree of bioadhesion, therefore, might aid in masking and neutralization of negative surface charge of polymeric nanoparticles.

Motivation

Due to ability to protect nanoencapsulated drugs from biodegradation in the harsh environment of gastrointestinal tract (GIT), as well as capability to design controlled drug release profiles, substantial effort is dedicated to development of effective oral drug delivery systems based on polymeric nanoparticles. However, most of the introduced nanomaterial gets entrapped and eliminated by protective mucosal lining of GIT, significantly reducing efficiency of such delivery systems. Therefore, it is important to understand the factors that influence the interactions between nanoparticles (NP) and mucin.

The goal of this study is to examine such interaction by looking for any substantial changes in DLS measurements of effective size and charge of NP in diluted purified mucin and water; and to correlate the degree of their interaction to various bioadhesive properties and physicochemical characteristics of the polymers used. The significance of this work is in elucidating possible factors that might influence the above interactions in order to improve oral drug delivery technologies via nanoencapsulated therapeutics.

Background

Dynamic Light Scattering

Dynamic Light Scattering is the most commonly used technique for size measurements of particles in the near and submicron region. As particles suspend in a solvent, they become subjected to the bombardment by the solvent molecules, thus creating Brownian motion. Instruments such as Malvern Zetasizer use laser beam to illuminate the sample and measure the intensity of fluctuation of the light, scattered from the particles due to their Brownian motion (Malvern Instruments, "Dynamic Light Scattering : An Introduction in 30 Minutes"). The velocity of the Brownian motion is called Translational Diffusion Coefficient. The larger the particle, the slower its velocity will be. Various manufacturers use different algorithms to relate the measurements of light fluctuation to the Translational Diffusion Coefficient. The instrument used in this study- Malvern Zetasizer- utilizes autocorrelation function, which works as signal comparator. It statistically correlates the obtained speck patterns taken at small time intervals to the probable position of particles as a function of time and through complex calculations derive the velocity of the Brownian motion. It will take longer for larger particle to diffuse in or out, thus the obtained signal will change slower over time, increasing correlation time, and therefore decreasing signal decay time (Malvern Instruments, "Dynamic Light Scattering : An Introduction in 30 Minutes"). Malvern instrument uses Cumulants analysis to derive average mean size (aka Z-average) and polydispersity index (PdI) (estimated width of the size distribution) by using single exponential fit into the obtained correlation function (Malvern Instruments, "Dynamic Light Scattering : An Introduction in 30 Minutes"). PdI is a unitless parameter with values ranging from zero to one. The lower the number is, the

narrower the width of the size distribution is, the more monodisperse the sample is. PdI is calculated in equation 1:

$$\text{PdI} = (\frac{\sigma}{d})^2 \qquad\qquad (1)$$

where σ is standard deviation of the measurement and d is the mean diameter (nanoComposix).

Z average size is the value most commonly used in DLS measurements. However, it accurately reflects the size of the sample only when certain conditions are met: the sample must be monodisperse (low PdI), have only one size population of particles, which must be spherical in shape (Malvern Instruments, "Dynamic Light Scattering : An Introduction in 30 Minutes"). If the sample contains two differently sized populations of particles, Z average will reflect in its value relative contribution of each intensity peak.

In this case, it is important to consider intensity, volume and number mean size distributions. Intensity mean is the most direct measurement out of the three. It derives the size distribution based on the measured intensity of the scattered light. By using Mie or Rayleighs theories it can be converted to volume mean, which reflects size distribution of the particles based on their volume or mass (Malvern Instruments, "Dynamic Light Scattering Common Terms Defined"). For particle sizes in the range of the laser wavelength Mie theory is used to convert intensity distribution to volume distribution. It is based on the complex minima and maxima function at a specific detection angle (usually 173 or 90 degrees). Rayleighs Scattering theory is useful for the particles of size approximately 10 times less that the wavelength of the laser beam used (633 nm for He-Ne laser). For such small particles (around 60 nm or less) this theory predicts that the

intensity of scattered light I is directly proportional to the diameter of the sphere d, according to Equation 2:

$$I \alpha d^6 \qquad (2)$$

For example, if the sample contains two distinct populations 5 nm and 50 nm in size, the intensity of the light scattered by the 50 nm particles will be a million folds higher compared to the smaller particles (**Fig.1**) (Malvern Instruments, "Dynamic Light Scattering : An Introduction in 30 Minutes"). Therefore, for equal concentration of the two size fractions, the intensity mean values will be skewed significantly towards bigger particles, overlooking the smaller population. Conversion to volume mean would reduce the ration between the two peaks to 1:1000, considering the respective volumes of the spheres $4/3\pi(d/2)^3$. Finally, number mean values for the two populations of equal concentration will be equal, because now the size distribution is based on the number of particles, rather than volume or intensity.
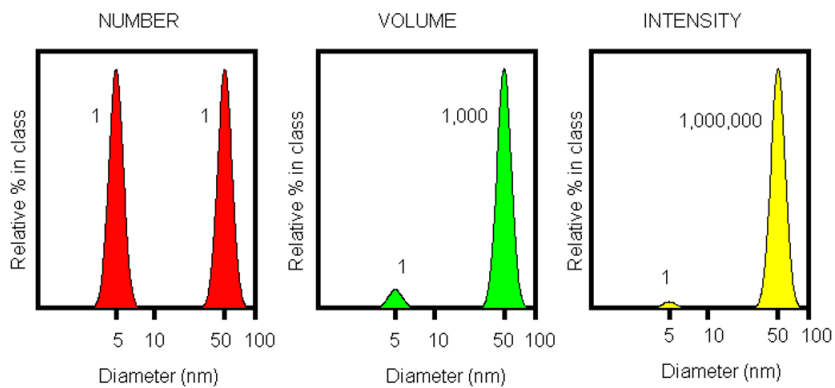
Figure 1: Schematic representation of bimodal DLS size peaks.

Shows differences in intensity, volume and number size distribution measurements of bimodal population of equal concentration (Malvern).

Hydrodynamic Diameter and Zeta Potential

When dispersed in solvent, particles acquire a diffusive electrical dipole double layer around their surface (**Fig. 2**). Hydrodynamic diameter of a particle is then defined not only by the core of the sphere, but also by its layer of strongly adherent solvent molecules, moving together with the particle as a whole. The thickness of the diffusive layer (Debye length) strongly depends on ionic strength of the solution. Less polar solvent results in thicker electric double layer, while more polar or conductive solvent (like water, for example) will suppress the layer by more tight adherence onto the surface of the particle (Malvern Instruments, "Dynamic Light Scattering : An Introduction in 30 Minutes"). Likewise, the nature of the surface of polymeric spheres and its degree of interaction with solvent will influence the thickness of the layer. Solvated, protruding chains of hydrophilic polymer in water will cause the apparent particle size to be larger, than compact hydrophobic surface in aqueous solution. The hydrodynamic diameter of the same particle, therefore, is solvent-dependent. Another word, the same particles will have different effective sizes in different solutions.
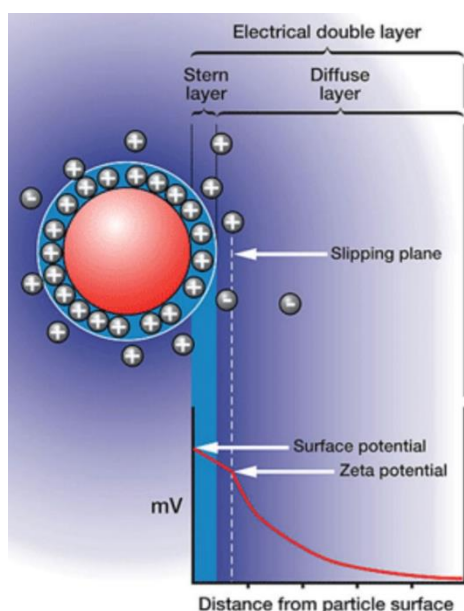
Figure 2: Schematic representation of electrical double layer.

It consists of closely packed Stern layer and looser diffusive layer. The slipping plane is located somewhere within diffusive layer. Zeta potential is measured at the surface of the slipping plane and gets smaller with increasing distance (pharmainfo.net).

Translational Diffusion Coefficient (D) is inversely proportional to the hydrodynamic diameter of the spheres as per Stokes-Einstein equation (Eq. 3):

$$d(H) = \frac{kT}{3\pi\eta D}$$ (3)

where d(H) is hydrodynamic diameter of a particle, k is Boltzman constant, T is absolute temperature and ŋ is viscosity of the medium. In other words, the larger the sphere, the smaller the diffusion coefficient. The viscosity of the solvent is extremely important to consider, since too viscous fluid will hinder Brownian motion of the particles, making the size measurements not feasible using DLS.

Due to the surface charge of a particle, an electric potential is established between the surface and the bulk of the solvent. Zeta potential is a charge at the surface of the slipping plane, located within diffusive layer, where solvent molecules are not tightly bound and start to slip away. This is the actual charge a particle exhibits in a particular solvent, thus it is solvent-dependent as well.

Zeta potential can be derived from measurement of electrophoretic mobility (velocity of particle per unit of electric field), using Henry's equation (Eq. 4):

(4)

$$U_E = \frac{2 \varepsilon z f(\kappa a)}{3\eta}$$

where U_E = electrophoretic mobility, z = zeta potential, ε viscosity and f(κa) = Henry's function.

Non-polar Media

Polar Media

Huckel approximation F(κa) = 1.0

Smoluchowski approximation F(κa) = 1.5
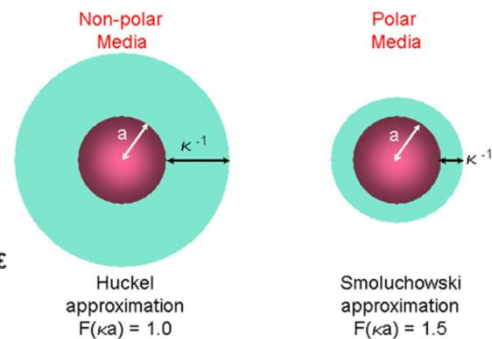
Henry's function relies on the radius of the particle core (a) and approximation of Debye length of the electrical double layer k (Malvern).

Phase Inversion Nanoencapsulation Method

To study the interaction between mucins and polymeric nanospheres, first the bulk polymeric material of interest must be transformed into nanomaterial. A large variety of nanoencapsulation techniques was developed over the past decades, which allow for entrapment of solids, liquids or gases inside one or several polymeric coatings (Mathiowitz, E. Kretiz M. R., Brannon-Peppas). While the chemical approach such as interfacial polycondensation) utilizes polymerization from monomers during the encapsulation process, physical methods employ controlled precipitation of already polymerized material by solidifying the emulsified liquid polymers (Mathiowitz, Chickering, et al.). The most common techniques for the former approach are Phase Inversion such as solvent evaporation and solvent removal, hot melt, spray drying, coacervation, and more. Usually, the choice of encapsulation method is influenced by the physical and chemical properties of the materials to be used, such as thermal and chemical stability, molecular weight, degree of hydrophobicity/hydrophilicity, etc (Mathiowitz, Chickering, et al.). In this study, there is no need for therapeutic agent encapsulation. Since the aim of this work is to investigate the affinity of mucins to various polymers, blank polymeric nanoparticles would suffice. Therefore, Phase Inversion Nanoencapsulation method (PIN) was chosen as the most suitable method due to its quick and easy procedure.

Phase Inversion is a physical process in which the polymer first dissolved in "good" solvent, forming one continuous homogenous liquid phase. By adding this mixture to the excess of non-solvent (or "bad" solvent), an unstable two phase mixture of polymer rich and polymer poor fractions is formed, causing the polymer to aggregate at the nucleation points (Mathiowitz, Chickering, et al.). When the polymer concentration

reaches a certain point (cloud point), polymeric particles phase separate, solidifying and precipitating from the solution (**Fig. 3**).

Unlike solvent removal or solvent evaporation methods, PIN does not require emulsification of the initial continuous phase polymer/solvent solution. It utilizes low polymer concentrations and low viscosities of the encapsulants. Also, the solvent and non-solvent pairs should be missible with at least ten times excess of non-solvent relative to solvent (Mathiowitz, Chickering, et al.). This special conditions allow for rapid addition of polymer dissolved in continuous solvent phase into non-solvent, which in turn results in spontaneous formation of nanomaterial. Since no emulsification required in this process and the nanospheres form spontaneously, the size of the resulting spheres is controlled not by the speed of stirring, but rather by changing the parameters of the procedure: polymer concentration, solvent to non-solvent ratio and their miscibility.
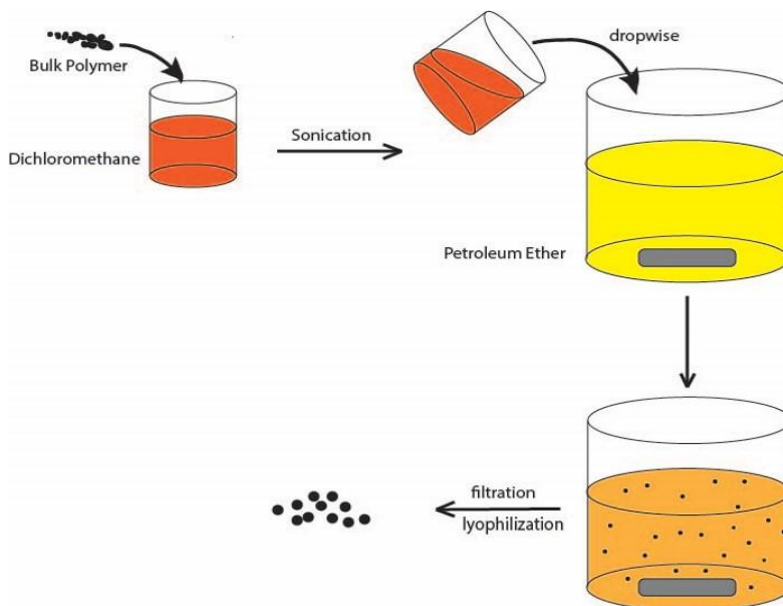
Figure 3: Schematic representation of Phase Inversion Nanoencapsulation

The bulk polymer is dissolved in DCM ("good" solvent), then added dropwise the excess of non-solvent Petroleum Ether. Upon phase inversion, the precipitates nanomaterial is filtered and then lyophilized.

Scanning Electron Microscopy

Scanning electron microscopy (SEM) provides direct visualization of the surface morphology, geometry and size distribution of nanomaterial (Pal et al.). Given the ease of the sample preparation and examination, it is one of the most widely used characterization method of nanoparticles. The sample of nanomaterial must be in a dry form with all residual solvents removed. It is mounted onto the sample holder and coated with conductive metal (usually gold) using sputter coater (Pal et al.). The imaging obtained from exposure of the sample to the accelerated beam of electrons at voltages ranging from 1 to 30 kV (Jacobs). The scattering of secondary electrons from the surface of the sample provides the morphological characteristics of the examined material (Pal et al.). Even though the size distribution of the particles can be estimated from the SEM images, it provides limited information regarding the true size average (Pal et al.). The number of particles available for examination in each frame is rather small, raising a significant problem in statistical analysis (Washington). For that purpose Dynamic Light Scattering (DLS) techniques are most commonly used, which will be discussed later.

Mucin and Mucus Lining of Gastrointestinal Tract

Mucus lines up the majority of organs exposed to the external environment, such as respiratory, reproductive, gastrointestinal and oculo-thino-otolaryngeal tracts (Bansil and Turner). Among its many functions are surface lubrication for better mechanical protection; creation of natural barrier for pathogens; and formation of permeable gel layer for gas and nutrients exchange (Allen). In GI tract it is comprised of two layers: firmly adherent unstirred mucus adjacent to epithelial lining followed by less

viscous loosely adherent layer, the thickness of the two layers varies throughout the gastrointestinal tract (**Fig. 4**).
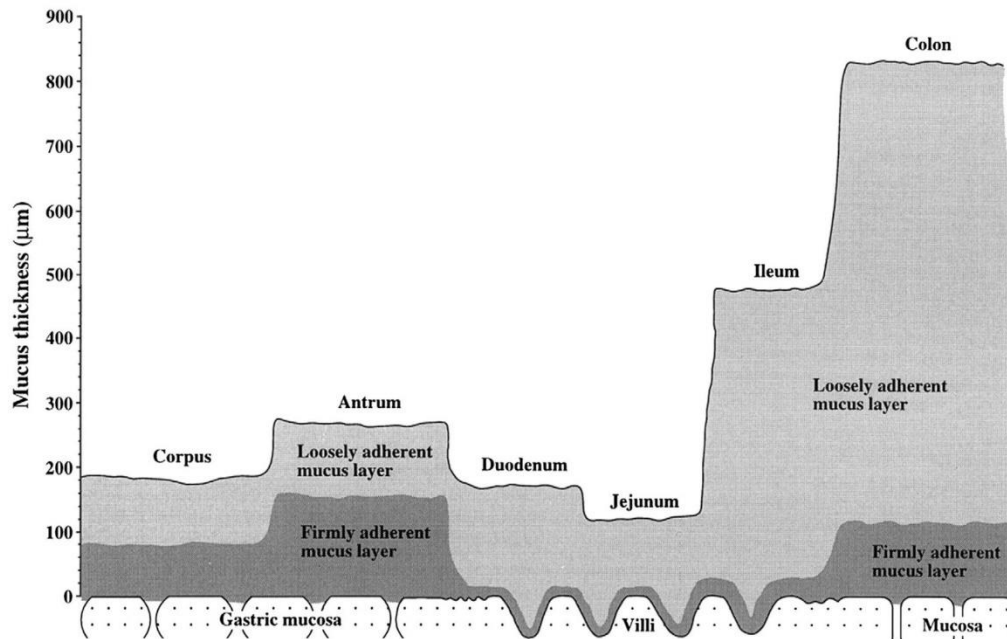
Figure 4: Schematic representation of firmly and loosely adherent mucus layers in rat GIT.

(Ensign, Cone, and Hanes)

The main constituent of mucus is water (around 95%), the rest includes salts, lipids, carbohydrates and proteins (Bansil and Turner). Glycoproteins, called mucins, are responsible for gel-like structure and properties of mucus; and represent 2-5% of mucus by wet weight (Ensign, Cone, and Hanes). Mucins are large flexible polydisperse proteins, ranging in size from 0.5-20 MDa, with reported strains as large as 40 MDa (Svensson and Arnebrant; Bansil and Turner). They consist of two alternating distinct domains: one having heavy glycosylation and another being hydrophobic, lipid-coated domain with little or no glycosylation (**Fig.5**). The long flexible fibers intertangle and crosslink via mucin-mucin interactions in hydrophobic regions. These regions are believed to be responsible to adhesive properties of mucus (Ensign, Cone, and Hanes).
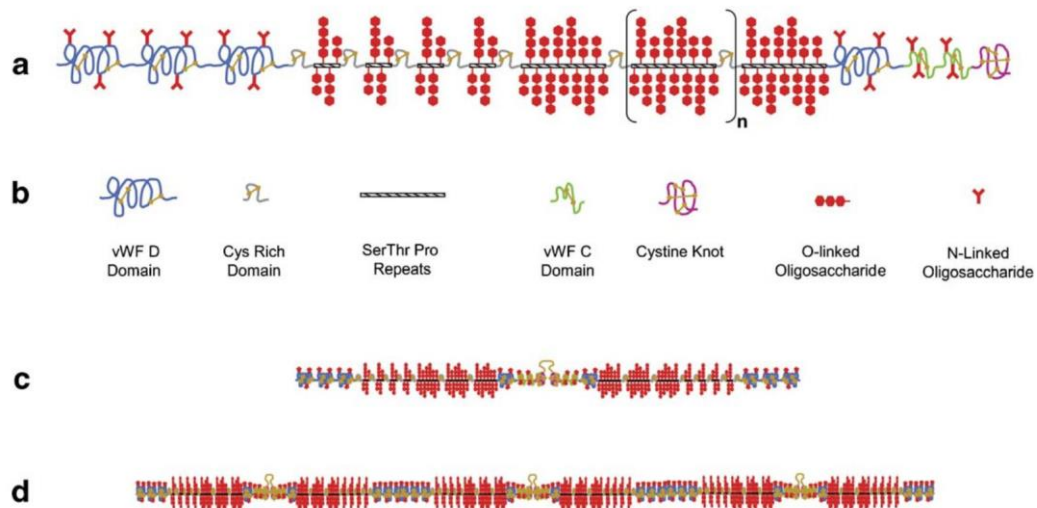
Figure 5: Schematic representation of mucin structure

a) pig gastric mucin monomer with glycosylated domain followed by "naked" region; b) symbols for different parts in sketch (a); c) a dimer formed via disulfide bonds in non-glycosylated domain; d) schematic representation of multimer. (Bansil and Turner)

Characterization of mucin by DLS revealed its random coil having radius of gyration around 100 nm, while AFM indicated that the length of individual mucin fibers is 200-600 nm (Bansil and Turner). SEM imaging revealed fibrous mesh structure with pores sizes between fibers up to 500 nm (**Fig. 6**). It is believed that physical dimensions of the

⊢1 μm⊣
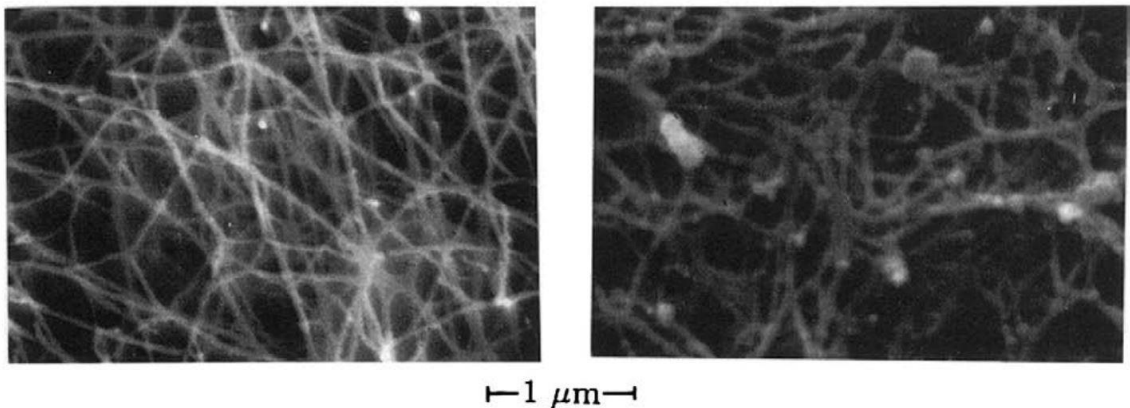
Figure 6: SEM image of human cervical mucus.

(Cu and Saltzman)

mesh pores may hinder and entrap orally introduced nanomaterials above certain size (Cu and Saltzman). Apart from steric hindrance, nanospheres may get entrapped by adhesion to the mucin fibers. This bioadhesion (adherence to biological surfaces) is predominantly governed by the ability of NP to form polyvalent low-affinity bonds with mucin, which might be electrostatic, van der Waal, hydrogen, dipole-dipole or hydrophobic in nature.

Introduction

Development of nanoparticle-based oral drug delivery systems (ODDS) gained widespread interest over the last few decades. Aside from providing better patient compliance, ODDS offers protection of therapeutics from harsh environment of Gastrointestinal tract (GIT); allows sustained and controlled release of drugs; enables to deliver the encapsulated cargo to desired site of action; and increases uptake of otherwise poorly permeable, water insoluble or metabolically unstable drugs (J. J. Reineke et al.; Thanos et al.) However, the very first limitation of such system lays in poor penetration of mucosal lining of GI tract. Mucus, a viscous adherent entangled gel, serves as a lubricant for the passage of objects, a permeable layer for nutrients and gas exchange, and as a natural barrier against pathogens and toxins (Allen; Neutra and Forstner; Bansil and Turner). It is also known to entrap and eliminate majority of orally introduced nanomaterials. Therefore, it became imperative gain in depth understanding of the barrier properties of mucus and its interaction with polymeric nanoparticle, for the sake of developing better muco-penetrating drug delivery systems.

Mucus is largely comprised from randomly interconnected protein fibers called mucins. They form a fibrous mesh with randomly located "pores", filled with water, through which solutes can diffuse (Cu and Saltzman). Poor permeability is often attributed to steric hindrance of the particles within the mesh and adhesion of the material to the mucin fibers. Since the pore size was found to be around 20-400 nm, for a long time it was thought that particles larger than 200 nm would not be able to penetrate the mucosal barrier (Jung et al.). Jani et al. demonstrated higher intestinal uptake for small 50-100 nm particle, compared to the larger ones (JANI et al.). The same observation was made for PLGA

nanospheres (Desai et al.). However, various studies showed successful uptake through GIT of much larger particles as well. For example, diffusion studies through undiluted human mucus by Hanes group indicated that smaller NP of 100 nm in diameter experienced more hindrance and immobilization by mucus, than NP of 200 and 500 nm in diameter (Lai et al.; Lai, Wang, and Hanes). It can be attributed to the interaction of the particles with mucin, which causes the gel to collapse and form large channels within its mesh (Cone). Furthermore, in vivo studies of NP uptake through GIT illustrated successful mucosal penetration and uptake of polystyrene particles ranging from 0.5 to 5 microns in size (J. J. Reineke et al.; Jani et al.). Yet another research group came to a conclusion that the mucus layer may not even be the rate-limiting barrier in NP uptake, and may only be responsible for 10% or less of total hindrance (Norris and Sinko).

Aside from a steric effect of the mucin mesh, the entrapment of the NP is also defined by physicochemical interactions between the mucin fibers and polymeric material. Mucin fibers consist of long glycosylated and highly hydrophilic domains, separated by hydrophobic regions. This flexible array of alternating hydrophilic and hydrophobic regions allows mucins to form variety of low-affinity hydrophilic or hydrophobic as well as hydrogen bonds with the surface of the nanospheres (Cone). For that reason, hydrophilicity/hydrophobicity of polymeric surface, its charge and degree of bioadhesion are important factors in defining their interaction with mucin.

With respect to charge, it is believed that highly positively charged particles may bind very tightly to the negatively charged regions of mucin, hindering their movement within the mucus. This was experimentally illustrated with chitosan spheres (Kas). Negatively charged particles, on the other hand, might resist entering and diffusing

through negatively charged mucin mesh altogether (Cone). Therefore, neutral charge is preferable for successful penetration through mucus, because will neither experience attraction nor repulsion towards negatively charged glycan regions of mucin (Cone). In fact, numerous studies have shown that coating of negatively charged particle with neutral PEG increases its diffusion and subsequent uptake through GI tract (Cone; Lai et al.; Griffiths et al.; Abdulkarim et al.) However, in vivo studies also demonstrated that negatively charged polystyrene NP are able to penetrate mucosal barrier and get through epithelial lining of GIT (J. J. Reineke et al.; Norris and Sinko; Jani et al.) Therefore, surface charge of particles, while important, is not the only factor influencing NP uptake.

Degree of hydrophobicity/hydrophilicity of polymeric surface greatly affects its interaction with mucosa. In general, particle's ability to make polyvalent low affinity bonds with the mucin network will more probably cause its entrapped within the mesh, as opposed to monovalent binding (Cone). Particles with pronounces hydrophobic surface will create multiple low-affinity bonds with "naked" hydrophobic domains of mucin; and consequently, adhere to the mucin fibers. This assumption was supported by early diffusion studies of highly hydrophobic PS spheres, which demonstrated complete immobilization of particles due to adherence to mucus (Olmsted et al.). Coating of the PS nanospheres with hydrophilic PEG proved to enhance their diffusion through human undiluted mucosa (Lai et al.). Another research group showed that surface modification of PLGA particles by PEGylation substantially increased its diffusion through mucus (Abdulkarim et al.). Yet another study demonstrated that coating hydrophobic PMMA nanoparticles with hydrophilic PBMAD polymer considerably improved their uptake through GIT (J. Reineke et al.). In contrast, Kissel research group claimed that intestinal uptake of hydrophobic

polymeric NP proved to be higher than for hydrophilic particles (Jung et al.), based on the fact that poloxamer coating of PS nanospheres caused the uptake through GIT to decrease (Hillery and Florence).

Since hydrophilic particles exhibit better absorption in GIT due to low interaction with mucins, and hydrophobic particles get entrapped in mucosal mesh due to high degree of interaction with mucin, it seems that bioadhesive properties of polymers also need to be considered. Bioadhesion is the ability of material to adhere to biological surfaces. Mucoadhesion of nanoparticles in the GI lumen can happen through one or more of the following: electrostatic, hydrophobic, van der Waals or hydrogen bond interactions,, as well as polymer chain interpenetration (Woodley). All polymeric materials, commonly used in DDS, have some degree of bioadhesion, but it varies from polymer to polymer. At first, it was thought that highly bioadhesive materials would get entrapped in loose mucosal layers and cleared (des Rieux et al.). However, for the uptake through GI walls to happen, the nanoparticles need first to diffuse through mucus layers at a faster rate, than the rate of mucosal secretion and clearance (Cone), which would require prolonged residence of the material in the GIT. To increase the residence time, attention was turned to bioadhesive polymers as possible materials for nanoencapsulation. When slightly bioadhesive PMMA nanoparticles were coated with highly bioadhesive PBMAD polymer, their gastrointestinal uptake improved significantly (J. J. Reineke et al.). Similarly, more bioadhesive P[FA:SA] provided prolonged NP retention in GI tract of rat, compared to weakly bioadherent alginate (Chickering et al.). Furthermore, Mathiowitz group demonstrated, that use of bioadhesive polymers as encapsulating material for oral delivery of insulin and dicumarol considerably increases the bioavailability of the therapeutic agents (Mathiowitz, Jacob, et

al.; Thanos et al.). The ability to enhance drug absorption by prolonging particle transit time trough GIT makes mucoadhesive drug delivery systems gain popularity in recent years.

Aims of the Study

One thing is clear: the interdependence of physicochemical properties of polymeric nanoparticles on their interaction with mucin is not well understood. There is profound need in systematic investigation of such interaction with close evaluation of factors such as composition, size, type, charge, hydrophobicity/hydrophilicity, and bioadhesion of the polymeric NP. In this study, we will use Dynamic Light Scattering (DLS) technique to evaluate the degree of interaction between mucin and polymers with various physicochemical properties. For this purpose, there is no need in freshly isolated mucus, since it contains less than 5% mucin w/v, the rest being water, lipids, etc. It is also highly viscous, which makes DLS measurements impossible to perform. Instead, purified mucin from porcine stomach by Sigma will be used. It is important to remember, that prediction of in vivo behavior of NP cannot be done based on this in vivo study. Different types of polymeric materials will be tested: biodegradable PLA and PLGA and nonerodable PS and PMMA; bioadhesive PBMAD, PS and P[FA:SA] as opposed to non-bioadhesive PEG-PLGA, PMMA, etc.; hydrophobic PS, P[FA:SA] vs hydrophilic PEG-PLGA and PBMAD, nearly neutrally charged PEG-PLGA vs the rest of the samples, which are negatively charged.

The degree of interaction between mucin and nanospheres will be evaluated by looking for any substantial changes in DLS measurements of hydrodynamic dimeter d(H) and zeta potential (ᵹ) of NP in diluted purified mucin and water. We are assuming

18
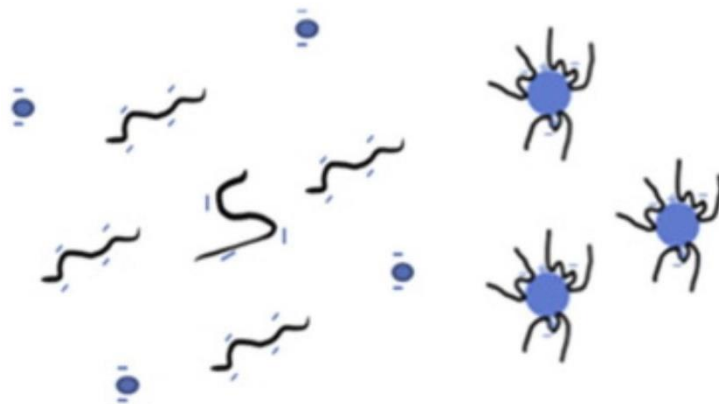
Figure 7: Schematic representation of assessment of interaction with mucin via DLS.

 DLS size measurements of nanoparticles with poor mucosal interaction (left) vs nanoparticles exhibiting high degree of interaction with mucin. (Griffiths et al.)

that in case of strong interaction, mucin strains would adhere to the surface of the nanosphere, creating thicker coating around the particle (**Fig. 7**). This coating would cause hindrance in diffusion through Brownian motion, resulting in smaller measurements in translational diffusion coefficient (D). Since D is inversely proportional to d(H) per Stokes-Einstein equation (see Eq. 3), adherence of mucins to the surface of the spheres should result in measurable difference by DLS in hydrodynamic diameter in mucin solution compared to one in water.

Zeta potential measurements will serve as another indication of mucin interaction with NP. In general, zeta potential decreases as the thickness of the electric double layer (Debye length) gets bigger. Therefore, strong interaction with mucin should considerably reduce the effective charge of the nanospheres. Bioadhesion assessment of polymers will be performed via measurements of fracture strength deformation.

The significance of this study lies in systematic approach of investigating the interaction of polymeric nanoparticles and mucin for deeper insight into possible factors that might influence the above interactions. The ultimate goal is to improve oral drug delivery technologies via nanoencapsulated therapeutics.

Materials and Methods

Materials

See **Table 1** for polymers used in this study.

Dichloromethane by Fisher Chemicals Cat#D143-4

Petroleum Ether by Fisher Chemicals Cat#E139-4

Methods

Fabrication of Nanospheres

Blank polymeric nanospheres were prepared using Phase Inversion Nanoencapsulation method (PIN), developed and patented by Mathiowitz lab (**Fig.3**) (Mathiowitz, Chickering, et al.). Around 80 mg of bulk polymeric material was dissolved in 5.3 mL of dichloromethane (DCM), keeping the ratio of polymer to DCM at 1.5% w/v. DCM in this case served as "good" solvent for all the polymers used, apart from PBMAD (ethanol was used instead). The solution was vortexed for about 30 seconds and then sonicated for 30 seconds using Ultrasonic Homogenizer CV26 (Cole-Palmer; Vernon-Hills, IL) until the polymer was completely dissolved, resulting in clear solution. Depending on polymer used, more vortexing/sonication rounds might have been performed for complete dissolution of the material. The obtained solution was then introduced dropwise to excess of "bad" solvent (or non-solvent), which in this case is 660 mL of petroleum ether (PE). In all productions, the volumetric ratio of solvent to non-solvent was kept at 1:125. The solution was stirred using magnet stirrer with enough speed to create vortex in the tall 1000 mL glass beaker for around 5-7 minutes or until the material started to aggregate into large snowflakes. The entire solution was then run through the positive

pressure filtration column with 0.2 µm PTFE filter (Millipore; Billerica, MA) to collect the resulting nanospheres. They were then scraped from the filter, flash frozen and lyophilized for at least 24 hours to remove the residual solvents. The PTFE filters were subjected to flash freezing and lyophilization as well to be used in SEM sample preparation. All PIN products were afterwards stored at -20 °C.

SEM Sample Preparation

SEM stubs and carbon-backed adhesive tape were obtained from Electron Microscopy Sciences (Hatfield, PA). Depending on sample, two methods of sample preparation was used. In first method, a small piece of filter (saved during the initial product preparation) was adhered onto the carbon adhesive tape. In second method, a small amount of the product was smeared onto the surface of the carbon adhesive tape using spatula. In both methods, the sample was sputter-coated with gold for 3 minutes at 20 mA using Emitech K550 sputter coater (Emitech; West Sussex, United Kingdom). The resulting samples were examined using Hitachi S-2700 scanning electron microscope (Hitachi, Peoria, IL). The accelerative voltage was 8 kV. Quartz PLI digital imaging system was used to obtain images of the samples.

Preparation of Mucin Porcine Solution

Mucin from porcine stomach by Sigma was prepared in 1 mg/mL, 3 mg/mL and 5 mg/mL concentrations. It was filtered with 0.2 µm syringe filter to remove large aggregates. It was either used freshly made, or stored overnight at -4°C. After storage, it was vortexed and sonicated for better resuspension and then filtered again. Even though mucin solution was evaluated for integrity for up to 7 days of storage and showed no signs

of apparent degradation, it nevertheless was discarded after 24 hour from its original preparation.
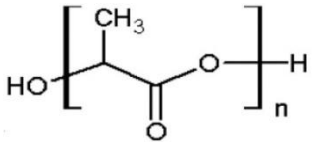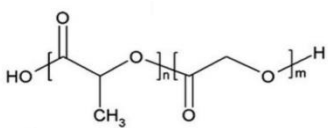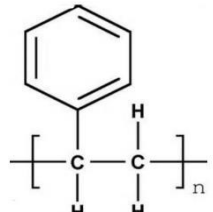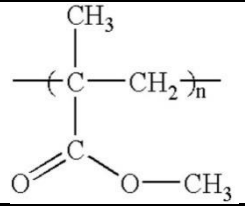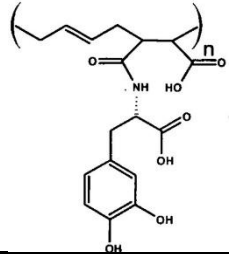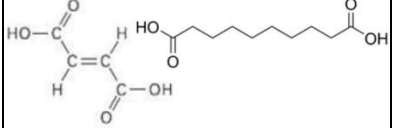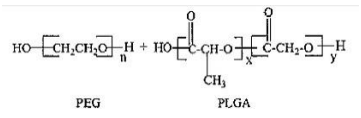
Dynamic Light Scattering Measurement by Zetasizer

The samples were prepared by suspending dry nanospheres in either DD water or mucin stock solution to achieve optimal concentration of 0.3-0.6 mg/ml. The samples were examined using Malvern Zetasizer Nanoseries. All size measurements were carried out at room temperature, using water parameters of viscosity 0.8872 cP, Dielectric constant of 78.50 and Refractive Index of 1.330 for both DD water and 0.1% w/v mucin solvents. Appropriate refractive index for each polymer known from literature was used. The scattered angle of 173° was used. Prior to each run the sample was vortexed and sonicated.

Bioadhesion Testing:

Glass-headed pins were coated with polymer in water solution (5% w/v). Small intestine of Sprague-Dawley rat was removed immediately post-mortem and washed with PBS. It was divided into Duodenum, Jejunum and Ileum; and each part was subdivided into 3 cm long segments. The tissue was cut along mesenteric border to expose lumen. Texture Analyzer XT was used to measure bioadhesive forces between the tissue and polymer-coated pins. The probe was set to descend at 5mm/s with 5 g of force. The polymer-coated probe was left in contact with the tissue for 7 minutes.

Table 1: List of polymeric materials used in this study

Polymer	Mw (kDa)	Manufacturer	Structure	Properties
Poly (lactic acid)	2	Polysciences Inc		Hydrophobic, slightly bioadhesive
	8	Takeda Pharmaceutical		
	18	Birminhgam Polymers Inc		
Poly (lactic-co-glycolic acid)	All samples	Takeda Pharmaceuticals		Hydrophobic, slightly bioadhesive
Polystyrene	2.5	Polysciences Inc		Highly hydrophobic and bioadhesive
	45	Scientific Polymer		
	125-250	Polysciences Inc		
Poly (methyl methacrylate)	75	Polysciences Inc		Hydrophobic, slightly bioadhesive
Poly (butadiene-maleic anhydride-co-L-DOPA)	All samples	Synthesized in Mathiowitz lab		Hydrophilic, highly bioadhesive
Poly(fumaric-co-sebatic anhydride)	All samples	Synthesized in Mathiowitz lab		Hydrophobic, very bioadhesive
PEG-PLGA	All samples	Birminhgam Polymers Inc		PEG is hydrophilic, non-bioadhesive, water soluble

Results and Discussion

Fabrication of Polymeric Nanospheres

The overall yield for all PIN productions in this study was $32 \pm 16\%$. The average yield for each polymer is given in Table 2, with PS polymer giving the lowest yield. Such a large loss is attributed to adhesion of the material to the glass walls of the reaction beaker.

Table 2: List of nanosphere fabrications for each polymer and yield for each production

Polymer	Production Date	Production Yield (mg)	Percent Yield (%)
PLA 2 kDa	10/20/2015	27	33.7
	11/17/2015	21	26
PLA 8 kDa	11/10/2015	13.3	16.6
PLA 18 kDa	11/9/2015	10.3	12.8
PLGA (50:50) 4 kDa	11/12/2015	36	44.3
	12/6/2016	23	28.7
PLGA (50:50) 6 kDa	11/12/2015	61.3	76.3
PLGA (50:50) 8 kDa	11/16/2015	26.9	33.2
	12/8/2016	18.0	22.5
PLGA (50:50) 10 kDa	11/16/2015	34.8	42.9
PLGA (50:50) 12 kDa	11/17/2015	13.6	16.9
PLGA (50:50) 14 kDa	12/21/2015	20.7	25.9
PLGA (50:50) 34-54 kDa	12/21/2015	32.7	40
PLGA (65:35) 6 kDa	1/14/2016	8.1	10.1
P[FA:SA] (20:80)	10/9/2015	N/A	N/A
P[FA:SA] (50:50)	2/14/2016	42.1	52.2
PLGA-Ester (75:25) 8 kDa	9/30/2016	22	27.5
Polystyrene 2.5 kDa	2/13/2017	2.2	2.8
Polystyrene 45 kDa	10/27/2016	10.2	12.8
Polystyrene 125-250 kDa	10/15/2015	N/A	N/A
	10/27/2016	8.6	10.6
	11/29/2016	25	31.3
	12/1/2016	31.76	39.7
	12/6/2016	20	25
PMMA 75 kDa	11/29/2016	27	33.9
PEG-PLGA (70:30) I.V. 0.79 g/dL	11/15/2016	30.8	38.2
PEG-PlGA (50:50) I.V. 1.28 g/dL	11/17/2016	34.37	42.8
PEG-PLGA (75:25) 0.45 g/dL	11/21/2016	41.29	51.6
PBMAD New	08/25/2015	N/A	N/A
	12/1/2016	39.02	48.8

Surface Morphology Characterization via SEM Imaging

SEM examination of PLA nanospheres of 2, 8 and 18 kDa (**Fig. 8 A-F**) revealed spherically shaped particles with estimated size of around 200-300 nm. However, wide variety of size populations were observed as well. As was mentioned previously, SEM provides visual inspection with respect to particle size, but it must be supplemented with DLS size measurements to obtain more accurate size distribution of the nanospheres. The particles looked well defined, not aggregated or fused. Increasing the molecular weight of the material seems to have no effect on the size of the resulting spheres.

Similarly, the assessment of surface morphology of PLGA (50:50) samples, made of various molecular weight bulk polymeric material (**Fig. 9 & 10**), showed well defined, round shaped spheres approximately 200-300 nm in size. As with PLA samples, a certain percent of much larger size particles can be seen in the images too. Increase of molecular weight of the starting polymeric material did not affect significantly the resulting size of the nanospheres. It is important to note, that PLGA (50:50) particles looked more aggregated into clusters, especially for the low molecular weight material, while PLA spheres were more spread out. With increased Mw of the material, a decrease in the aggregation of the spheres was observed.

Figure 8 G and H represents SEM images of PLGA-Ester (75:25) of 8 kDa. The nanoparticles look spherical in shape and spread out akin to PLA particles. This polymer has greater number of lactic acid monomers incorporated in the structure than glycolic acid: 75 percent and 25 percent respectively. Therefore, its surface morphology closely resembles the one of PLA. The SEM images of PLGA (65:35) polymer of 6 kDa (**Fig. 10 G & H**) reveal defined spherical particles, which are aggregated into larger clusters

similarly to low Mw PLGA (50:50). This polymer has only slightly higher number of lactic acid monomers incorporated: 65 percent as opposed to 50 percent in PLGA (50:50), thus exhibiting similar morphological properties.

Nanoparticles made of low molecular weight Polystyrene (**Fig. 11 A & B**) are predominantly aggregated into large clusters and, though still possessing spherical shape, look less defined and more fused together. With increasing molecular weight of the polymer, the degree of aggregation was reduced, the spheres became more defined and separated (**Fig. 11 C-F**). The best quality PS nanospheres, per SEM, were produced from high molecular weight polymer of 125-250 kDa. However, increasing molecular weight did not seem to influence the size of the resulting spheres.

PEG-PLGA nanospheres of varying ratios of PEG to PLGA as well as molecular weight of the bulk material were examined for morphological characteristics. High degree of fusion of the spheres was observed (**Fig. 12 A -H**). The spheres looked less spherically defined. Also, particles predominantly were aggregated into large clusters. The dual nature of the copolymer might be accountable for such observations. PEG is polar, while PLGA is mostly hydrophobic in nature. During the PIN process, while the polymer is exposed to organic solvent, PEG parts of the polymeric chains would try to aggregate, leaving PLGA exposed to the solution. However, if there would be not enough time for the polymer to regroup, it might not form individual spheres, but rather fused network of nanoparticles.

P[FA:SA] (20:80) and (50:50) (**Fig. 13 C-F**) also showed high degree of fusion between the nanospheres. The particles did not possess spherical geometry, but rather resembled a network of agglomerated particulates. This polymer is very sensitive to water and humidity. Upon contact with water, it quickly becomes subjected to hydrolysis. It is

possible that during PIN sample handling over long period (SEM image was taken several months after production of nanospheres took place), the nanomaterial started to degrade.

Figure 13 A,B represents nanoencapsulated PBMAD polymer. The spheres are round, well defined and separated. No aggregation or agglomeration was observed. Similarly, the PMMA NP exhibited well defined spherical geometry, with no agglomeration or fusion present (**Fig.13 G & H**). Estimated size of the spheres in both samples was in 200-300 nm range.

Conclusion

Various polymeric nanospheres were prepared by PIN method. The average yield of the preparation method was 31.3%. The resulting NP were visually examined for morphological and geometrical characteristics using SEM imaging. PEG-PLGA materials of different ratios and molecular weight and well as P[FA:SA] samples revealed high degree of fusion and agglomeration, as well as poorly defined spherical shape of the particles. The rest of the tested polymers exhibited well separated, discreet, spherically defined nanoparticles. Upon visual inspection of the samples it was concluded that all polymeric nanospheres were approximately 200-300 nm in diameter. However, as was mentioned previously, this technique is statistically unreliable with respect to size determination. Also, it provides the size of dry, lyophilized spheres. In biological conditions, however, the nanomaterial would be suspended in fluid and it apparent size would be greatly influenced by the polymer interactions with molecules of the solvent. Therefore, DLS measurements of hydrodynamic diameter of each sample should serve as more accurate representation of the size distribution of the nanospheres.
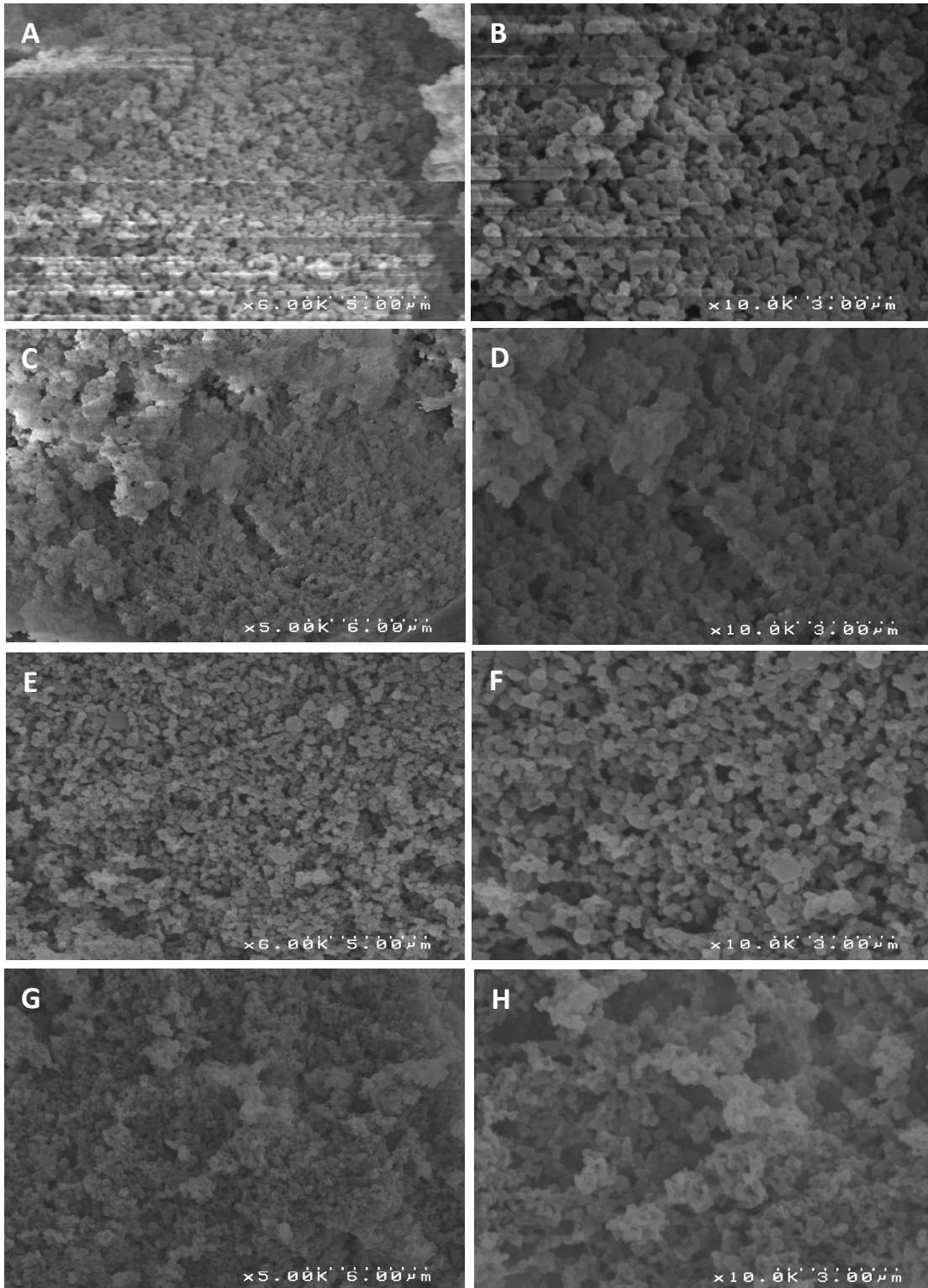
Figure 8: SEM images of PLA particles of increasing molecular weight.

Low (left column) and high (right column) magnification: (A and B) 2 kDa; (C and D) 8 kDa; (E and F) 18 kDa; (G and H) is PLGA-Ester (75:25) 8 kDa
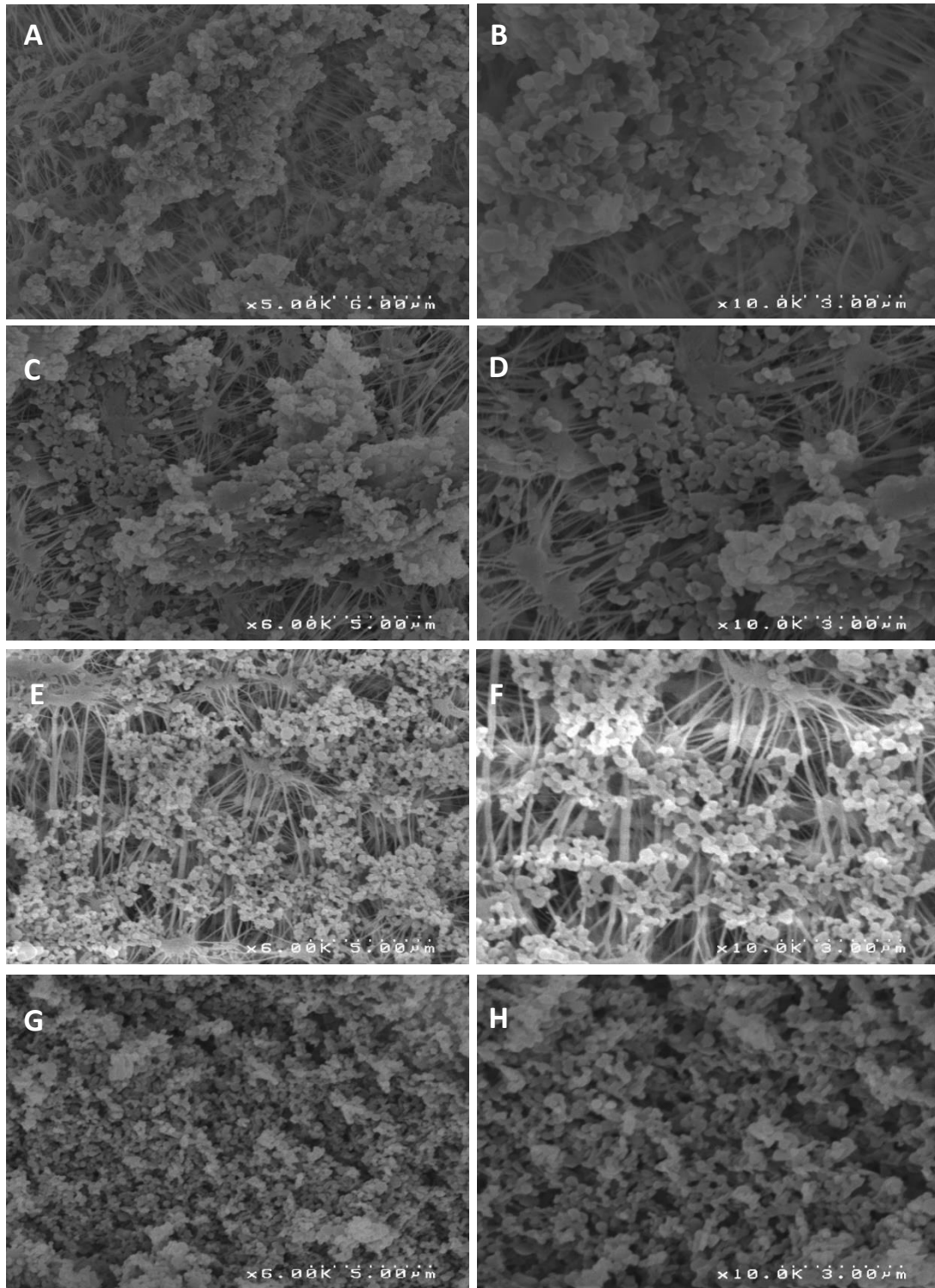
Figure 9: SEM images of PLGA (50:50) particles of increasing molecular weight.

Low (left column) and high (right column) magnification (A and B) 4 kDa; (C and D) 6 kDa; (E and F) 8 kDa; (G and H) 10 kDa
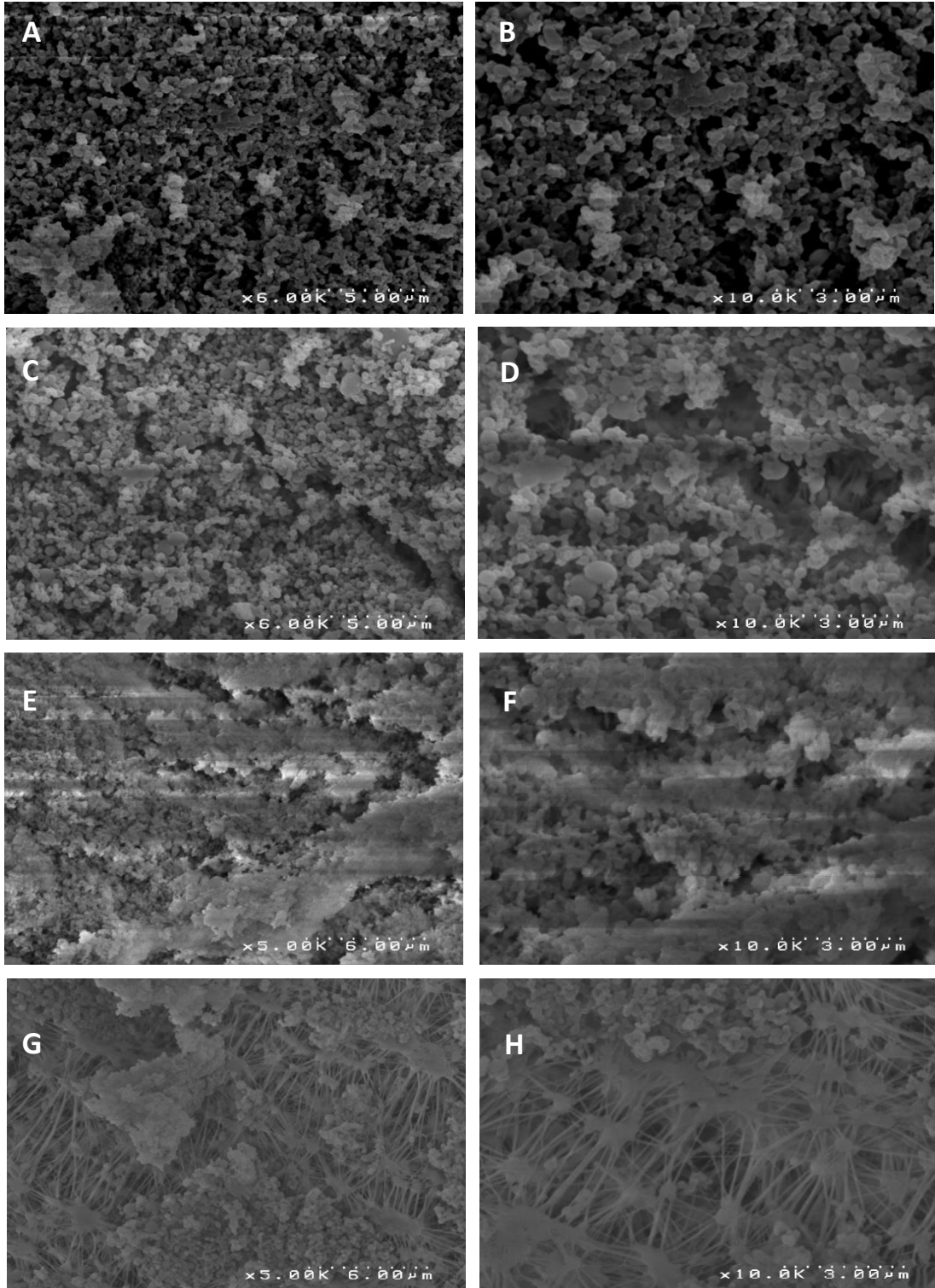
Figure 10 SEM images of PLGA (50:50) particles of increasing molecular weight.

Low (left column) and high (right column) magnification (A and B) 12 kDa; (C and D) 14 kDa; (E and F) 34-54 kDa; and (G and H) PLGA (65:35) 6 kDa
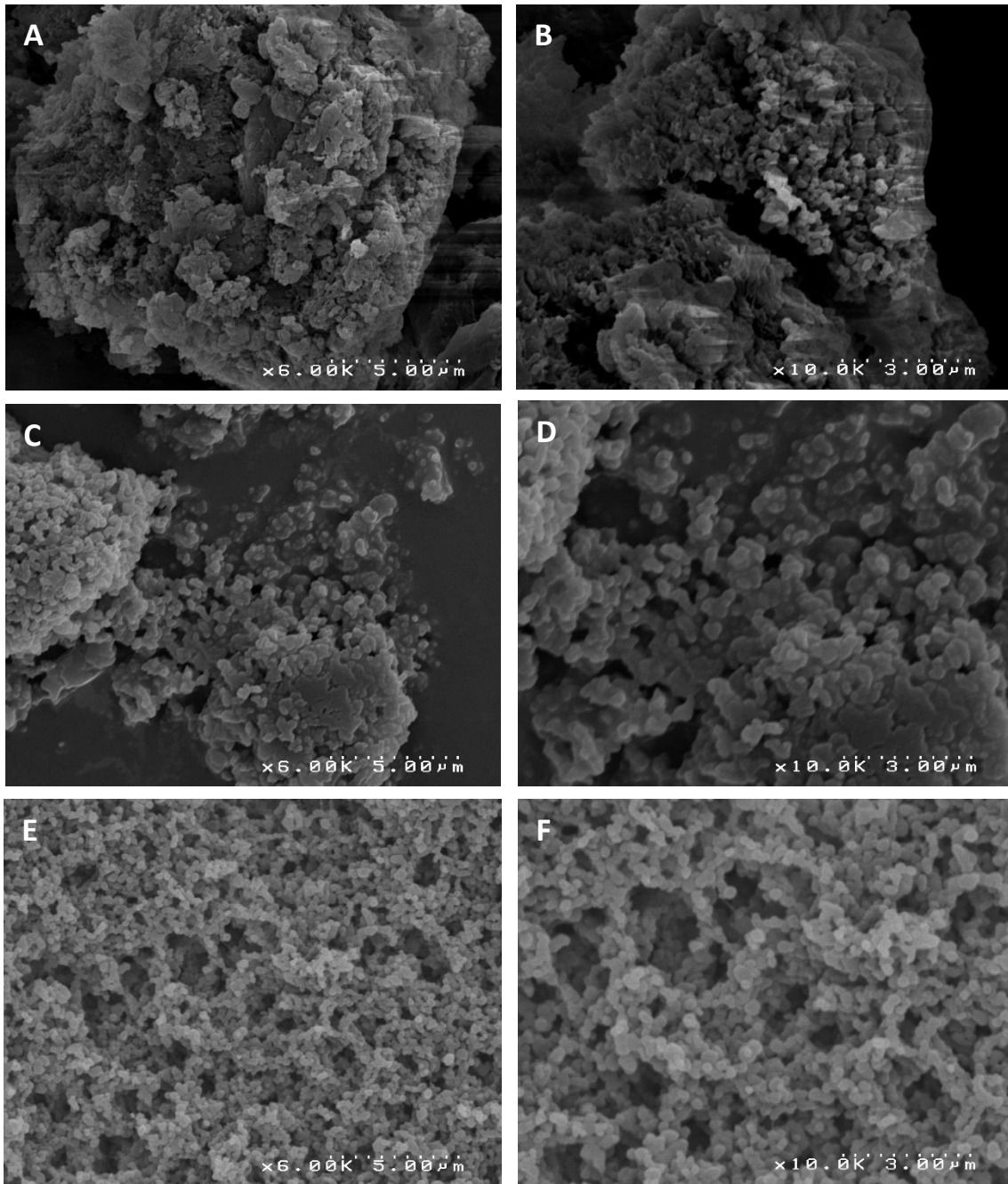
Figure 11: SEM images of Polystyrene particles of increasing molecular weight.

Low (left column) and high (right column) magnification (A and B) 2.5 kDa; (C and D) 45 kDa; (E and F) 125-250 kDa
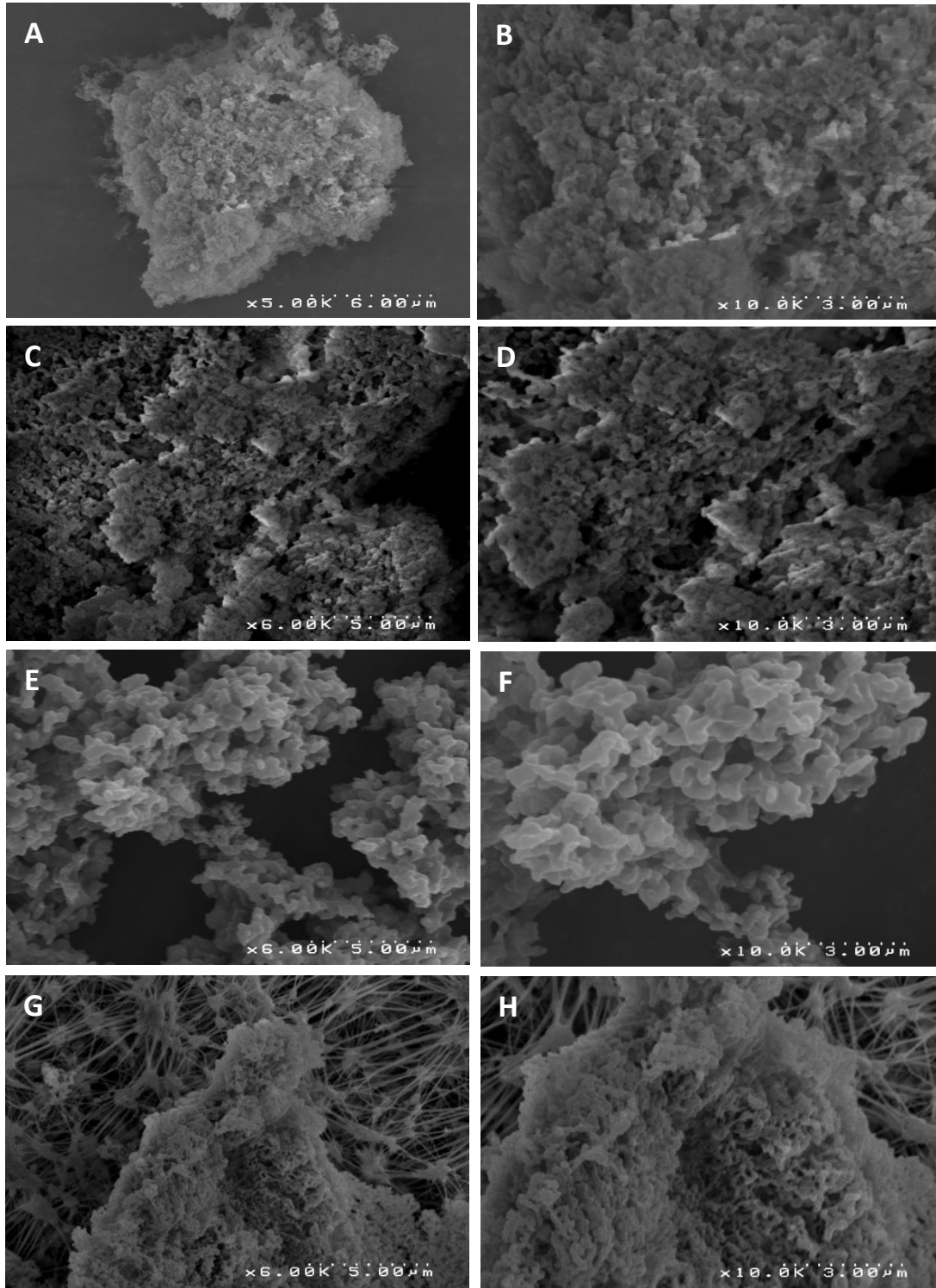
Figure 12: SEM images of PEG-PLGA nanospheres.

.Low (left column) and high (right column) magnification: (A and B) PEG-PLGA (70:30) I.V. 0. 79 g/dL; (C and D) PEG-PLGA (70:30) I.V. 0.73 g/dL; (E and F) PEG-PLGA (75:25) I.V. 0.45 g/dL; (G and H) PEG-PLGA (50:50) I.V. 1.28 g/dL
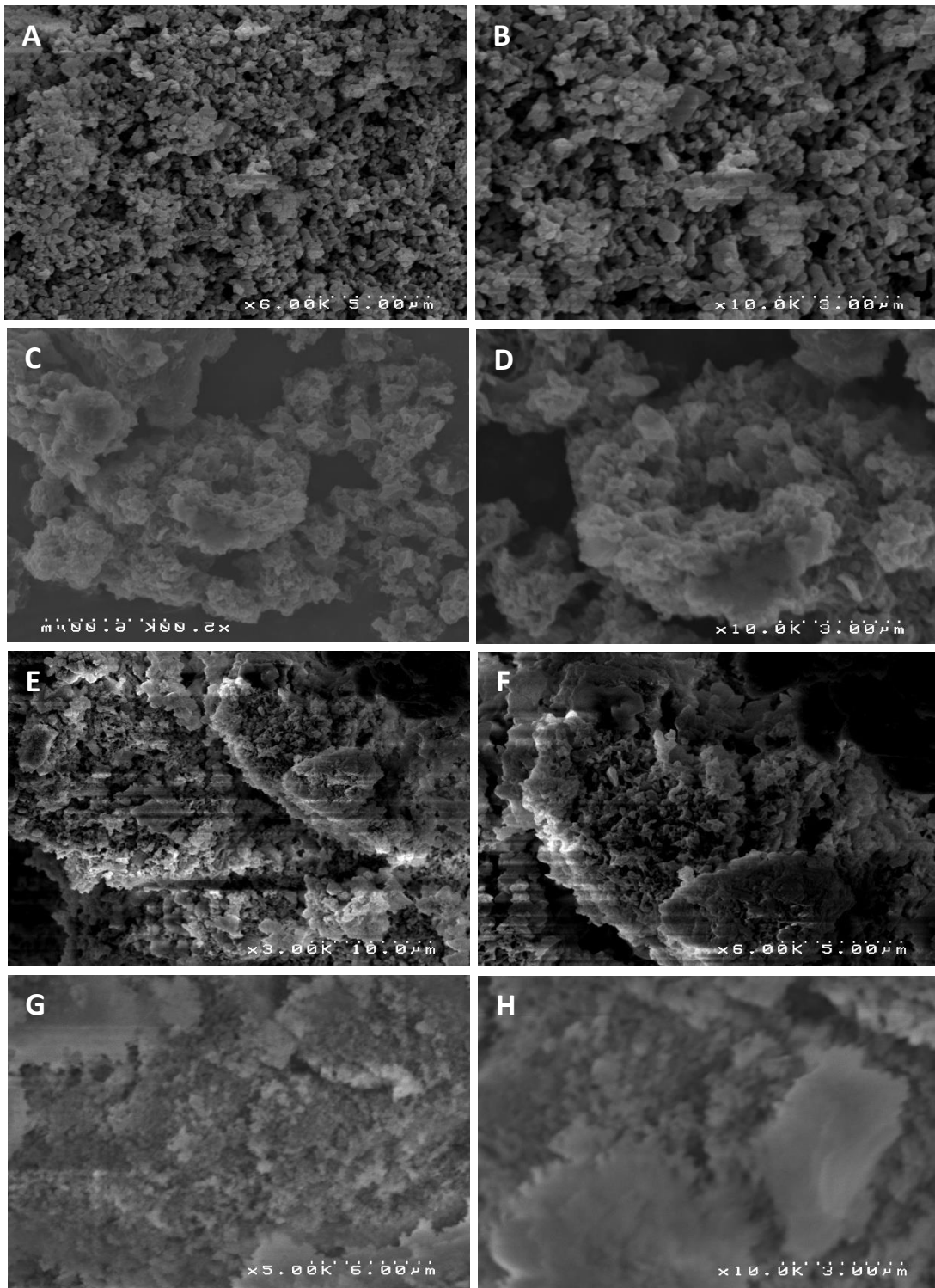
Figure 13: SEM images of PBMAD, P[FA:SA] and PMMA nanoparticles.

Low (left column) and high (right column) magnification (A and B) PBMAD New; (C and D) P[FA:SA] (70:30); (E and F) P[FA:SA] (50:50); (G and H) PMMA 75 kDa

Establishment and Optimization of DLS Protocol for Investigation of Polymeric Nanospheres' Interaction with Mucin

Stability Evaluation of Blank Mucin Porcine Solution

To address potential concern regarding possible mucin degradation or aggregation during the time of the experiments and to evaluate the appropriate storage time of the stock solution, a series of DLS runs of freshly prepared mucin of 1 mg/mL concentration were made at different timepoints. Figure 14 (Run 246) shows the representative size distributions for freshly made and filtered mucosal solution. It contains two size populations: 122 and 17 nm. Figure 14 (Run 230) represents mucin sample 1 h after preparation and filtration. It contains three different size distribution peaks: 109 nm, 22 nm and a small peak at 4552 nm (1.1% of the entire population), indicating that large aggregates started to form. After 24 hours DLS of the sample shows no significant change in aggregation: the intensity peaks are 126 nm, 21 nm and 4519 nm for large aggregates, also being only 1.1% on the entire population (Run 238). Even after 7 days the degree of protein aggregation remains almost unchanged (**Table 3**). If to filter the sample, the size peak for large aggregates disappears. Overall, it seems that the stock solution is stable over at least a week, but needs to be filtered prior to use.

It is important to note, however, how such minute quantities of large aggregates affect the overall numbers of size measurements. For example, in run 238 (**Table 3**) the most predominant intensity peak value is 126 nm, which represents 92% of all populations. However, the Intensity Mean value is 169 nm, because it "favors" much larger particles. Since Rayleigh theory postulates that intensity is directly proportional to the diameter to

the six power d^6, even small quantities of very large particles will skew size values toward bigger particles.

Table 3: hydrodynamic diameter of empty mucin as a function of time

Time point	Rec #	Z-Avg	Pk 1 Avg (I)	Pk 2 Avg (I)	Pk 3 Avg (I)	Intensity Mean	Volume Mean	Number Mean	PdI
		d.nm	d.nm	d.nm	d.nm	d.nm	d.nm	d.nm	
Fresh	246	81.18	122.1	17.39	0	118.5	29	14.12	0.279
1 h	230	76.15	108.6	21.8	4252	272	73.98	17.35	0.379
24 h	238	86.67	126.1	20.61	4519	168.5	39.29	15.76	0.287
7 days	268	89.19	132.3	23.42	4751	173.2	46.01	18.06	0.295

However, if in the same example to consider actual volume peaks and volume mean value (**Fig. 14** second row Run 238), since now the peak intensity is proportional only d^3, large aggregate peak now represents only 0.3% of the entire population and does not affect volume mean significantly. In this particular run, volume mean is skewed towards smaller particles, due to their much higher concentration. Finally, number peaks, which correlate to the actual number of each size population, does not even have large aggregate peak and the peak around 100 nm (**Fig. 14** third row, run 238). Zeta Average number also incorporates all different sizes obtained, similarly to Intensity Mean value.

When dealing with multimodal samples it is important to use the values, that DLS runs can provide, which would most accurately describe the system. Malvern Instruments advises to use Zeta Average value or Intensity Mean, because they are based on the actual parameters the instrument measures; and it is indeed the best option for monodisperse samples with only one size distribution. However, with multimodal population it is better to use direct volume peaks from the DLS reports, because will be skewed the least for both large aggregates and sediments and small mucin oligomers.
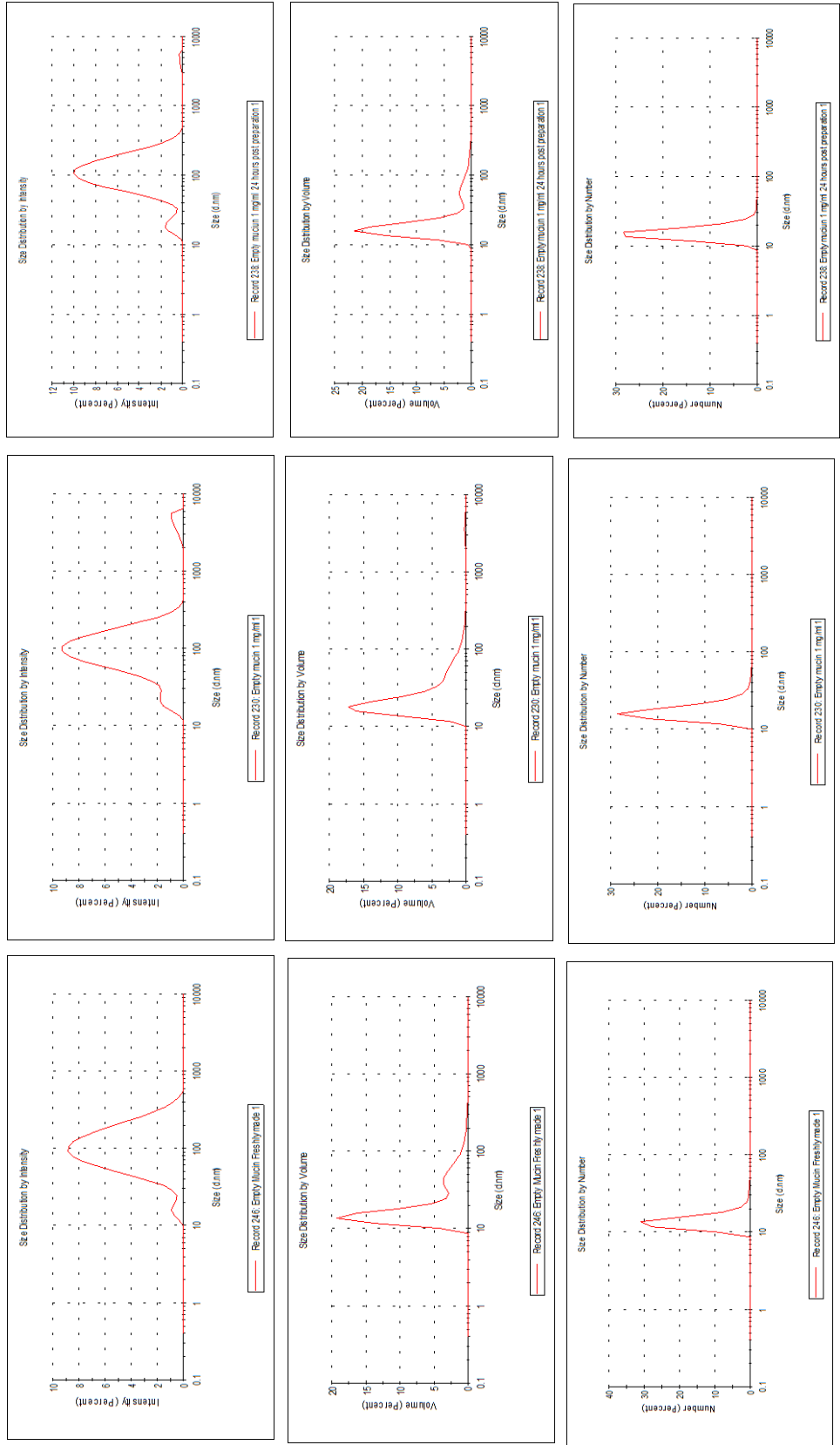
Figure 14: Hydrodynamic diameter of 1 mg/mL mucin porcine stock solution.

Run 241: freshly made; Run 230: 1 hour post prep; Run 238: 24 hour post prep. First row graphs represent size distribution by intensity, second row- by volume; and third row- by number.

Rec #	Z-Avg	Pk 1 Avg (I)	Pk 2 Avg (I)	Pk 3 Avg (I)	DCR	Intensity M	Volume M	Number M	PdI
	d.nm	d.nm	d.nm	d.nm	kcps	d.nm	d.nm	d.nm	
192	374.2	671.4	83.15	31.62	5440.5	476.1	389.2	26.68	0.547
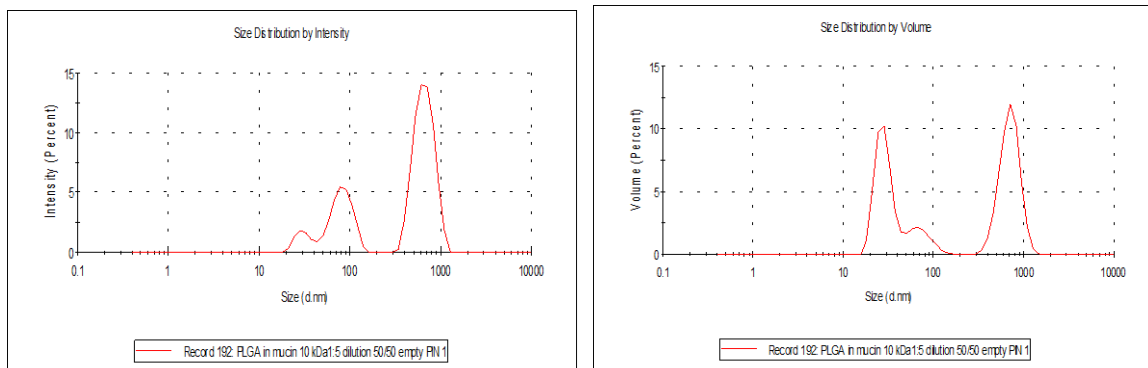
Figure 15: Hydrodynamic diameter of PLGA (50:50) 10 kDa nanospheres in mucin porcine 0.1% w/v

The second concern that needs to be addressed is whether mucin peaks would interfere with peaks of the nanospheres, making the measurements hard to interpret. DLS runs of samples containing nanospheres in water and in mucin showed that the range for the size distribution peaks of the particles is in 300-1500 nm, while peaks of filtered mucin are in the range of 150 nm and less. Figure 15 represents DLS run of PLGA (50:50) nanospheres in 1 mg/mL mucin solution. On the graphs of size by intensity and by volume distribution the first two small peaks closely resemble the empty mucin peaks, while the third large peak belongs to PLGA nanospheres. In this case, it is easy to assign each peak to its corresponding moiety. As with empty mucin, Zeta Average value of 374 nm represents cumulative size of both populations, which is twice smaller than the individual peak assigned to the polymer. Same goes to the mean values of intensity and volume. Therefore, as was stated before, in this study the direct size distribution by volume values will be used as data points.

Determination of Appropriate Concentration of Polymer Sample

As was described previously, DLS measures the intensity of the scattered light from particles, which are subjected to Brownian motion. By correlating the speckle patterns (areas of dark and light patches) at different timepoints, the instrument can "track" the moving particles and calculate the translational diffusion coefficient. The hydrodynamic diameter of the sphere can then be calculated, using Stokes-Einstein equation (Eq. 3). This theory assumes that the particles are at infinite dilution, meaning that they cannot interact with each other and thus alter their motion. Therefore, it is important to establish the appropriate sample concentration range.

Study was conducted, where initial sample of approximately 0.3 mg/mL was diluted to 1:2 and 1:3 ratios, giving 0.15 and 0.10 mg/mL samples. The graphs below (**Fig. 16-17**) represent the effective size and charge measurements of several different polymers at the three above concentrations. In all tested polymers, there was no statistically significant effect of dilution on the hydrodynamic diameter measurements. In general, the size measurements in mucin decreased with increased dilution factor. As the concentration of the nanospheres in the sample decreased, small mucin population predominated the size readings. Zeta potential measurements also did not show dependence on sample concentration (**Fig. 18-19**). However, as the dilution factor increased, the reports started to have "poor expert advice" due to low sample concentration. Therefore, it was decided to use sample concentration in the range of 0.3-0.5 mg/mL for both hydrodynamic and zeta potential measurements.
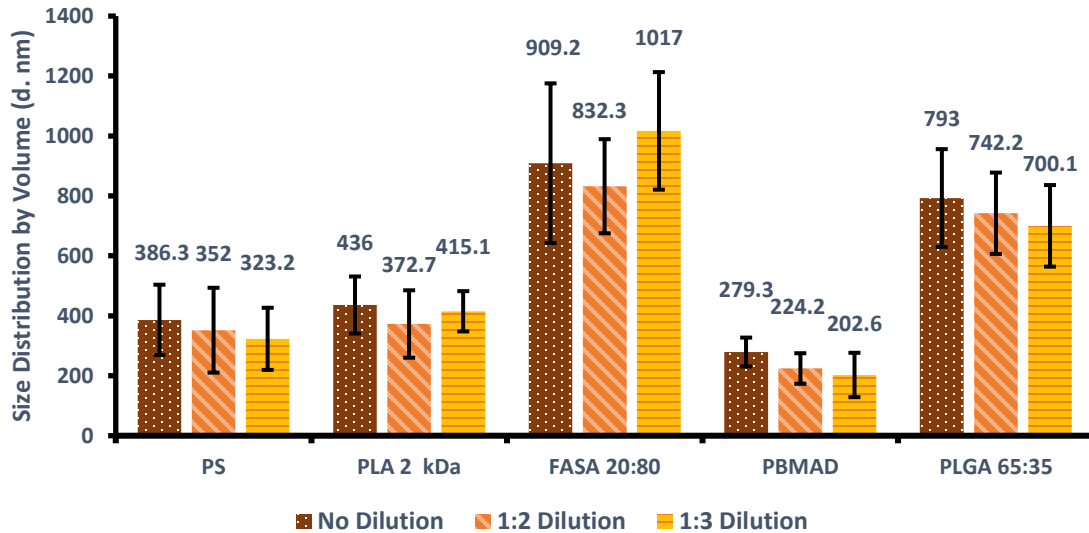
Figure 16: D(H) in water of several polymeric nanospheres at three different concentrations.
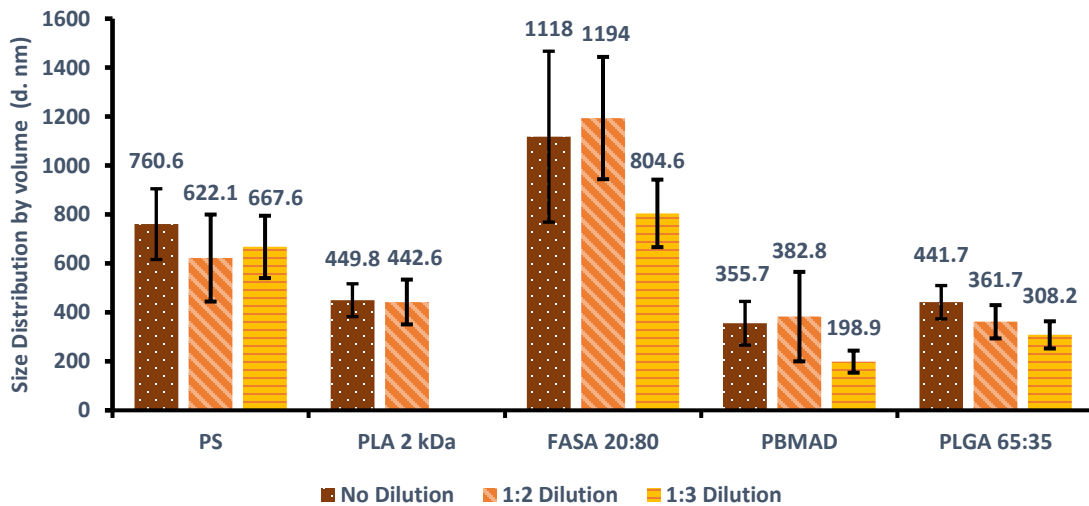
Figure 17: D(H) of several polymeric nanospheres at three different concentrations in mucin 0.1 w/v.
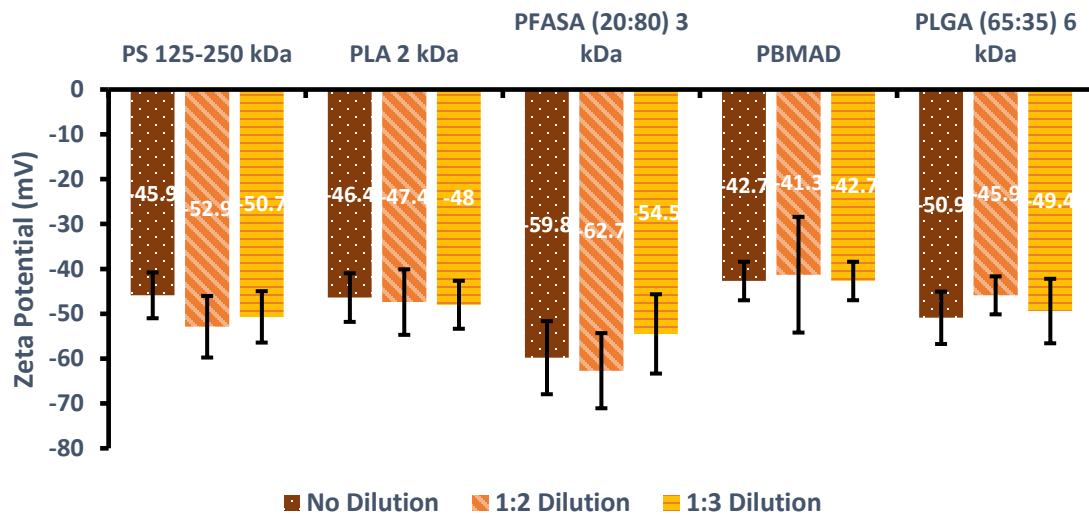
Figure 18: Zeta potential measurements of several polymeric nanospheres at different concentrations in water.
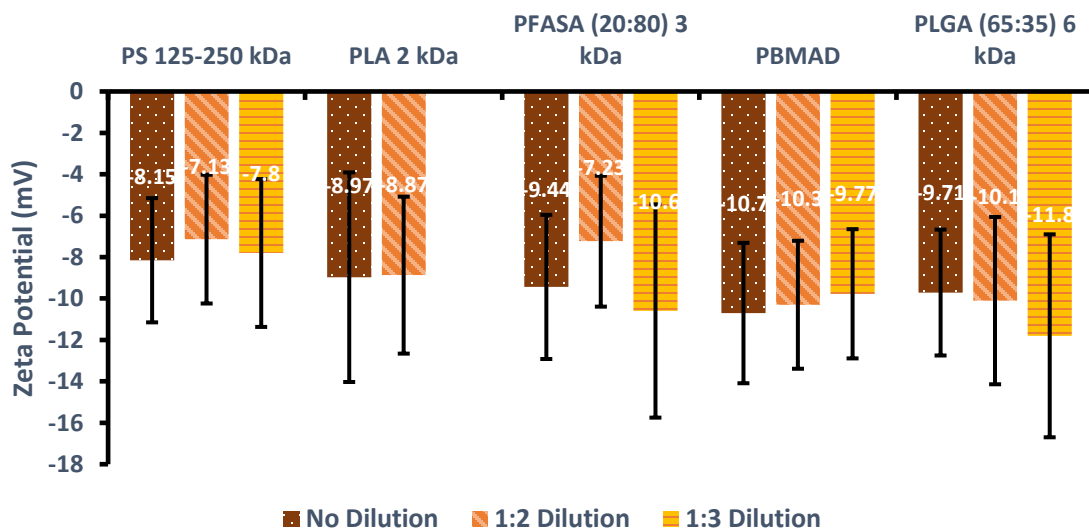
Figure 19: Zeta potential measurements of several polymeric nanospheres at different concentrations in 0.1% w/v mucin.

Determination of Appropriate Concentration of Mucin

Ideally the concentration of mucins should be high enough to be able to detect their interaction with nanospheres. On the other hand, increasing mucosal concentration would also increase the viscosity (**see Appendix A**) and refractive index of the sample, thus making DLS measurements difficult to perform. Three different concentrations of mucin were evaluated to determine the optimal one for further experimental use: 1 mg/mL, 3 mg/mL and 5 mg/mL. Polystyrene nanospheres were suspended in each of the above solutions the hydrodynamic diameter was compared against one PS nanospheres in DD water (**Table 4**). All three cases the interaction of the nanospheres with mucin was observed: the hydrodynamic diameter in mucin was at least two folds bigger than in water. However, as the concentration of mucin increased, it began interfere with the measurements, resulting much higher polydispersity index of the DLS runs. Therefore, it was concluded that mucin concentration of 1 mg/mL is high enough to study the effect of mucin-nanoparticle interaction without interference; and at the same time has viscosity comparable to water.

Table 4: hydrodynamic diameter of polystyrene nanospheres in mucin of various concentrations

PS 125-250 kda polymer	Volume Size Distribution ave	STD	# of Runs	Ave PdI
In water	383.8	104.3	10	0.113
1 mg/mL mucin	762.7	232.2	7	0.364
3 mg/mL mucin	647.9	103.3	9	0.43
5 mg/mL mucin	918.2	179.2	8	0.531

Reproducibility of the Measurements Using Polystyrene and P[FA:SA] 20:80 Nanoparticles

Due to the time constrains and large number of polymers to be tested in this study, most nanospheres had come from a single production batch for each polymer. Therefore, it was important to determine that measurements of samples from a single batch would be representative for that particular polymer. In the study below (**Fig. 20**) five different PIN productions of Polystyrene 125-250 kDa were prepared. Each batch was used in effective size measurements to determine the degree of variability from batch to batch.
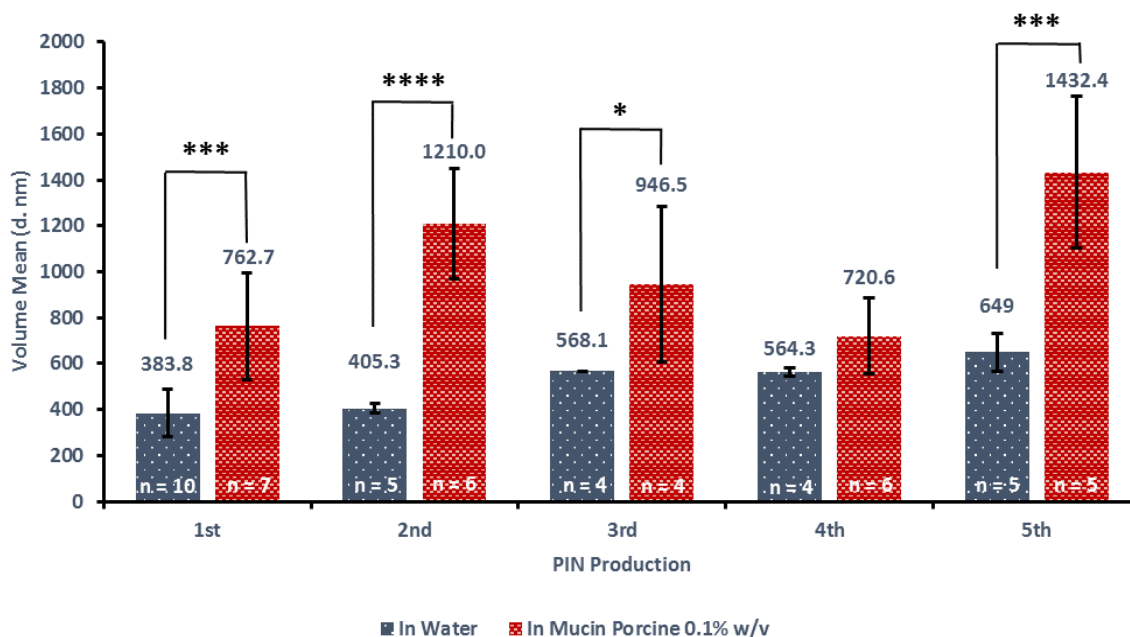
Figure 20: Reproducibility in DLS measurements of different PIN productions.

5 different nanoencapsulation productions of polystyrene were examined for the degree of variability in hydrodynamic diameter. No statistically significant changes in size in the same solvent observed (blue- in DD water, red- in mucin).

Effective size in water did not fluctuate much neither between different PIN samples, nor within the same production. Standard deviation for the measurements in mucin was higher relatively to one in water, however the variations between the samples were not statistically significant. If to compare the hydrodynamic diameter between water and mucin samples, apart from one, all the batches showed much larger effective size in mucin than in water. It may serve as an indication that the nanospheres had interaction with mucin, adhering to the polymeric surface. The particles now had to move with much thicker layer of mucin oligomers around them, compared to the layer of water molecules. Polystyrene, being a hydrophobic polymer due to bulky styrene rings as side groups; is also known for its bioadhesive properties (Norris and Sinko). The interaction between PS and mucins is most probably hydrophobic-hydrophobic one. Therefore, it was hypothesized that PS would exhibit high affinity to mucin, resulting in much higher size distribution peaks in that solvent, compared to water.

Figure 21 represents yet another reproducibility experiment within the same batch, but using different polymer. Five DLS samples were prepared from one batch and examined for variability. P[FA:SA] is known to undergo rapid hydrolysis in aqueous environment. This process manifests itself in increase of particles' size with time. It happens because backbone is being cleaved and the chains in the erosion zone get untangled and spread out, creating the appearance of expansion and size increase. Therefore, in general, P[FA:SA] has relatively high standard deviation. However, the variations in measurements are yet again not significant.

Figure 21: Reproducibility in size measurements of different samples from single PIN production

Hydrodynamic diameter of five samples of P[FA:SA] from the same production batch was measured in water. No statistically significant differences between each measurement were observed.

Conclusion

Overall, the optimization of DLS method of measuring hydrodynamic diameter and zeta potential of polymeric nanospheres in this study resulted in reproducible measurements. It was also confirmed that this method is suitable to analyze the degree of mucin interaction with the nanoparticles.

Analysis of Interaction Between Mucin and Polymeric Nanospheres

Effect of Mucin on Hydrodynamic Diameter and Zeta Potential of Polymeric Nanospheres

Each polymer in this study possess different chemical and physical characteristics that might influence its interaction with mucin. Polystyrene is highly hydrophobic, PBMAD is highly hydrophilic, while the rest of the polymers have moderate degree of hydrophobicity. All of them are bioadhesive (**Fig 23**), but some are more than others. Finally, due to carboxylic end groups, all the polymers examined are negatively charged. But how all these parameters will affect the degree of interaction with mucin?

In this study, we performed DLS measurements of hydrodynamic diameter d(H) and zeta potential ȝ of polymeric NP in dilute solution of purified mucin from porcine stomach and compared the obtained values to the same measurements in DD water. The goal of this study is to look for any substantial changes in measurements between the two solvents, that would indicate presence of NP interaction with mucins; and to correlate the degree of interaction to various physicochemical characteristics and bioadhesive properties of the polymers used. The significance of this work is in elucidating possible factors that might influence the above interactions in order to improve oral drug delivery technologies via nanoencapsulated therapeutics.

Figure 22 shows that the hydrodynamic diameter of PBMAD is more than tripled compared to one in water, suggesting a strong interaction between the surface of the nanospheres and mucin in the solution. From the measurements of bioadhesion (**Fig. 23** credit to Stephanie Hojsak and Soham Rege), (J. Reineke et al.) it is clear that PBMAD is
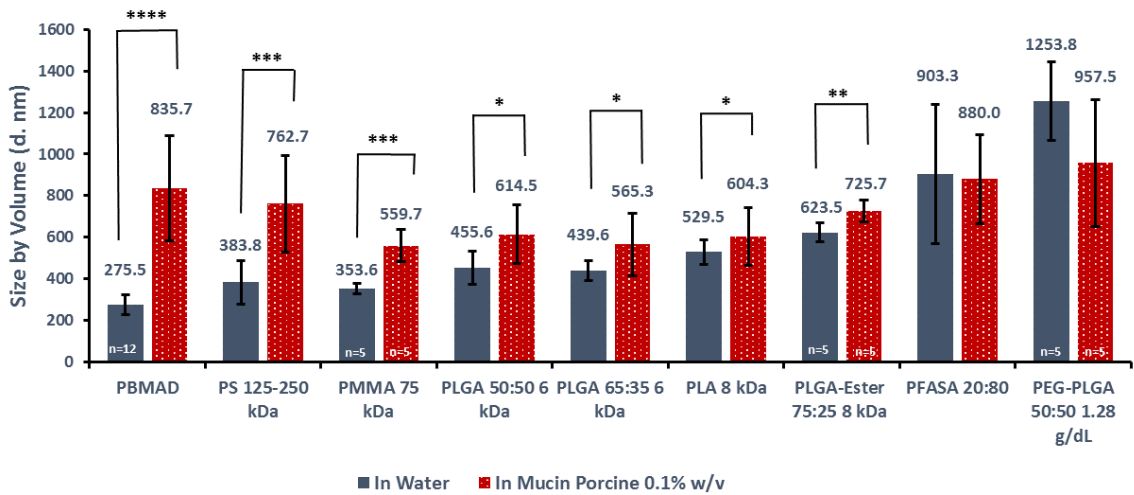
Figure 23: D(H) measurements of different polymeric NP in mucin and water.

High degree of interaction inferred between mucin and hydrophilic PBMAD and hydrophobic PS, both bioadhesive. * $p < 0.1$; ** $p < 0.05$; *** $p < 0.005$, **** $p < 0.0005$
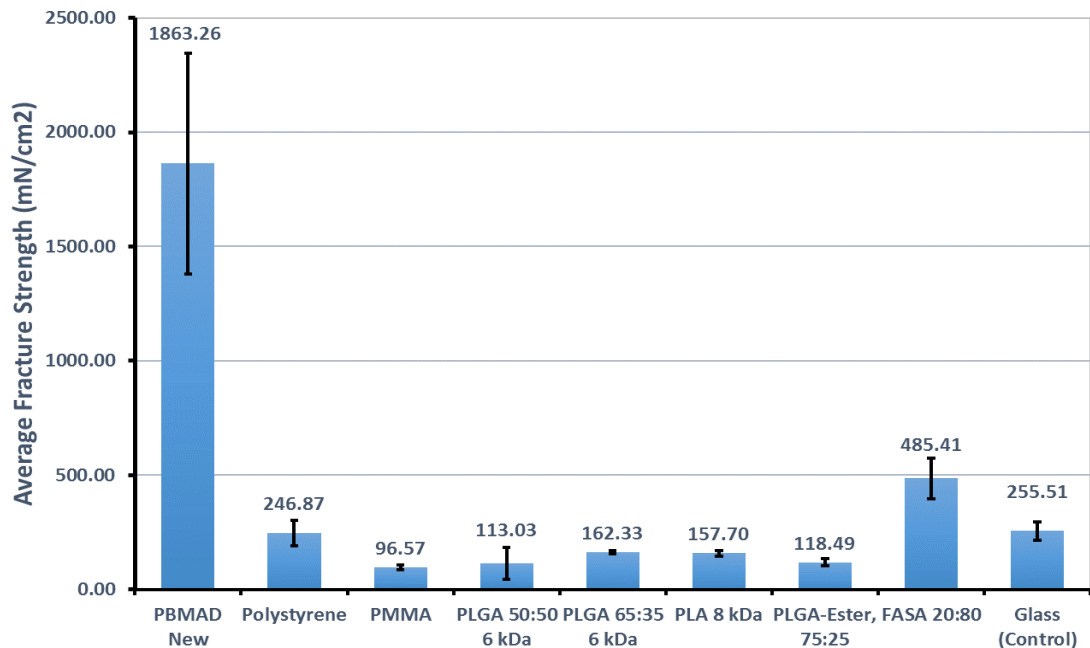
Figure 22: Quantification of bulk polymers' bioadhesion by measurements of average fracture strength-deformation.

Measurements were done by Texture Analyzer XT with rat small intestine substrate. Work credit to Stephanie Hojsak and Soham Rege

highly bioadhesive . Such high degree of bioadhesion can be attributed to a high number of hydrogen bonds formed between hydrophilic parts of mucins and polar size groups of the polymer. PEG and PBMAD are both hydrophilic polymers. But unlike PEG, which is non-bioadhesive and does not form interactions with mucin, PBMAD is highly bioadhesive due to strong H bond formation. PBMAD is sensitive to pH: stable in acidic environment and dissolving in basic; and therefore, can be used in design of pH- activated drug delivery systems (for pH-dependent DLS study of PBMAD see **Appendix C**). Since pH gets progressively basic going from the stomach (pH <3) to small intestine (6.5-7.0) to colon (7.8) (Balamuralidhara et al.), an external coating of PBMAD can be applied on a polymeric nanosphere, containing therapeutic agent. This outer coating will be stable as the particle travels through stomach, and will start to dissolve upon reaching the intestine.
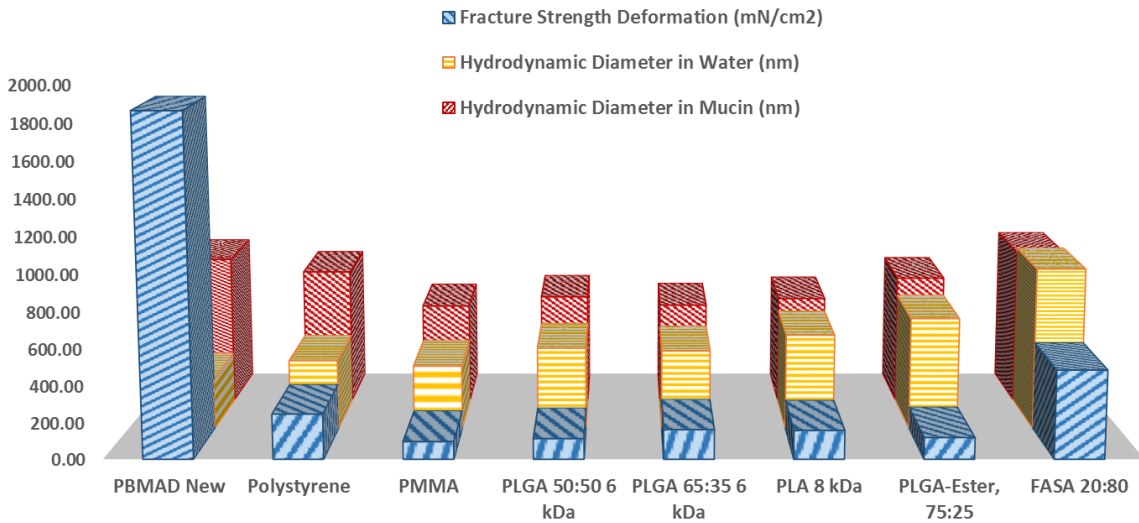
Figure 24: Bioadhesion vs change in hydrodynamic diameter.

Comparison between bioadhesion of polymers and the change in hydrodynamic diameter of their corresponding nanospheres in water vs mucin 0.1% w/v. Bioadhesion work credit to Stephanie Hojsak and Soham Rege

Reineke et. al. did isolated loop experiments, where they introduced PMMA nanoparticles and PBMAD-coated PMMA to GI tract of a rat. PMMA showed very little intestinal uptake (5.8%). However, addition of external coating of PBMAD significantly increased the uptake of the PMMA nanoparticles to 66.9% (J. Reineke et al.).

Polystyrene (PS) possess the second most pronounced change in hydrodynamic diameter going from water to mucous solution. Its effective size more than doubled, pointing to the strong interaction with mucin as well. PS is known for its bulk bioadhesive properties (J. Reineke et al.), however they are mainly due to the polyvalent hydrophobic interaction with hydrophobic domains of mucin fibers. From the bioadhesion measurements (**Fig. 23**) PS exhibit two -three times more fracture-strength deformation that other polymers such as PLA or PLGA, but it is not nearly as high as PBMAD. Studies of intestinal uptake of PS nanoparticles show that they are able to penetrate the mucus layers are get through intestinal wall into the bloodstream (J. Reineke et al.; Jani et al.).

P[FA:SA] (20:80) in another hydrophobic yet bioerodable polymer that displays relatively high degree of bioadhesion (**Fig. 23**) and (Chickering and Mathiowitz). Interestingly, its effective size in water and mucin is virtually unchanged. It is important to note that the size measured by DLS in both solvents is relatively large (800-900 nm), while visual inspection demonstrated particles around 300 nm. As was indicated in previous section, this polymer is very sensitive to water and upon contact with aqueous solution undergoes rapid hydrolysis. The chains in the water erosion zone begin to spread out and untangle, leading to larger effective size of the nanospheres. For more studies of P[FA:SA] in different pH as a function of time see **Appendix C**. Also, SEM of this sample (**Fig. 13 C & D**) did not show well defined spherical spheres, but rather aggregated network of

nanoparticles. Therefore, it is possible that we measured the size of clusters or small aggregates of particles instead of the individual spheres.

PEG-PLGA is another polymer, which did not demonstrate any changes in hydrodynamic diameter between two solvents. This hydrophilic polymer is known for its non-adhesive properties towards mucin. Studies show that coating the surface of the sphere with PEG creates a water interface and does not allow to form any sort of interaction with mucins (Lai et al.). PEGylation of nanospheres facilitates their diffusion through mucus layers promotes the increase in intestinal uptake (Abdulkarim et al.)

PMMA, the nonerodable polymer, has the lowest fracture strength deformation values, much lower that the glass, used for control (**Fig. 23**) and (J. Reineke et al.). However, it does exhibit statistically significant increase in hydrodynamic diameter in mucin, compared to one in water (**Fig. 22**). It is relatively hydrophobic polymer, but due do the presence of ester side group, it can possibly form hydrogen, dipole-dipole or other electrostatic interactions with mucin. However, the isolated loop studies show (J. Reineke et al.) very low uptake of PMMA nanoparticles in the GI tract.

The rest of the polymers, such as biodegradable PLA and PLGA, show moderate increase in their effective size in mucin, indicating some degree of interaction with mucin. Texture Analyzer measurements also show low to moderate bioadhesive forces of these materials. They are predominantly hydrophobic, with some degree of hydrophilicity due to the carboxylic end groups.

We also examined another parameter- zeta potential of the nanospheres in water and in mucin solution. This is the charge measured at the slipping plane within the electric

double layer, and it is solvent-dependent. In general, for the particle to be efficient in mucus penetration, neutral charge is preferable (Cone). Numerous studies indicated that coating of negatively charged particle with neutral PEG increases its diffusion and subsequent uptake through GI tract (Cone; Lai et al.; Griffiths et al.; Abdulkarim et al.) Positively charged particles might have too strong interactions with negatively charged mucin, entrapping them within the mucosal mesh, as was illustrated with chitosan spheres (Kas). On the other hand, highly negatively charged particle might have repulsive forces with negatively charges mucin, thus reducing the chance of mucus penetration by simply getting cleared from the body. However, in vivo studies also demonstrated that negatively charged polystyrene NP are able to penetrate mucosal barrier and get through epithelial lining of GIT (J. J. Reineke et al.; Norris and Sinko; Jani et al.)
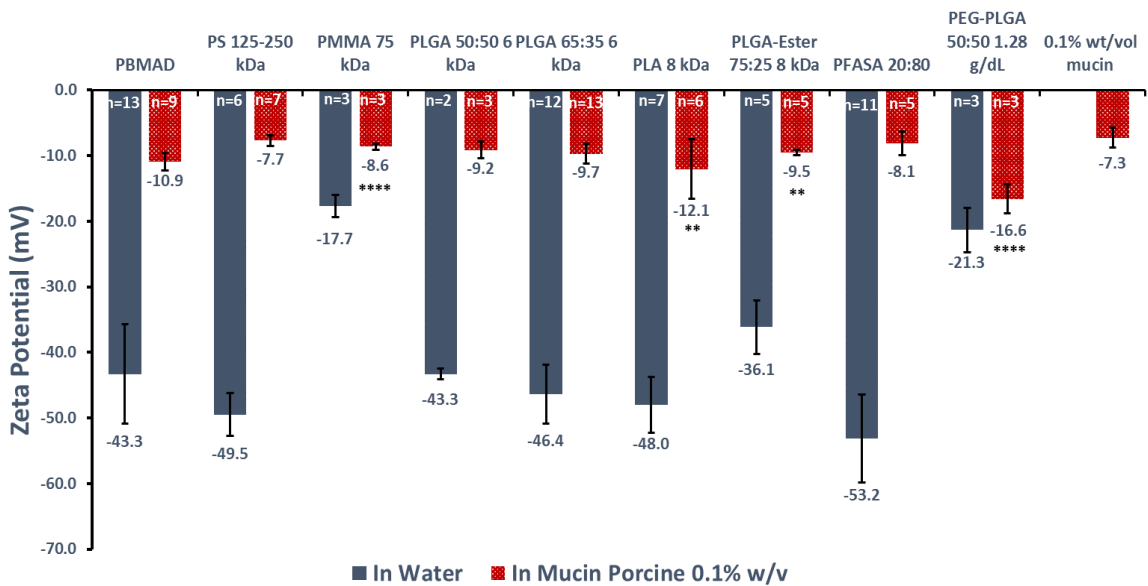

Figure 25: Effect of mucin on zeta potential of nanospheres in water vs mucin

Zeta potential in water is substantially more negative that in mucin. Mucin masks the charge of the spheres.

All the particles have negative charge in water, ranging from -17 to -53 mV (**Fig. 25**). In mucin, however, the charge is significantly reduced. While the charge of mucin without any nanomaterial was found to be -7.3 mV, the charge of nanospheres in mucin ranges from -16 to -7.7 mV. It seems that mucin greatly masks the charge of all the particles. PMMA and PEG-PLGA stands out by having much lower effective charge in water, compared to the rest for the tested polymers. As a result, there was no substantial charge reduction in mucin for these two polymers.

Since nanospheres produced from various polymers have different hydrodynamic diameters, to compare the charges across the polymers, we need to normalize the measurements by calculating charge per surface are for each sample. PBMAD has the highest negative charge concentration on its surface in both water and mucin (**Fig. 26-27**). It is logical, because it has large amount of polar negatively charged side groups. In addition, in water, for example, its effective size is relatively small. Therefore, the charge per surface area is high. Polystyrene nanospheres have also high negative charge density on their surface in water (**Fig. 26**). In mucin, on the other hand, this charge is substantially reduced (**Fig. 27**). PS alongside P[FA:SA] has the smallest surface charge in mucin out of all the tested polymers. The rest of them exhibit various degree of charge reduction in mucin. Even though that the charges of all the samples seemed to be masked to very similar values,when taking into account the changes in effective size of the NP, it becomes evident that the degree of charge reduction varies from sample to sample.

To better represent the amount of the charge reduction, Figure 28 compares the charge per surface area in mucin (red) to the surface charge in water (red plus yellow). The yellow then represents the difference in charge density in the two solvents (the amount of
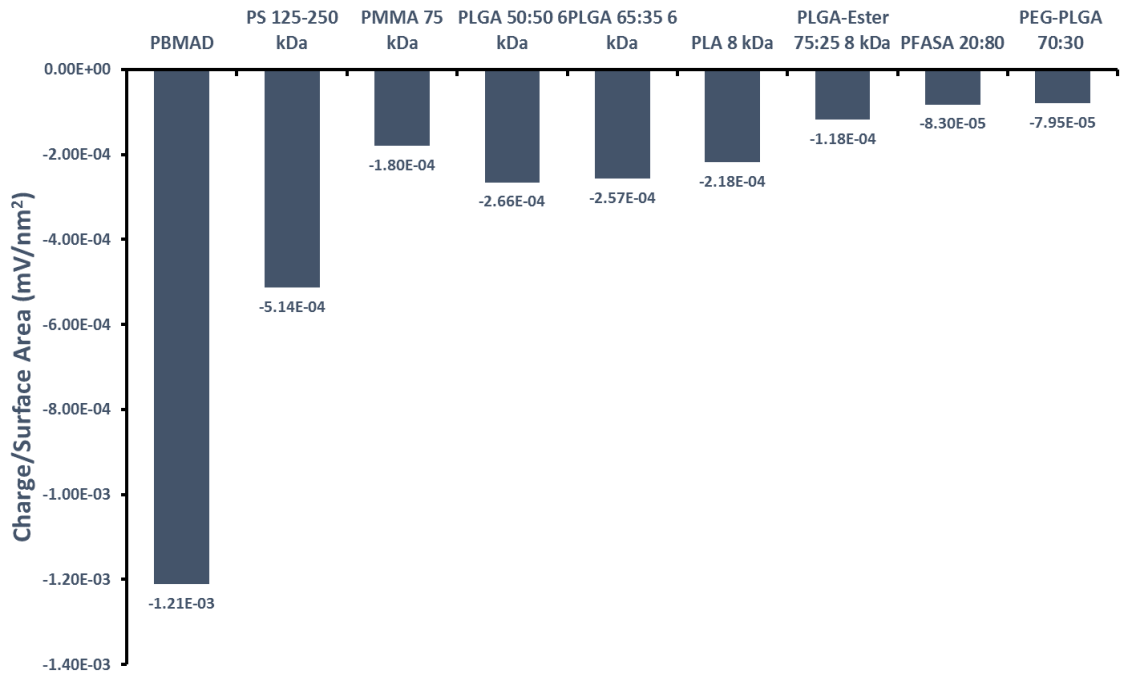
Figure 26: Charge per surface area of various nanospheres in water.

Zeta potential measurements were divided by surface area of each polymeric sample $\zeta/\pi(r(H))^2$. Surface area was calculated using hydrodynamic radius measurements, r(H) in water
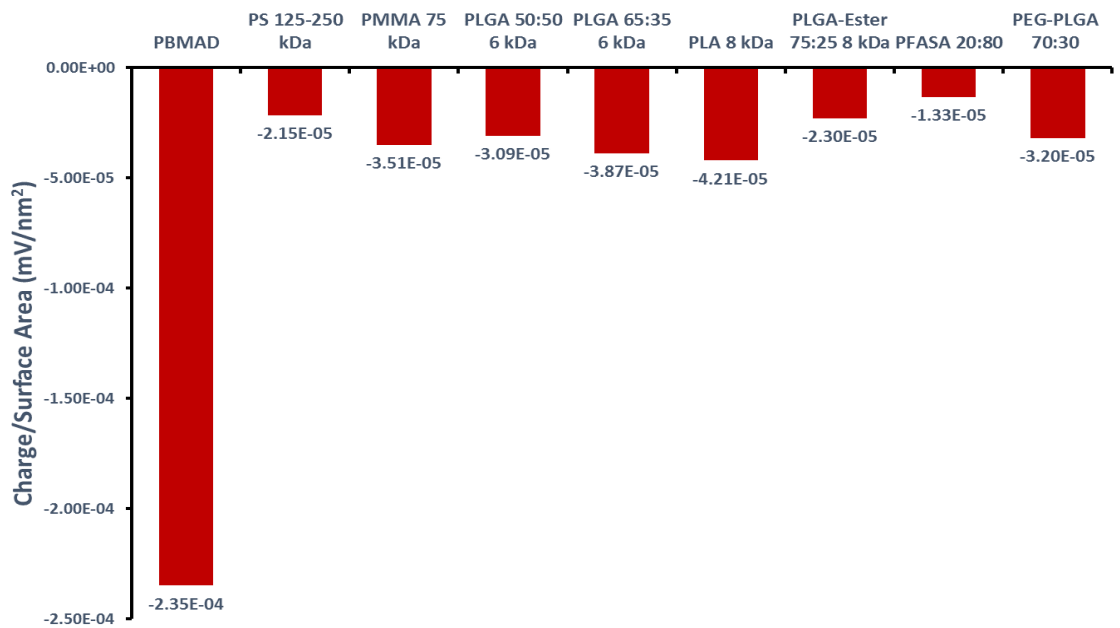
Figure 27: Charge per surface area of various polymeric nanospheres in mucin.
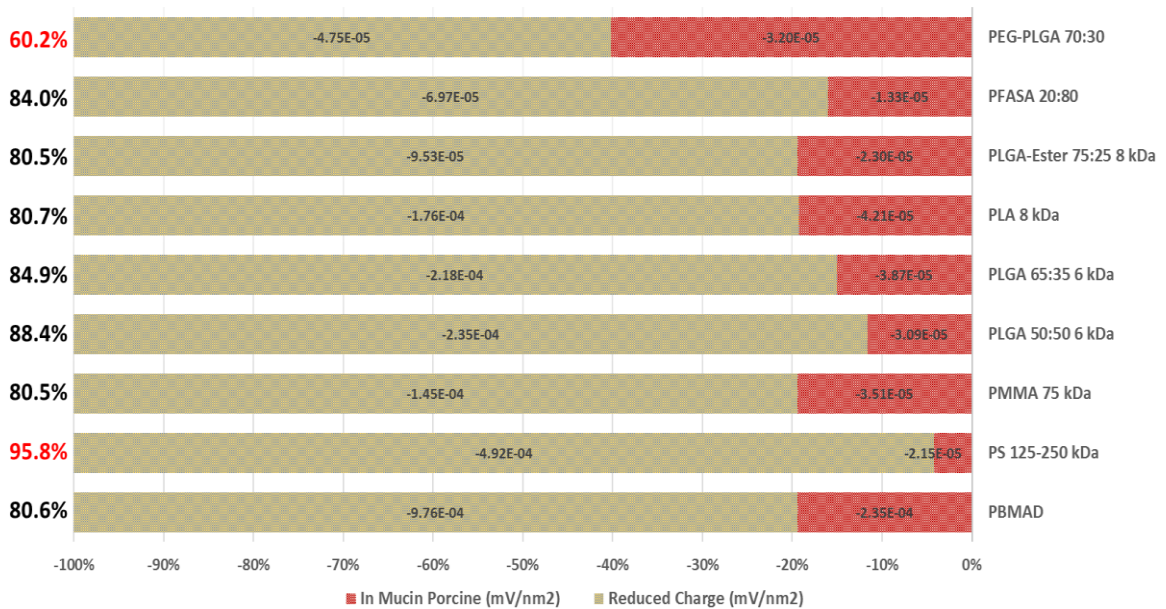
Zeta potential measurements were divided by surface area of each polymeric sample $\zeta/\pi(r(H))^2$. Surface area was calculated using hydrodynamic radius measurements, r(H) in mucin.

reduced charge). Immediately it is clear that PS is subjected to the highest degree of charge reduction: its original surface charge in water is reduced by more than 95% in

mucin. It is another indication that bioadhesive PS nanoparticles extensively interact with mucin: their effective size is increasing, while zeta potential is decreasing, leading to such profound masking of the charge by mucin. Previous studies indicate that PS nanoparticles succeed in penetrating mucosal layers of GI tract (J. J. Reineke et al.; Norris and Sinko; Jani et al.). High degree of charge masking, therefore, may promote the diffusion of the nanomaterial through negatively charged mucin; and subsequently increase its uptake though negatively charged membranes.

60.2%	-4.75E-05	-3.20E-05	PEG-PLGA 70:30
84.0%	-6.97E-05	-1.33E-05	PFASA 20:80
80.5%	-9.53E-05	-2.30E-05	PLGA-Ester 75:25 8 kDa
80.7%	-1.76E-04	-4.21E-05	PLA 8 kDa
84.9%	-2.18E-04	-3.87E-05	PLGA 65:35 6 kDa
88.4%	-2.35E-04	-3.09E-05	PLGA 50:50 6 kDa
80.5%	-1.45E-04	-3.51E-05	PMMA 75 kDa
95.8%	-4.92E-04	-2.15E-05	PS 125-250 kDa
80.6%	-9.76E-04	-2.35E-04	PBMAD

-100% -90% -80% -70% -60% -50% -40% -30% -20% -10% 0%

■ In Mucin Porcine (mV/nm2)   ■ Reduced Charge (mV/nm2)

Figure 28: Percent reduction of surface charge density.

Comparison of the calculated values in mucin (red) to water (the sum of red and yellow). The values' units are mV/nm^2

53

PEG-PLGA, on the other hand, experience the lowest change in surface charge density. Only 60% of its original charge density in water is reduced in mucin. That is due to the fact that for this particular polymer, both hydrodynamic diameter (**Fig. 22-23**) and zeta potential (**Fig. 25**) did not change much across the two solvents. This polymer was classified as non-bioadhesive (Lai et al.); and widely used as external coating of nanoencapsulated material to promote the uptake though GIT.

Previously we observed that PBMAD had the highest surface charge density in both water and mucin. However, the charge is being reduced to the same degree as for the rest of the polymers tested: 80-88%. P[FA:SA], having the smallest charge density, experience 84% masking of the charge in mucin.

Effect of Mucin on Hydrodynamic Diameter and Zeta Potential of Polymeric Nanospheres as a Function of Increasing Molecular Weight

PLGA Nanospheres

Polylactic acid and poly(lactic-co-glycolic acid) copolymer are widely used in drug delivery systems due to their biocompatibility and biodegradability properties. PLA has methyl side chain group, which makes the polymer chain bulkier and less flexible compared to PLGA, which lacks some of the methyl groups due to glycolic acid copolymer. It also gives PLA greater hydrophobicity, compared to PLGA. In general, the more lactic acid monomers are present in the copolymer, the more hydrophobic it becomes. In addition, with increasing molecular weight of the polymeric chains the amount of polar end groups decreases, which should in turn increase the overall hydrophobicity of the polymer. We decided to test PLA and PLGA of different copolymer ratios and molecular weights, to see whether degree of hydrophobicity influences NP interaction with mucin.
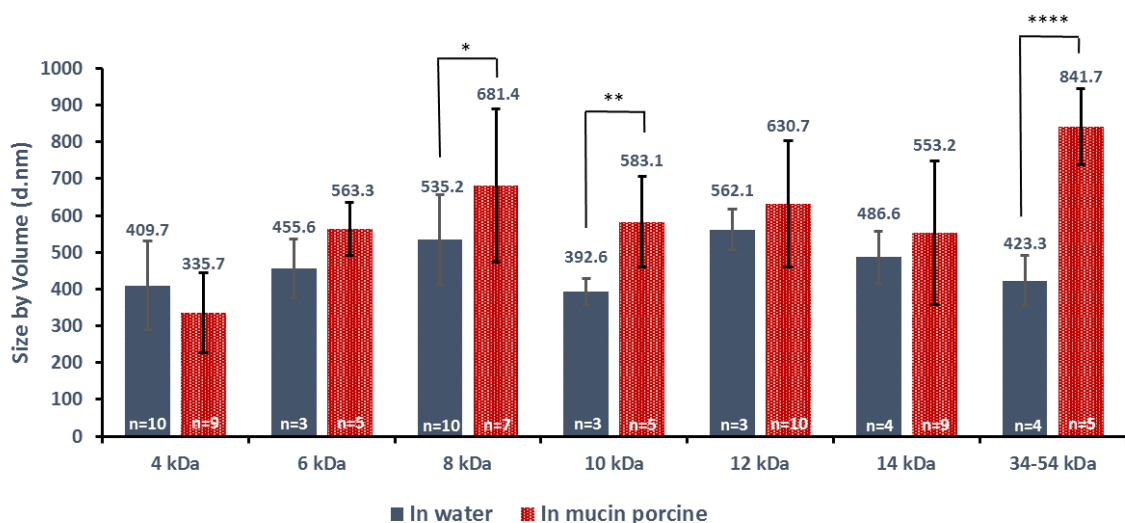

Figure 29: Hydrodynamic diameter of PLGA nanospheres as a function of molecular weight.

$* \ p< 0.1; \ ** \ p< 0.05; \ **** \ p < 0.0005$

Hydrodynamic diameter measurements in water showed no obvious trends as the molecular weight of the polymer increased (**Fig. 29**). All samples were measured at 400-600 nm in size. Effective size in mucin for the most part was larger compared to water, but only 8,10 and 34-54 kDa samples has statistically significant change. It is important to note that the largest Mw PLGA nanospheres doubled in size in mucin, indicating much stronger interaction with mucin, than the rest of the samples. It seems that polymeric chain must reach a certain length to attain enough hydrophobicity in order to strongly interact with hydrophobic parts of mucin chains.
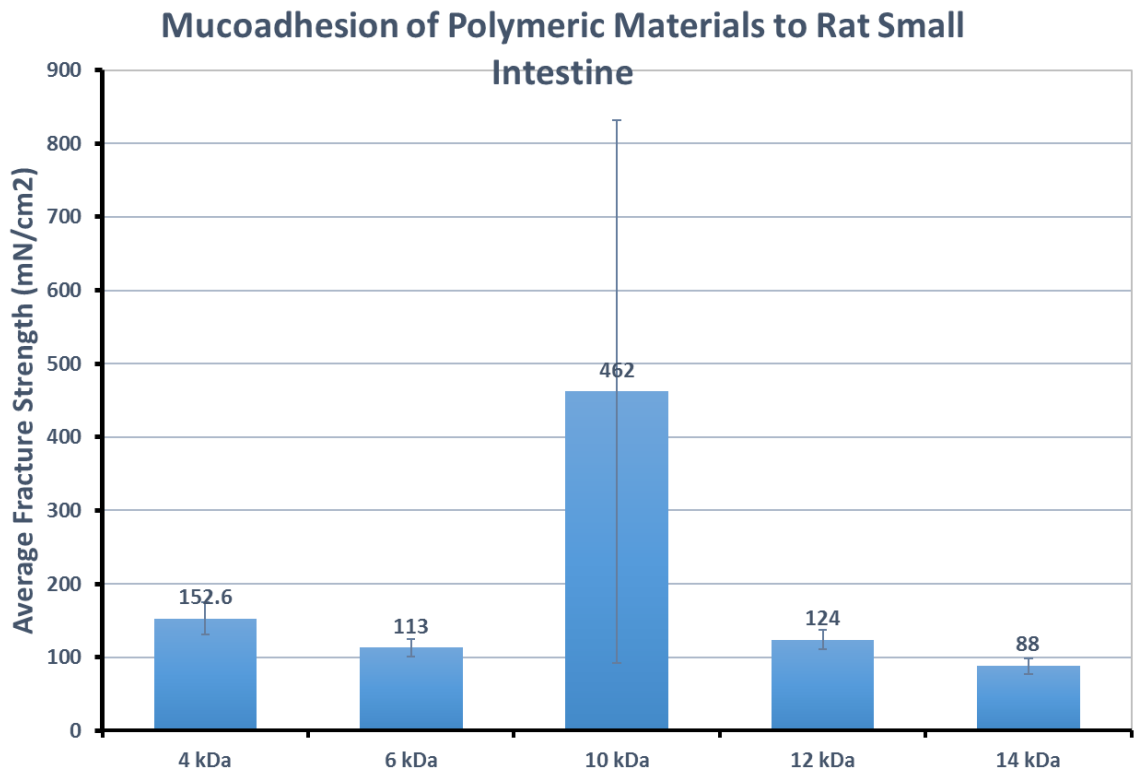

Figure 30: Quantification of bioadhesive properties of bulk PLGA (50:50) polymers by measurements of average fracture strength-deformation

Measurements were done by Texture Analyzer XT with rat small intestine substrate. Work credit to Stephanie Hojsak and Soham Rege

Fracture-strength deformation measurements indicate that PLGA bulk polymers possess analogous degree of bioadhesion across different molecular weight samples.

4 kDa PLGA had smaller hydrodynamic diameter in mucin as opposed to water, unlike the rest of the tested polymers. Another PIN batch was produced for more testing. The second sample generated the same trend in results. It is important to note, however, that the difference in values was not statistically significant. Nevertheless, we decided to perform FTIR analysis of the sample in order to determine whether this particular polymer had carboxylic end groups or ester-protected end groups. The FTIR of the sample was compared to PLGA polymer with ester end groups as well as to PLGA with acid end groups (**Fig. 31**). FTIR transmittance peaks of 4 kDa PLGA matched to the ones of 8 kDa PLGA-with known acid end groups. PLGA-Ester was different from both 4 and 8 kDa polymers: it had peak at 3660 cm^{-1} and was lacking peak at 1631cm^{-1}. The differences may account or the presence of ester groups and absence of carboxylic groups. FTIR results also shows that 4 kDa PLGA had carboxylic end groups after all.

As with all other tested polymers, zeta potential of PLGA nanospheres is more negative in water, than in mucin (**Fig. 32**). Mucin masks the charge of the spheres, reducing its value substantially. Usually zeta potential measurements are indicative of the stability of the suspension, with values below $|\pm30|$ signifying instability of the particles in the solution. However, from our measurements it seems that mucin stabilized the charge of the nanospheres, hence much smaller standard deviation values in mucosal solution compared to ones in water.
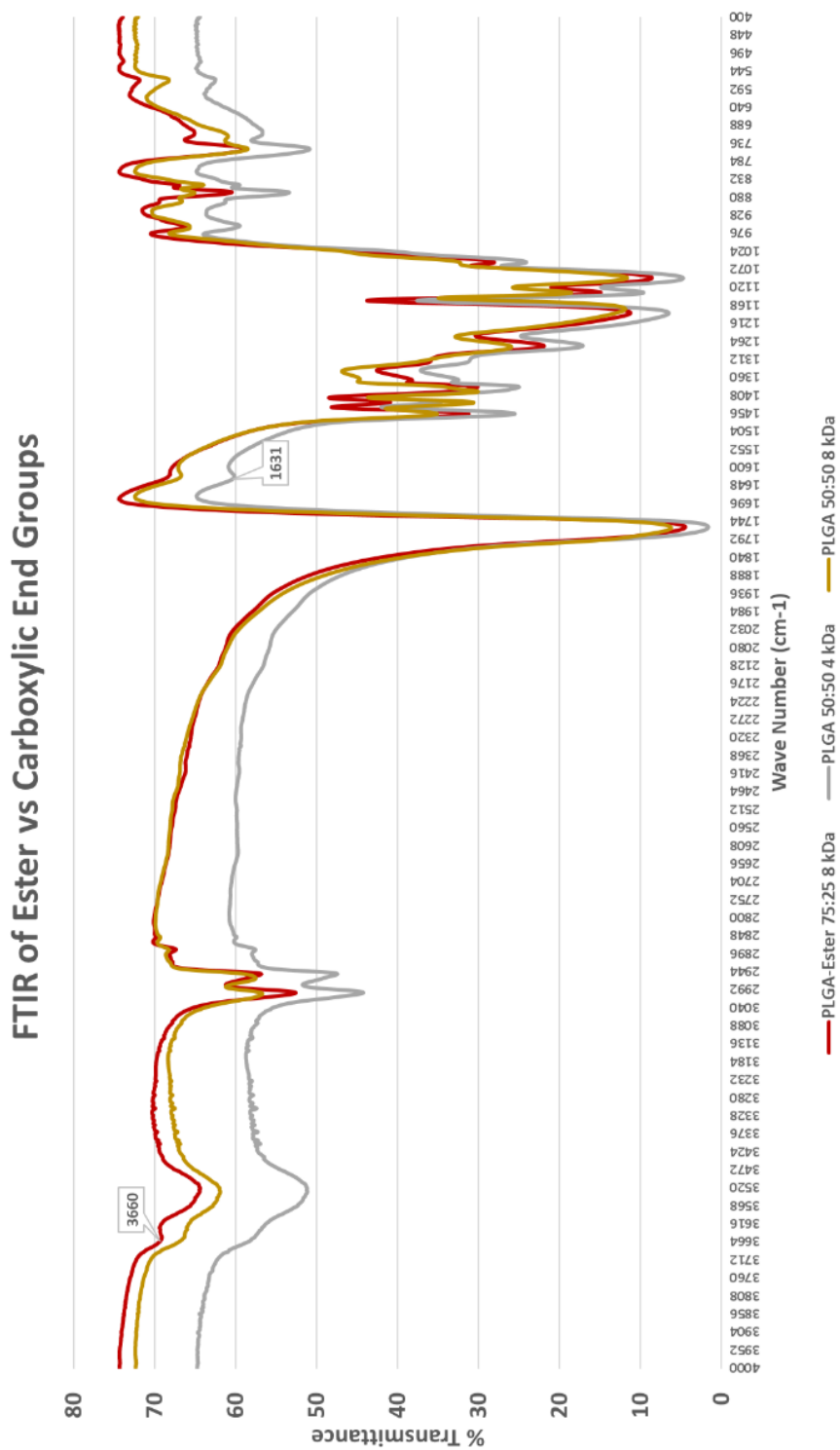
Figure 31: FTIR analysis of PLGA samples with carboxylic vs ester end groups.
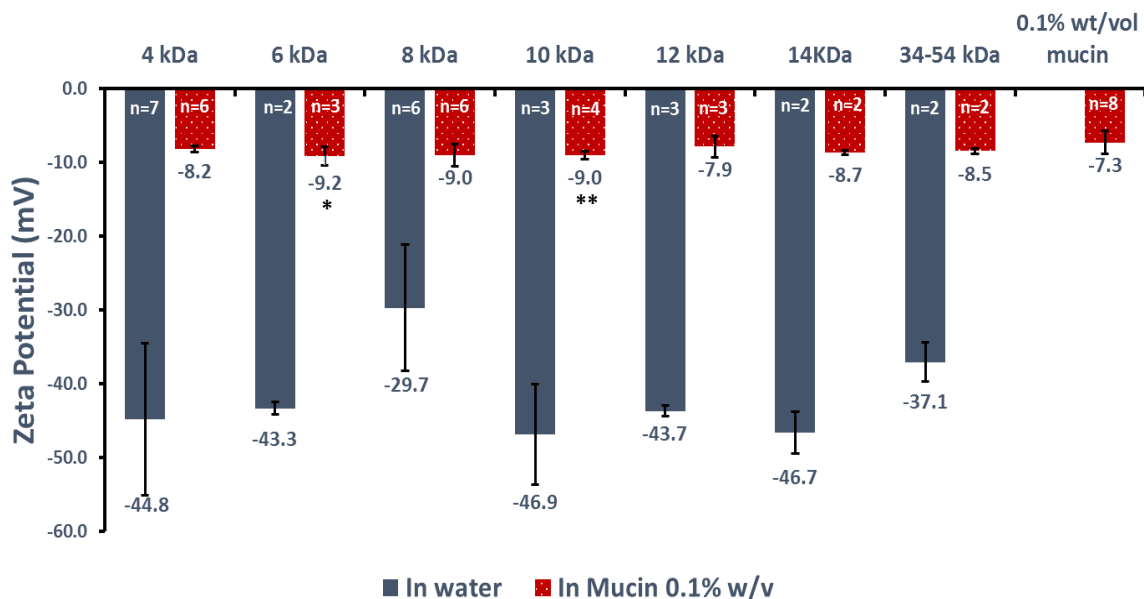
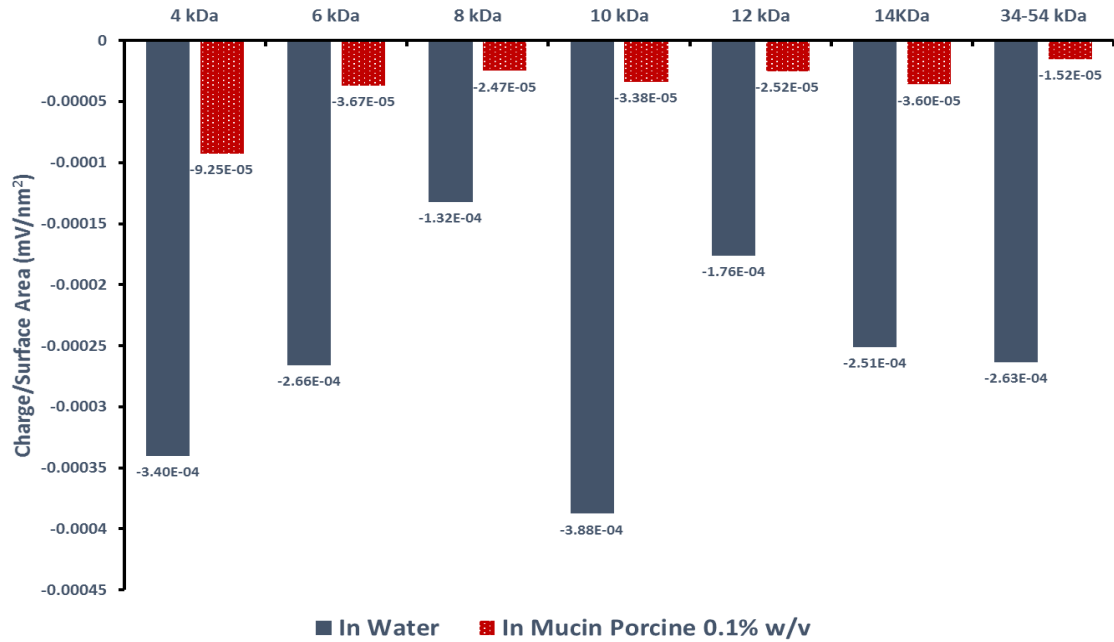**Figure 32:** Zeta potential of PLGA nanospheres as a function of molecular weight. In water ʒ is substantially more negative that in mucin. Mucin masks the charge of the spheres.

Calculations of charge density on the surface of the spheres revealed that the smallest Mw polymer (4 kDa) had the highest value, while the largest Mw polymer (34-54 kDa) had the smallest value in mucin (**Fig. 33**). It may be attributed to decrease in number of carboxylic groups as the polymeric chains become longer, which makes the polymer less polar and more hydrophobic in nature. Even though bioadhesion forces among the PLGA polymers are comparable, DLS measurements of effective size indicated stronger interaction with mucin for larger Mw sample, and non-significant one for low Mw sample. Therefore, hydrophobicity of the sample may play important role alongside bioadhesion and charge as a factor, determining degree of interaction between polymers and mucin.

Figure 34 visualizes the amount of surface charge that was reduced by dispersing the nanospheres in mucin compared to water. The red bars represent charge per surface

area in mucin, while the yellow bars show the difference between the charge in water and mucin. The surface charge density get smaller with increasing Mw of the sample. 4 kDa PLGA had only 72.8% of its charge in water reduced by mucin. 34-54 kDa PLGA, on the other hand, experienced over 94% charge reduction.

Figure 33: Charge per surface area of PLGA (50:50) nanospheres with increasing molecular weight.

Zeta potential measurements were divided by surface area of each polymeric sample $\zeta/\pi(r(H))^2$. Surface area was calculated using hydrodynamic radius measurements, r(H) in water and mucin
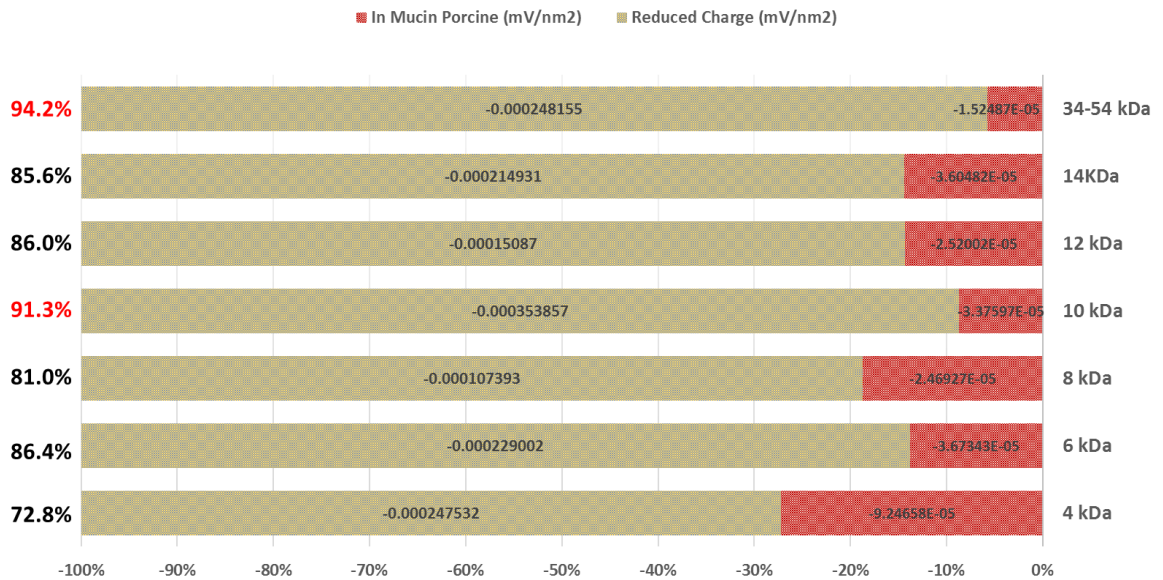
Figure 34: Percent reduction of surface charge density for PLGA (50:50) nanospheres with increasing molecular weight.

Comparison of the calculated values in mucin (red) to water (the sum of red and yellow). The values' units are mV/nm^2

PLA Nanospheres

PLA, as previously stated, is one of the most widely used polymers in drug delivery systems. It is biodegradable and biocompatible, thus being FDA approved for use in humans. It has methyl as a side chain group, making the polymer bulkier and less flexible and more hydrophobic in nature compared to PGA or PLGA.

We investigated the dependency of hydrodynamic diameter and zeta potential of PLA nanospheres on the molecular weight of the material. DLS measurements of the effective size in water and mucin did not show any significant differences as the polymeric chains increased in size (**Fig.35 A**). Zeta potential of all samples was significantly lower in mucin compared to water (**Fig. 35 B**). Normalization of the charge per unit of surface area indicated that the lowest Mw PLA had the highest charge in water, which can be explained by greater number of polar carboxylic end groups in the sample (**Fig.35 D**). However, all three samples had similar degree of charge masking by mucin, varying from 79 to 84% (**Fig. 35 C**).
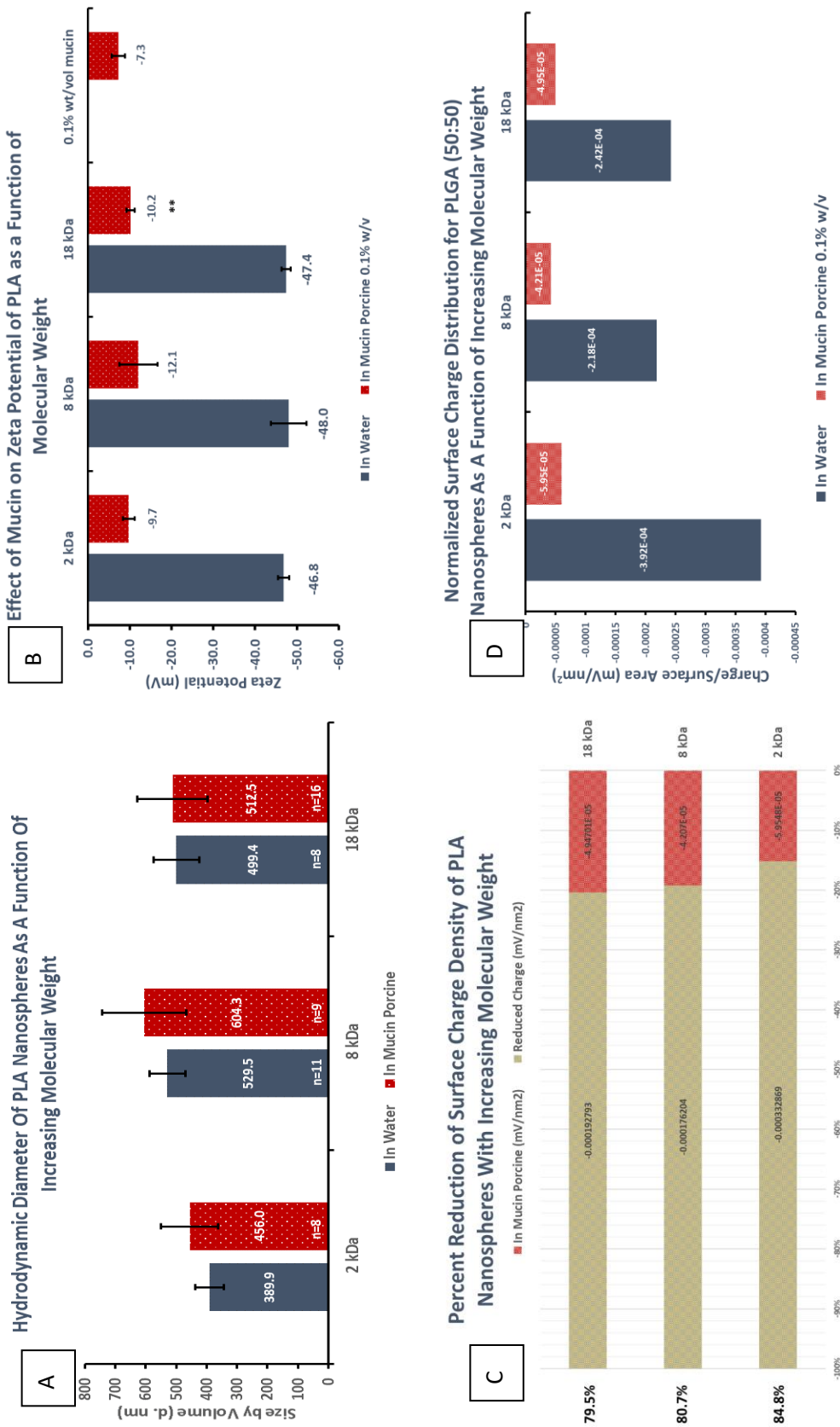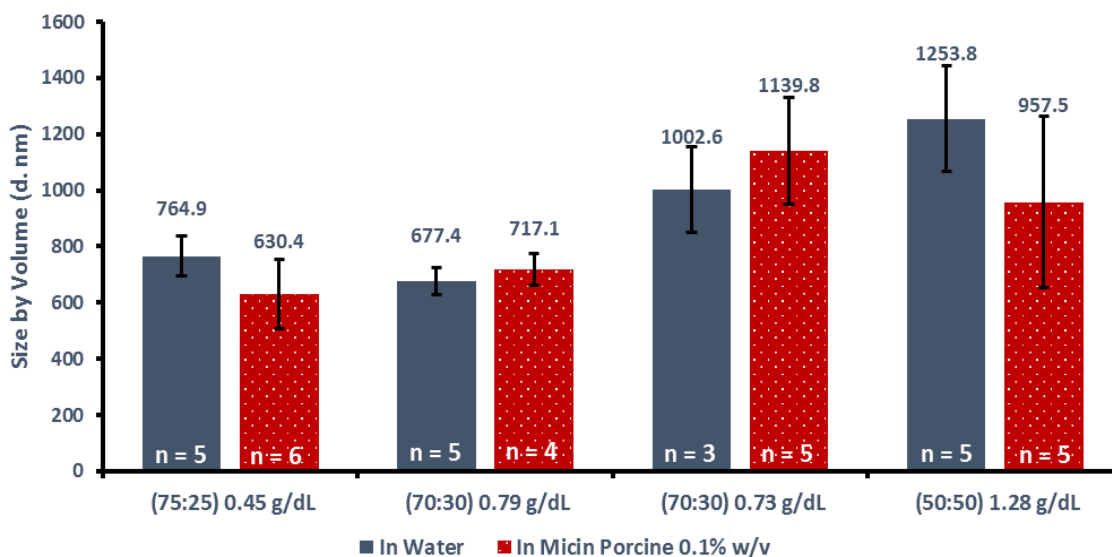
Figure 35: Effect of mucin on hydrodynamic diameter and zeta potential of PLA nanospheres.

A) Effect of mucin on d(H) of PLA NP with increasing Mw; B) ζ of PLA NP in mucin is substantially less negative compared to water; C) percent reduction of calculated surface charge density compared to water; D) normalization of ζ by dividing effective charge by NP surface area in each solvent

PEG-PLGA Nanospheres

Polyethylene Glycol or PEG is non-toxic, non-immunogenic, FDA approved polymer, which is extensively used in the field of drug delivery. It is water soluble polymer with low bioadhesive forces. Recent studies show that PEGylation of polymeric nanoparticle considerably improves their uptake through GIT(Lai et al.; Lai, Wang, and Hanes; Abdulkarim et al.). The increase in uptake is attributed to low interaction with mucin in mucosal layers, which allows for rapid diffusion through mucosal layers. Multiple Particle Tracking studies shows that nearly neutral PEG-PLGA achieve much higher diffusion through freshly isolated porcine mucus, than negatively charged PLGA nanospheres (Abdulkarim et al.) The nearly neutral surface charge of the nanospheres aids in penetration across negatively charged cell membranes (Cone). In light of the resent

Figure 36: Hydrodynamic diameter of PEG-PLGA nanospheres as a function of molecular weight.

findings, we decided to investigate effect mucin exhibits on the effective size and charge of PEG-PLGA nanospheres to better understand the interaction between PEGylated polymers and mucin.

Different ratios of copolymers and molecular weights were explored. Hydrodynamic diameter of the nanospheres was significantly larger than SEM- estimated size. Since SEM images revealed poorly defined spherical particles with large agglomeration, such large numbers can be explained by measuring aggregates rather than single particles. Alternatively, increase in effective size may be attributed to PEG copolymer chains solubility in water. The PEG parts of the polymeric chains might be spreading out into the aqueous solvent, enlarging the diameter of the spheres. Two samples of 70:30 ratio PEG to PLGA showed slight, but not statistically significant, increase in hydrodynamic diameter going from water to mucin (**Fig. 36**). Another two samples (one
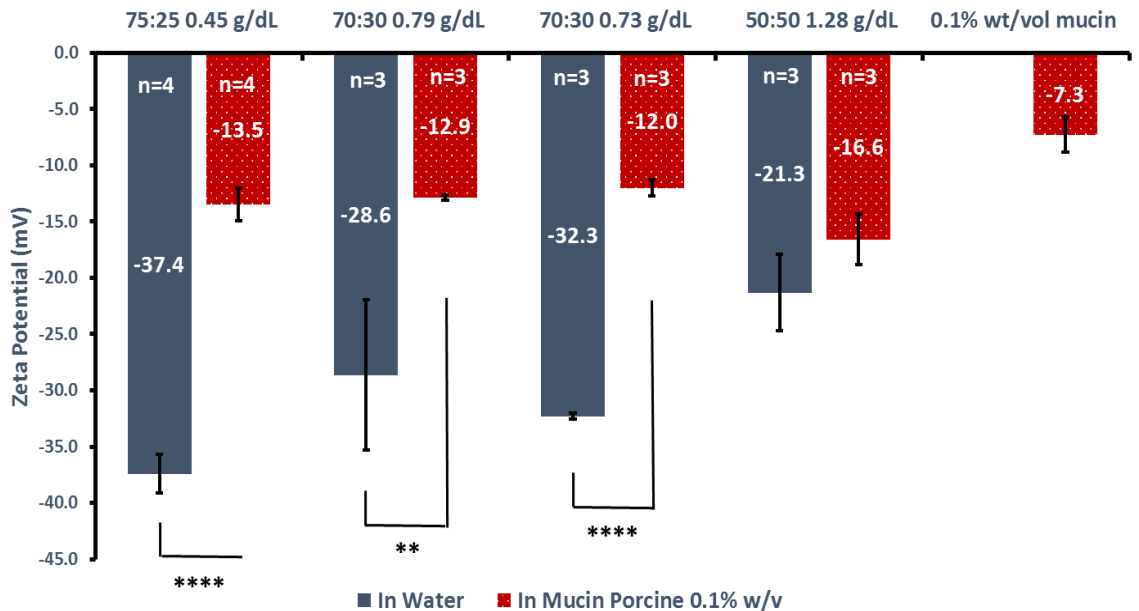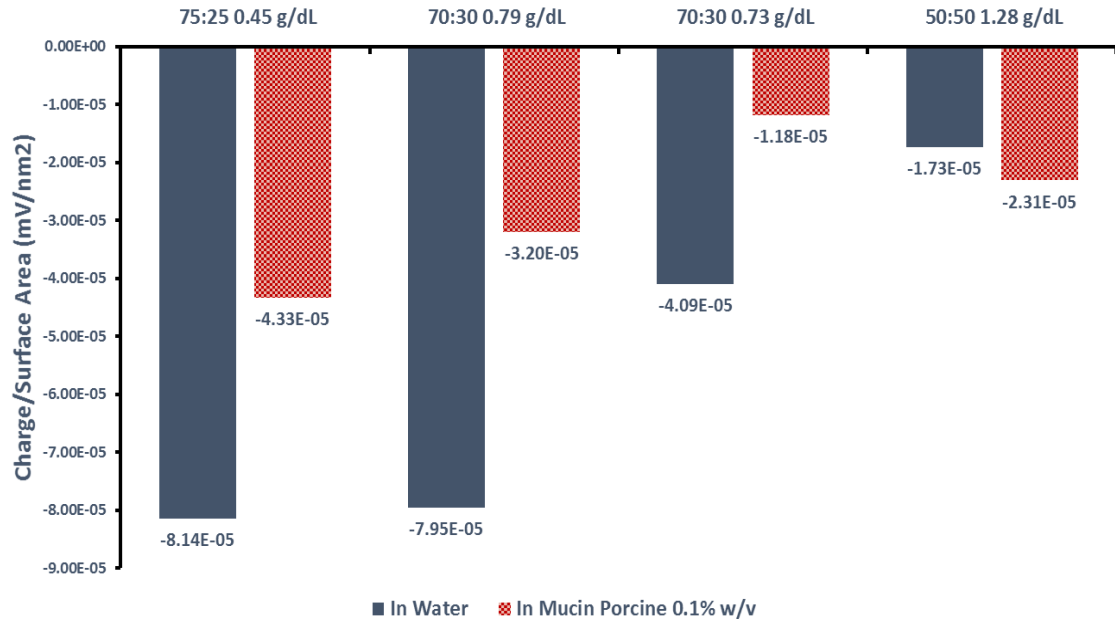

Figure 37: Zeta potential of PEG-PLGA nanospheres as a function of molecular weight.
Zeta potential of nanospheres in water is more negative that in mucin, signifying masking of the surface charge.

with the highest PEG content but lowest Mw; and one with lowest PEG content but highest Mw) displayed decrease in effective size in mucin compared to water. This reduction in apparent size signifies poor interaction of mucin with the surface of the spheres. The DLS measurements agree with well-known non-bioadhesive properties of PEG.

Zeta potential of PEG-PLGA is lower in water compared to mucin (**Fig. 37**). However, for the sample with highest Mw the difference in measured charge in not statistically significant. Overall, the charge of the nanospheres in mucin is higher that empty mucin (no nanomaterial present), indicating relatively poor masking of the charge. Normalization of zeta potential in each solvent further supports the conclusion that mucin masks the charge of PEGylated spheres to much lesser extent than the rest of the polymers tested in this study (**Fig. 38**). In case of PEG-PLGA 50:50 the charge per surface area in mucin is higher than in water by 20% (**Fig. 39**). The rest of the samples also show unusually low degree of masking, ranging from 49 to 71%, while the rest of the polymers tested typically had at least 80% reduction in charge in mucin.

Figure 38: Normalized charge per surface area of PEG-PLGA nanospheres.

Zeta potential measurements were divided by surface area of each polymeric sample $\zeta/\pi(r(H))^2$. Surface area was calculated using hydrodynamic radius measurements, r(H) in water and mucin
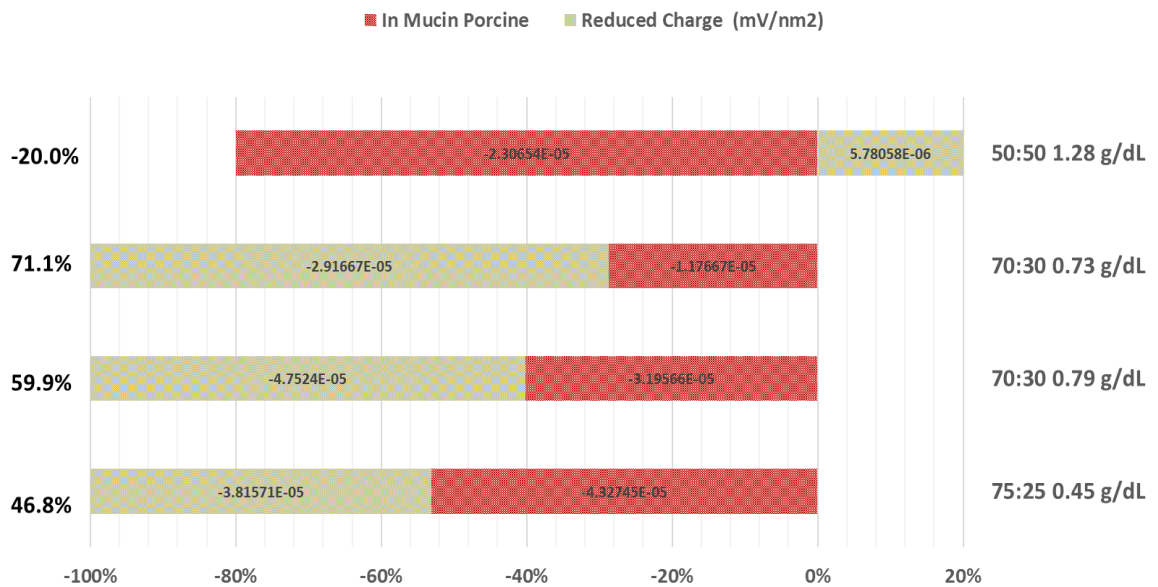
Figure 39: Percent reduction of surface charge density for PEG-PLGA nanospheres.

Comparison of the calculated values in mucin (red) to water (the sum of red and yellow). The values' units are mV/nm^2
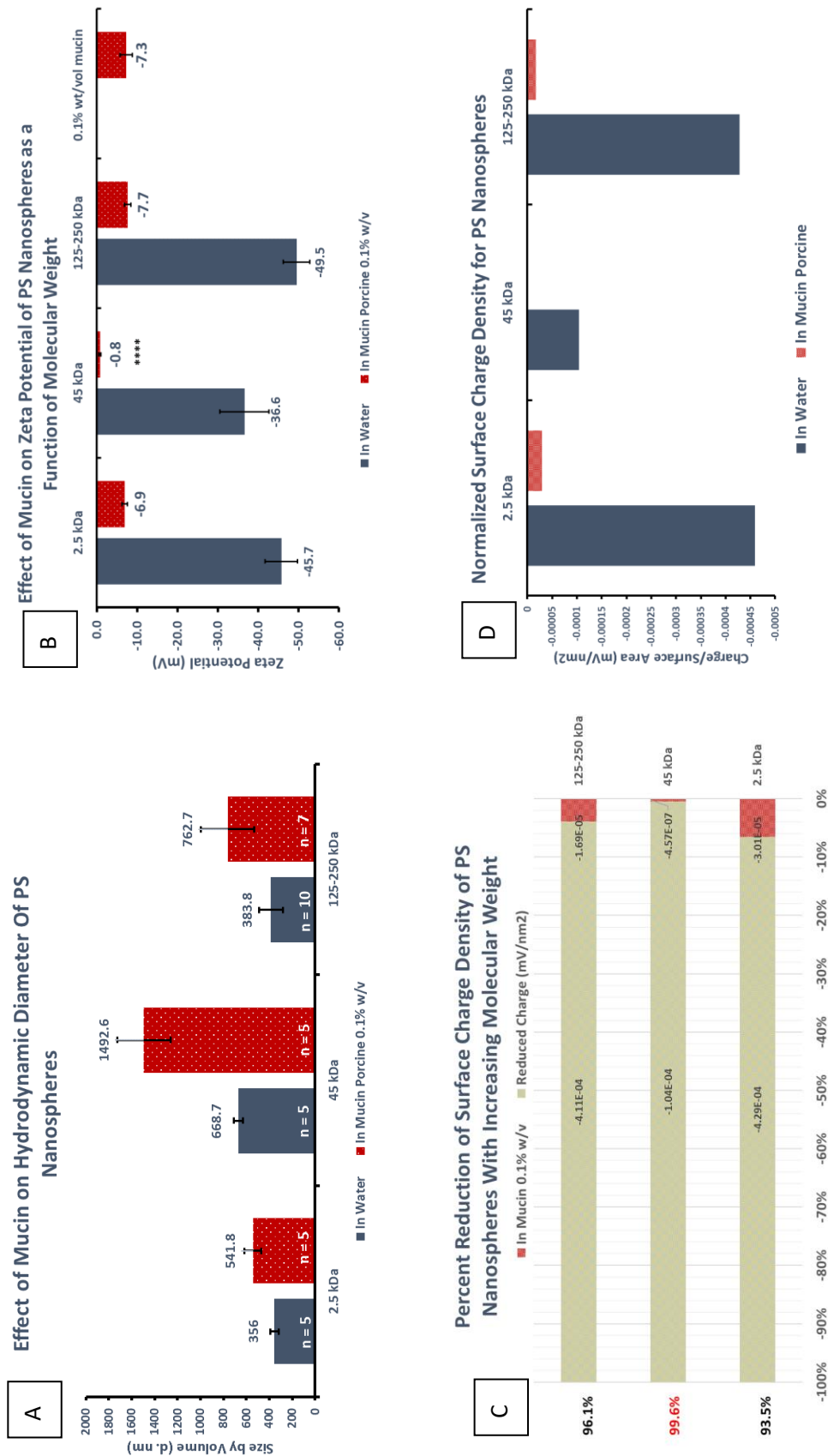
Polystyrene Nanospheres

Polystyrene was chosen for the study for several reasons: it is nondegradabe and robust, providing good quality DLS measurements with low PdI. This hydrophobic polymer is also known for its bioadhesive properties (Norris and Sinko) and could hypothetically exhibit substantial degree of interaction with mucin. PS is non-biodegradable polymer, consequently it cannot be utilized in designing drug delivery systems. Nevertheless, it is being widely used in diffusion studies through mucosal layers and its subsequent uptake though GIT. Due to its robust nature, it is easier to track nonerodable PS particles, than biodegradable material. As described in previous section, PS showed substantial increase in hydrodynamic diameter in mucin; and calculations of surface charge density revealed more than 96% masking of the original charge by mucin. This is indicative of high degree of hydrophobic-hydrophobic interactions between PS nanospheres and mucin strains. We decided to pay closer look to this polymer and investigate how increasing Mw of the polymer affects its effective size and charge.

All three PS samples revealed considerable increase in effective size going from water to mucin solvent (**Fig. 40 A**) $p < 0.005$ in two-tailed student t.test). There was no apparent effect of increasing Mw of the polymer on the degree of interaction with mucin; all three polymers nearly doubled in size in mucin. Zeta potential in water was substantially more negative than in mucin, indicating high degree of charge masking by interaction of mucin strains with the nanospheres' surface (**Fig. 40 B**). 45 kDa sample showed unexpectedly lower, close to neutral, effective charge in mucin compared to the rest of the samples. Calculation of surface charge density of the PS samples showed much higher negative charges in water and much lower charges in mucin (**Fig. 40 D**). 45 kDa PS

exhibited the lowest surface charge in water and almost non-existent charge in mucin (due to its largest hydrodynamic size in both solvents out of the three samples). To better visualize the reduction in surface charge density by mucin, the charges in mucin were plotted against original charges in water and percent reduction was calculated (**Fig. 40 C**). The surface charge of all PS samples was reduced by more than 90%. The charge density on the surface of 45 kDa PS sample in mucin constituted only mere 0.4% of its charge in water. The degree of interaction between this polymer and mucin is so extensive, that it succeeds in complete neutralization of negatively charged polymeric surface. As was mentioned previously, neutral charge is preferable for successful penetration of particles across negatively charges cell membranes. That makes this polymer particularly attractive material for in vivo studies of NP uptake.

We decided to investigate further how increasing concentration of mucin may affect the hydrodynamic diameter of the nanospheres. Figure 41 reinstated previous finding that indeed there is significant difference in hydrodynamic diameter of the spheres in water and in mucin. In 1 and 3 mg/mL mucosal concentrations, the particles nearly doubled in size. At higher concentration of mucins the size of the spheres almost tripled. It seems that increasing mucosal concentration promotes the interaction of mucins with polymeric surface.

Figure 40: Effect of mucin on hydrodynamic diameter and zeta potential of Polystyrene nanospheres.

A) Effect of mucin on d(H) of PS NP with increasing Mw; B) ζ of PS NP in mucin is substantially less negative compared to water; C) percent reduction of calculated surface charge density compared to water; D) normalization of ζ by dividing effective charge by NP surface area in each solvent
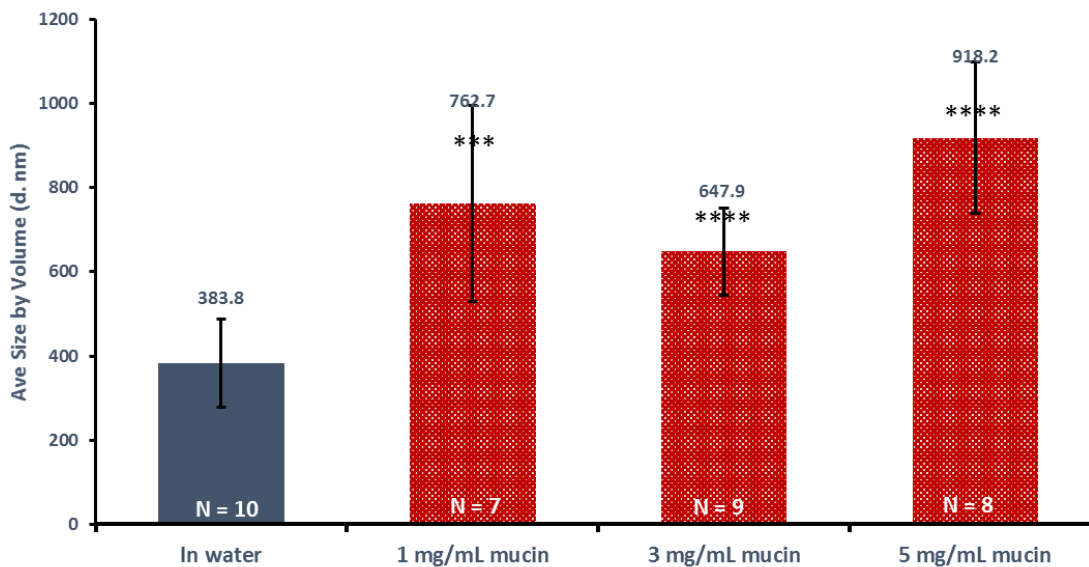
Figure 41: Effect of mucosal concentration of hydrodynamic diameter of PS 125-250 kDa nanoparticles.

Hydrodynamic diameter of polystyrene nanospheres in 1, 3 and 5 mg/mL mucin solution was compared to the measurements in DD water. Effective size in mucin increased by at least two folds. As the concentration of mucin increases, the effective size becomes larger.

Conclusion

Thus far, it is obvious that there is a relationship between bioadhesive forces of the polymers and their interaction with mucin; and its subsequent amount of intestinal uptake. The higher the bioadhesion, the better the interaction with mucin (which is evident from DLS measurements), which in turn may promote higher intestinal uptake of the orally delivered nanoparticles. However, it is also obvious that this is not the entire picture because we already observed exception of the rule. P[FA:SA], while highly bioadhesive and has been uptaken though GI tract, did not show significant change in hydrodynamic diameter. This, on the other hand, can be attributed to the rapid hydrolysis of the polymer in water, which exposes carboxylic acid end groups on the surface of the nanospheres. As a consequence, nanoparticles become more hydrophilic in nature. PMMA, on the other hand, while having the lowest bioadhesion out of all polymers tested, as well as low intestinal uptake, exhibits statistically significant increase in effective size, indicating mucin adhesion on its surface via polyvalent hydrophobic interactions.

All nanoparticles experienced substantial reduction on surface charge concentration in mucin solution, ranging from 60 to 96%. Less bioadhesive polymer PEG-PLGA had only 60% of its charge reduced, indicating on poor adherence of mucin strains on its surface. This is indicative of low interaction of the spheres with mucosal fibers, which is consistent with known poor bioadhesive properties of this polymer. More bioadhesive polymers, such as PS, experienced near complete charge inhibition by mucin, which might possibly explain its successful gastrointestinal uptake.

DLS measurements of d(H) and ʒ of PLGA NP with increasing molecular weight demonstrated stronger interaction with mucin for larger Mw PLGA nanospheres. Therefore, in cases where only the degree of hydrophobicity changes, while other parameters such as composition and bioadhesion stays unchanged, it can be concluded that affinity to mucin increases with increasing hydrophobicity of polymeric surface. However, it appears that a polymer must reach a certain threshold in its degree of hydrophobicity for it to have prominent effect on mucosal adherence.

Overall, an observation was made that polymers whose chemical composition allows them to create multiple bonds with mucin will exhibit more bioadhesive forces and also have the greatest difference in DLS measurements. Hydrogen bond formation between polymer and mucin results in higher bioadhesion and greater difference in d(h) and ʒ. The next strongest interaction with mucin comes from higher degree of hydrophobicity. If polymer is hydrophobic enough, it will create multiple low-affinity bonds to such extend, that mucin strains might completely mask negatively charged surfaces of the nanospheres. Therefore, a charge of a particle, thought important, is not an exclusively determining factor in the degree of mucosal interactions with polymeric materials.

Future directions include evaluating the interactions between mucin and positively charged nanoparticles; testing greater variety of highly hydrophilic and highly hydrophobic polymeric nanospheres; as well as polymers with high vs low degree of bioadhesion. It is imperative to perform the study of mucin effect on hydrodynamic diameter and zeta potential at biologically relevant pH, since it greatly affects the conformation of mucin fibers; hence may influence their interaction with polymeric nanoparticles.

References

Abdulkarim, Muthanna et al. "Nanoparticle Diffusion within Intestinal Mucus: Three-Dimensional Response Analysis Dissecting the Impact of Particle Surface Charge, Size and Heterogeneity across Polyelectrolyte, Pegylated and Viral Particles." *European journal of pharmaceutics and biopharmaceutics : official journal of Arbeitsgemeinschaft fur Pharmazeutische Verfahrenstechnik e.V* 97.Pt A (2015): 230–8. Web. 2 Feb. 2017.

Allen, A. *Structure and Function of Gastrointestinal Mucus*. Ed. L Johnson. 1st ed. New York: Raven Press, 1981. Print.

Balamuralidhara, V. et al. "pH Sensitive Drug Delivery Systems: A Review." *American Journal of Drug Deiscovery and development* 1.1 (2011): 24–28. Web.

Bansil, Rama, and Bradley S. Turner. "Mucin Structure, Aggregation, Physiological Functions and Biomedical Applications." *Current Opinion in Colloid & Interface Science* 11.2 (2006): 164–170. Web. 29 Mar. 2017.

Chickering, D.E et al. "Bioadhesive Microspheres: III. An in Vivo Transit and Bioavailability Study of Drug-Loaded Alginate and Poly(fumaric-Co-Sebacic Anhydride) Microspheres." *Journal of Controlled Release* 48.1 (1997): 35–46. Web. 10 Apr. 2017.

Chickering, D E, and E Mathiowitz. "Controlled Release Bioadhesive Microspheres : I . A Novel Electrobalance-Based Method to Study Adhesive Interactions between Individual Microspheres and Intestinal Mucosa." 34 (1995): 251–261. Print.

Cone, Richard A. "Barrier Properties of Mucus." *Advanced Drug Delivery Reviews* 61.2 (2009): 75–85. Web. 29 Mar. 2017.

Cu, Yen, and W. Mark Saltzman. "Mathematical Modeling of Molecular Diffusion through Mucus." *Advanced Drug Delivery Reviews* 61.2 (2009): 101–114. Web. 29 Mar. 2017.

Desai, Manisha P et al. "Gastrointestinal Uptake of Biodegradable Microparticles: Effect of Particle Size." *Pharmaceutical Research* 13.12 (1996): 1838–1845. Web.

des Rieux, Anne et al. "Nanoparticles as Potential Oral Delivery Systems of Proteins and Vaccines: A Mechanistic Approach." *Journal of Controlled Release* 116.1 (2006): 1–27. Web. 10 Apr. 2017.

Ensign, Laura M., Richard Cone, and Justin Hanes. "Oral Drug Delivery with Polymeric Nanoparticles: The Gastrointestinal Mucus Barriers." *Advanced Drug Delivery Reviews* 64.6 (2012): 557–570. Web. 29 Mar. 2017.

Griffiths, Peter Charles et al. "Probing the Interaction of Nanoparticles with Mucin for Drug Delivery Applications Using Dynamic Light Scattering." *European journal of pharmaceutics and biopharmaceutics : official journal of Arbeitsgemeinschaft fur Pharmazeutische Verfahrenstechnik e.V* 97.Pt A (2015): 218–22. Web. 31 Jan. 2017.

Hillery, Anya M., and Alexander T. Florence. "The Effect of Adsorbed Poloxamer 188 and 407 Surfactants on the Intestinal Uptake of 60-Nm Polystyrene Particles after Oral Administration in the Rat." *International Journal of Pharmaceutics* 132.1–2 (1996): 123–130. Web. 10 Apr. 2017.

Jacobs, J.S. "Characterization of Delivery Systems, Microscopy." *Encyclopedia of Controlled Drug Delivery* 1999: n. pag. Print.

Jani, P. et al. "The Uptake and Translocation of Latex Nanospheres and Microspheres after Oral Administration in Rats." *J. Pharm. Pharmacol.* 41 (1989): 809–812. Print.

JANI, PRAFUL et al. "Nanoparticle Uptake by the Rat Gastrointestinal Mucosa: Quantitation and Particle Size Dependency." *Journal of Pharmacy and Pharmacology* 42.12 (1990): 821–826. Web.

Jung, T et al. "Biodegradable Nanoparticles for Oral Delivery of Peptides: Is There a Role for Polymers to Affect Mucosal Uptake?" *European Journal of Pharmaceutics and Biopharmaceutics* 50.1 (2000): 147–160. Web. 29 Mar. 2017.

Kas, H.S. "Chitosan: Properties, Preparations and Application to Microparticulate Systems." *J. Microencapsulation* 14.6 (1997): 689–711. Print.

Lai, Samuel K et al. "Rapid Transport of Large Polymeric Nanoparticles in Fresh Undiluted Human Mucus." *Proceedings of the National Academy of Sciences of the United States of America* 104.5 (2007): 1482–7. Web.

Lai, Samuel K., Ying-Ying Wang, and Justin Hanes. "Mucus-Penetrating Nanoparticles for Drug and Gene Delivery to Mucosal Tissues." *Advanced Drug Delivery Reviews* 61.2 (2009): 158–171. Web. 29 Mar. 2017.

Malvern Instruments. "Dynamic Light Scattering : An Introduction in 30 Minutes." *Http://Www.Malvern.Com/En/Products/Technology/Dynamic-Light-Scattering/* (2014): 1–8. Web.

---. "Dynamic Light Scattering Common Terms Defined." 2011. Web.

Mathiowitz, E. Kretiz M. R., Brannon-Peppas, L. "Microencapsulation." *Encyclopedia of Controlled Drug Delivery* 1999: n. pag. Print.

Mathiowitz, Edith, Jules S Jacob, et al. "Biologically Erodable Microspheres as Potential Oral Drug Delivery Systems." *Nature* 386.6623 (1997): 410–414. Web.

Mathiowitz, Edith, Donald Chickering, et al. "Process for Preparing Microparticles Through Phase Inversion Phenomena." Web.

nanoComposix. "NANOCOMPOSIX'S GUIDE TO DYNAMIC LIGHT SCATTERING MEASUREMENT AND ANALYSIS." (2015): 1–8. Print.

Neutra, M, and J Forstner. "Gastrointestinal Mucus: Synthesis, Secretion, and Function." *Physiology of Gastrointestinal Tract*. Ed. L Johnson. 2nd ed. New York: Raven Press, 1987. chapter 34. Print.

Norris, Daniel A, and Patrick J Sinko. "Effect of Size , Surface Charge , and

Hydrophobicity on the Translocation of Polystyrene Microspheres Through Gastrointestinal Mucin." (1996): 1481–1492. Print.

Olmsted, SS et al. "No Title." *Biophys* 81 (2001): 1930–1937. Print.

Pal, Sovan Lal et al. "Nanoparticle : An Overview of Preparation and Characterization." *Journal of Applied Pharmaceutical Science* 1.6 (2011): 228–234. Print.

Reineke, J et al. "Can Bioadhesive Nanoparticles Allow for More Effective Particle Uptake from the Small Intestine ?" *Journal of Controlled Release* 170.3 (2013): 477–484. Web.

Reineke, Joshua J et al. "Unique Insights into the Intestinal Absorption , Transit , and Subsequent Biodistribution of Polymer-Derived Microspheres." *PNAS* 110.34 (2013): 13803–13808. Web.

Svensson, Olof, and Thomas Arnebrant. "Mucin Layers and Multilayers — Physicochemical Properties and Applications." *Current Opinion in Colloid & Interface Science* 15.6 (2010): 395–405. Web. 29 Mar. 2017.

Thanos, CG et al. "Enhancingthe Oral Bioavailability of the Poorly Soluble Drug Dicumarol with a Bioadhesive Polymer." *J Pharm Sci* 92.8 (2003): 1677–1689. Print.

Washington, Clive. *PARTICLE SIZE ANALYSIS IN PHARMACEUTICS AND OTHER INDUSTRIES Theory and Practice*. Ellis Horwood Limited, 1992. Print.

Woodley, John. "New Possibilities for Drug Administration ?" 40.2 (2001): 77–84. Print.

Appendix A:

Viscosity measurements of Mucin Porcine Solution at Different Concentrations

Materials and Methods

Mucin from porcine stomach by Sigma was prepared in different concentrations, ranging from 1 mg/mL to 30 mg/mL. It was filtered with 0.2 µm syringe filter to remove large aggregates. Two methods of viscosity measurements were used: Gilmont Falling Ball Viscometer by Cole Parmer and by Brookfield Rheometer DV3T.

Gilmont Viscometer

Size 1 (GV-2101) glass tube and size 1 glass ball were used in the measurements. This settings allow for measurements of viscosities in 0.2-2 cP region. Approximately 10 mL of tested mucin solution was added to the clean tube. The tube was leveled in aligned vertical position. The glass ball was then dropped into the liquid and the time of its movements between two red lines was recorded.

Viscosity then was calculated according to Equation 4 :

$$\mu = K \left(\rho f - \rho\right)t \tag{4}$$

where µ is viscosity in cP
K- viscometer constant (0.3 for size 1)
ρf is density of glass ball (2.53 for glass)
ρ is density of the tested liquid
t is measured time of descent

Brookfield Rheometer

Spindle 40 (CP-40) was used in the measurements. For mucin of 1-10 mg/mL concentration rpm setting was set to 50. For higher mucin concentrations, the speed of 150

rpm was used. In this study, mucin samples were unfiltered. 1 mL of each sample was placed into spindle compartment at 22°C.

Results and Discussion

Gilmont Dropping Ball Viscometer was used to measure the viscosity of filtered mucin at 1-5 mg/mL concentrations, which were used in the course of the study. For zero concentration sample DD water was used. The obtained results showed that there is lineal increase in viscosity with increasing mucin concentration. However, the increase is not too large, especially for the lowest concentration of mucin. Therefore, use of the water parameters for mucin solvent in DLS settings should not create significant error in the obtained data for hydrodynamic dimeter and zeta potential.
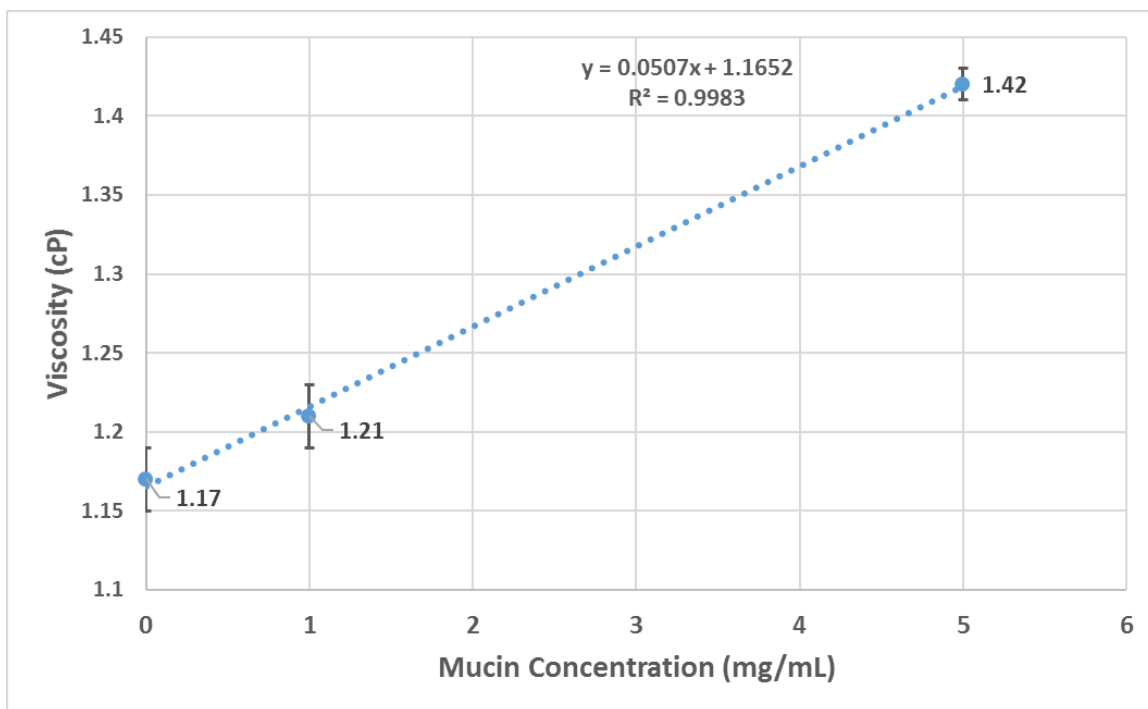
Figure 42: Viscosity of filtered mucin at various concentrations.

Viscosity values of filtered mucin, measured by Gilmont Falling Ball Viscometer at 22°C, do not differ significantly from water.

Viscosities of unfiltered mucin solution in the range of 1-30 mg/mL were measured using Brookfields Rheometer with CP-40 spindle. Each measurement was repeated 3 times, producing very small to nonexistent standard deviation values. The overall trend observed is a linear increase in viscosity with increasing mucosal concentration.
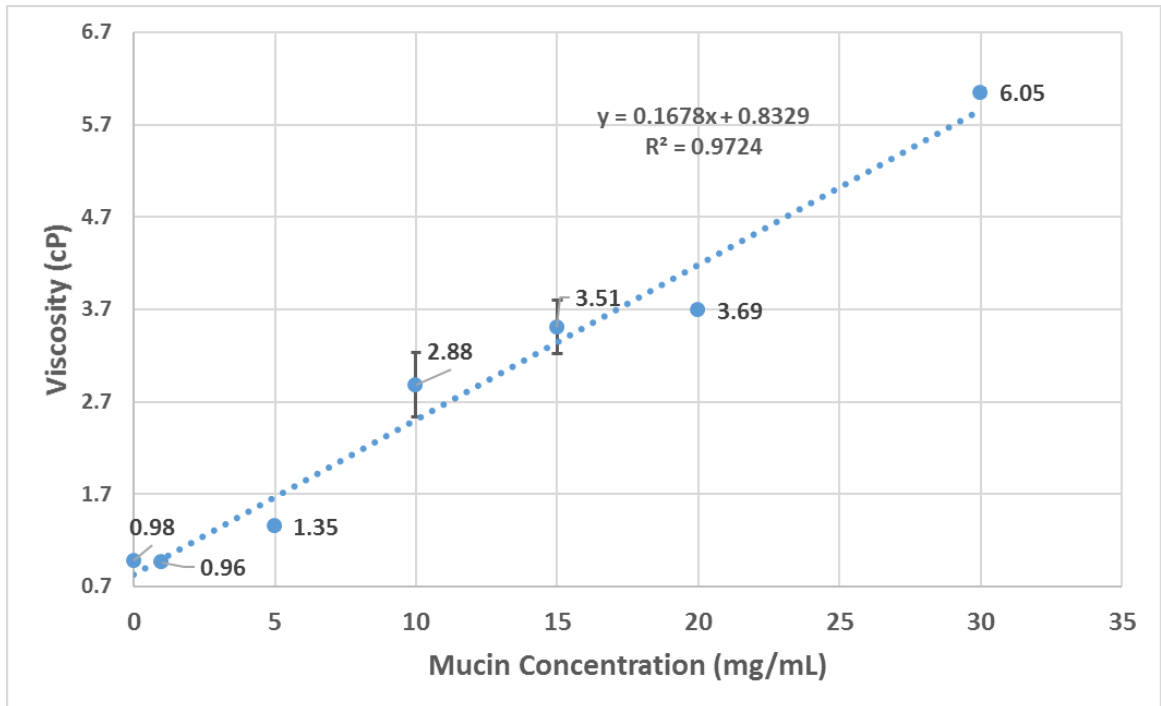

Figure 43: Viscosity of unfiltered mucin of various concentrations.

Viscosity of unfiltered mucin, measured by Brookfield Rheometer at 22°C, follows linear increase in values as a function of increasing concentration.

Appendix B:

## Effect of Polymer Aging and Storage Conditions on Hydrodynamic Diameter of PBMAD Nanospheres

Two batched of PBMAD nanospheres were used for DLS measurements in this study. The first batch was produced on 8/25/2015 and stored in desiccator at room temperature. The second batch was made on 12/1/2016 and stored at -80°C. Examination of the first batch took place more than half a year after its original production, while the second batch was used for SEM and DLS testing shortly after the production was made. SEM images of the two batches did not show any morphological differences. Both samples revealed well defined, spherical nanospheres with no evident aggregation (**Fig. 44**)
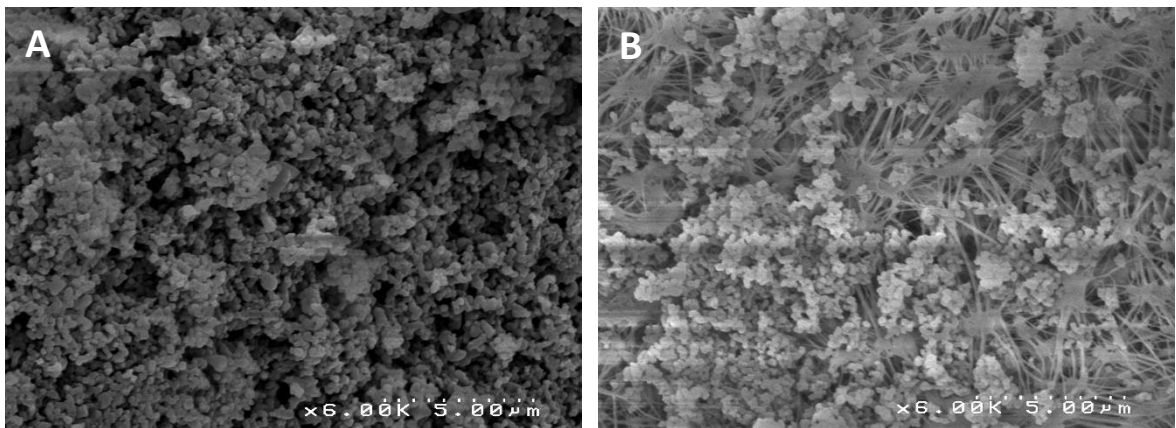
**Figure 44**: SEM images of old and fresh samples of PBMAD nanospheres.

A) old PIN batch B) freshly prepared batch of nanospheres. Particle in both samples have similar size, shape and morphological characteristics

While zeta potential measurements for both samples were similar in both water and mucin (**Fig. 45**), hydrodynamic diameter in mucin was higher (but not statistically significant) for freshly produced nanospheres, compared to old production, while the size in water did not change much. For fresh sample, stored at -80°C, the interaction with mucin proved to be
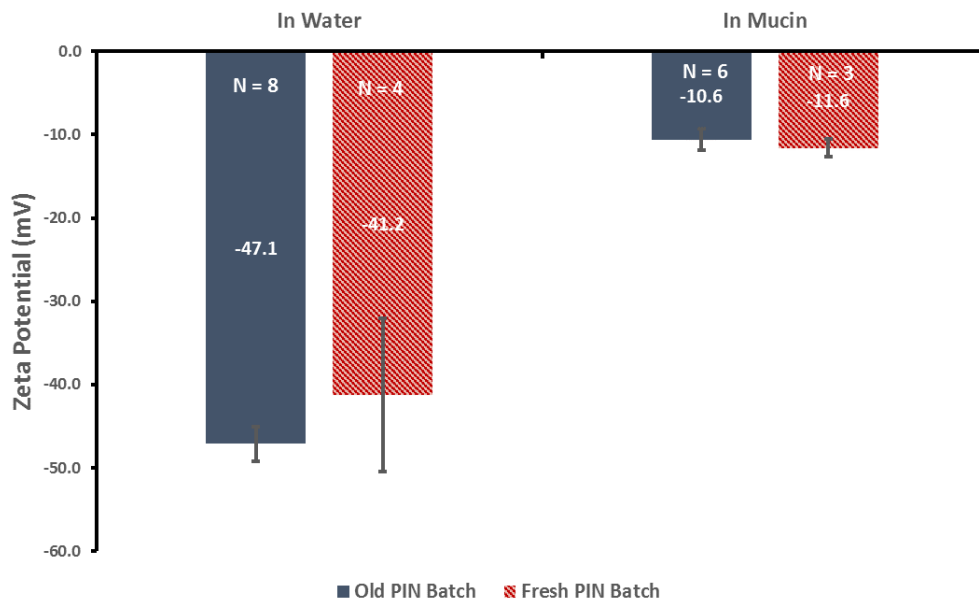
Figure 45: Effect of sample aging on zeta potentila of PBMAD nanospheres.

Zeta potential of old and freshly produces samples of PBMAD nanoparticles show no significant difference in values.
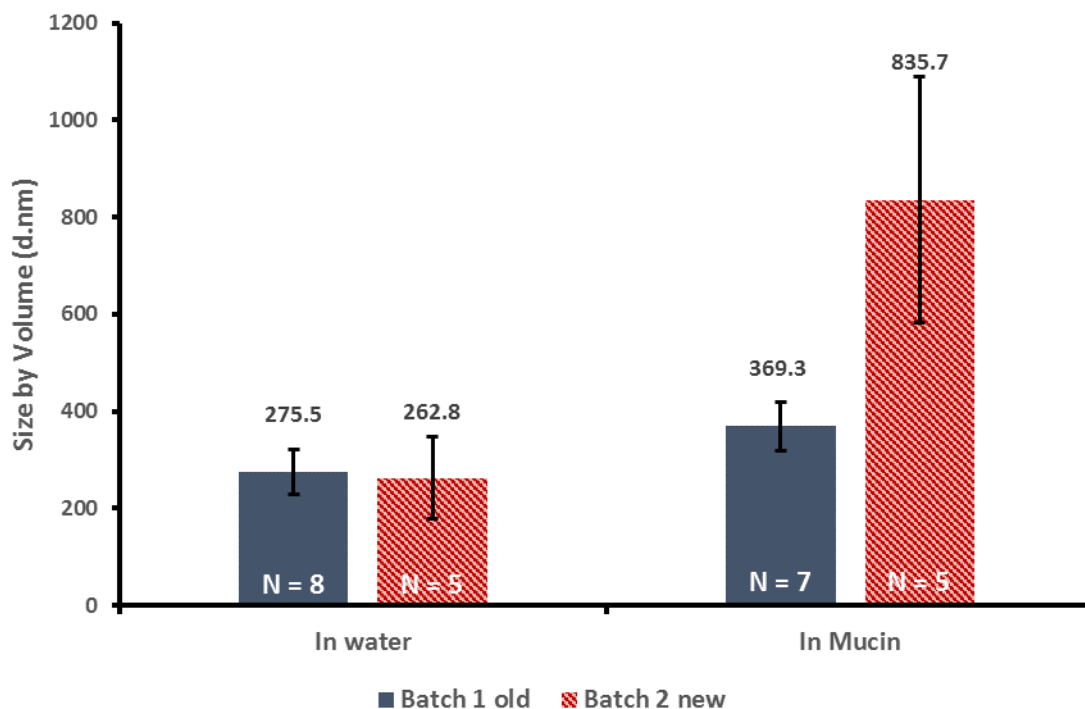
Figure 46: Effect of sample aging on d(H) of PBMAD nanospheres.

Hydrodynamic diameter in mucin of old PBMAD nanospheres was twice as less than the size of the fresh sample. However, the change proved to be not statistically significant.

much stronger. Since PBMAD is highly bioadhesive as well as hydrophilic polymer (J. Reineke et al.), we predicted high degree of interaction with mucin, which was true in the case of fresh sample. Bioadhesive properties of this polymer are mainly attributed to the high amount of carboxylic and hydroxyl groups in its side chains (J. Reineke et al.). It is possible that with time the number of polar groups decreases. FTIR study of the two samples is advisable to elucidate the reason behind such behavior.

On the other hand, it is possible that for PBMAD polymer PIN procedure simply resulted in nanospheres of different surface chemistry characteristics. Variability in amount polar side chain groups on the surface of the spheres can drastically influence its interaction with mucins. Future directions include productions and characterization of more PBMAD batches of nanospheres, as well as examination by DLS and FTIR to understand the underlying cause for such large difference with mucosal interaction.

Appendix C:

Effect of pH on Hydrodynamic Diameter and Zeta Potential of PBMAD and P[FA:SA] Nanospheres

Effect of pH on Hydrodynamic Diameter of P[FA:SA] (20:80)

P[FA:SA] proceeds to degrade rapidly upon contact with water. To determine the stability of the nanospheres, hydrodynamic diameter of P[FA:SA] (20:80) nanoparticles was measured in different pH solutions as a function of time.
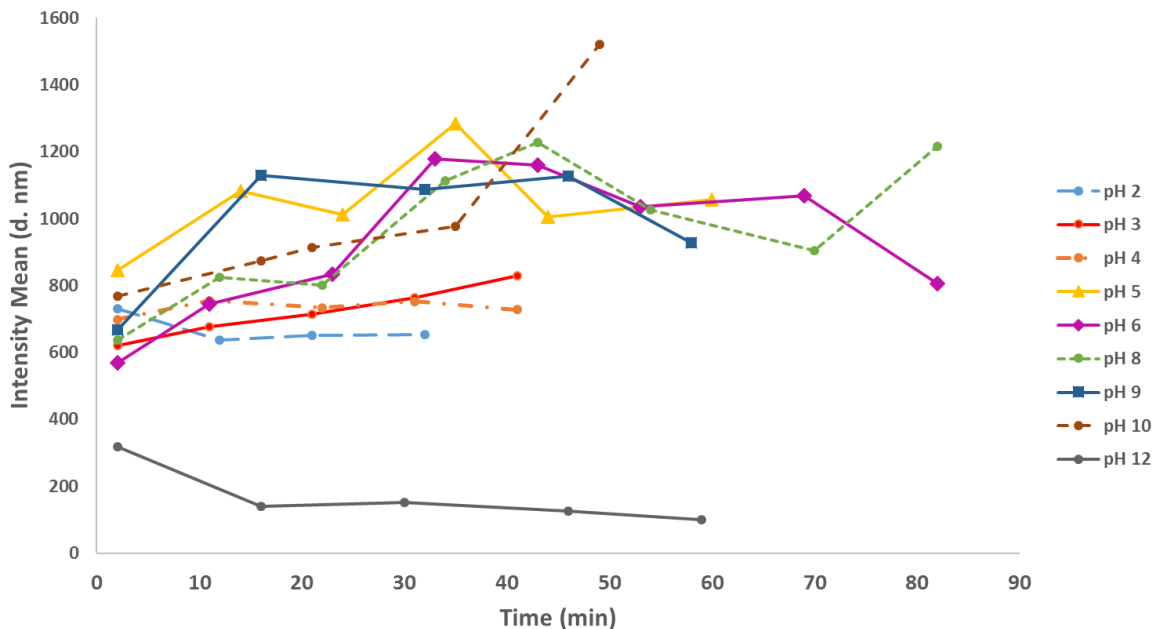

Figure 47: pH and time effect on hydrodynamic diameter of P[FA:SA] nanoparticles.

D(H) of P[FA:SA] (20:80) was measured as a function of time at different pH solutions. Rapid degradation is observed at high pH of 12. In general, effective particle size increased with time, indicating hydrolysis process.

Nanospheres were rapidly degrading at pH 12. While at lower pH the particles were all relatively large (around 800 nm), at lower pH solutions the size did not change with

time, while with increasing pH the effective size increased with time, signifying ongoing

hydrolysis process.
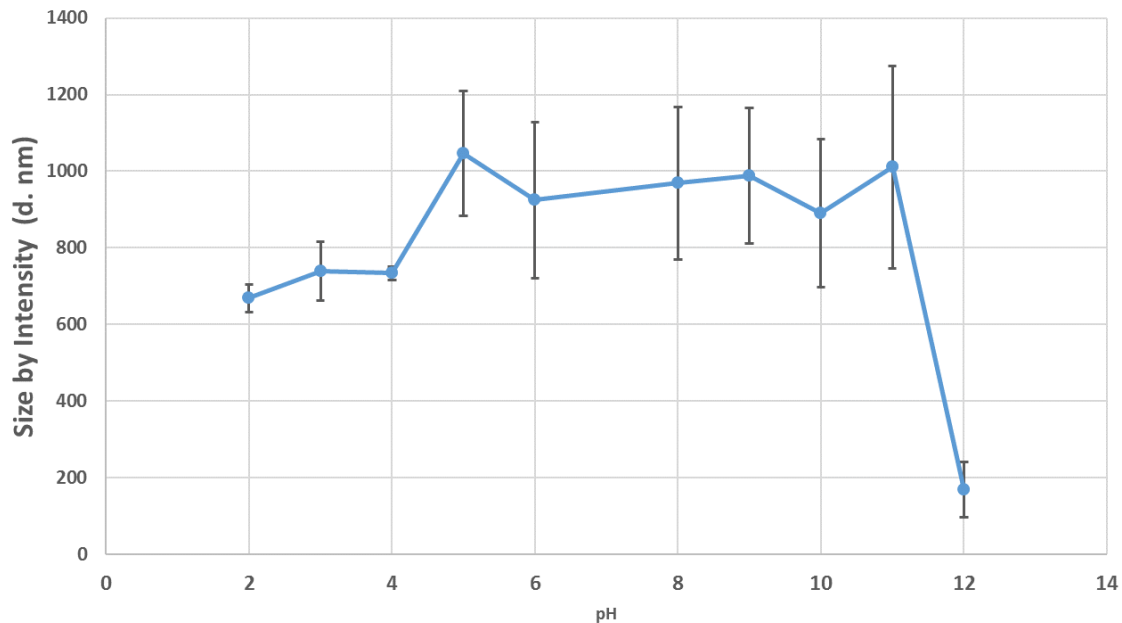
**Figure 48**: D(H) of P[FA:SA] (20:80) as a function of various pH

 Rapid degradation is observed at high pH of 12. In general, effective particle size
increased with increasing pH, indicating hydrolysis process.

From Figure 48 can be inferred that nanoparticles made out of P[FA:SA] in general

is more stable in acidic solutions that in basic. The standard deviation of effective sizes at

lower pH are smaller than that at higher pH. The size values at pH 2-4 are smaller as well

(around 700 nm, increasing to 900 nm and up with increasing pH. The double-tailed student

T. test between size at pH 4 and pH 8 is $p<0.05$. The size of the spheres rapidly decreases

at pH 12, as the polymer degrades and probably diaaspear. Double tailed T. Test of

hydrodynamic diameters between pH 11 and 12 is $p < 0.0005$.

Effect of pH on Hydrodynamic Diameter of P[FA:SA] (20:80)

Zeta potential of P[FA:SA] was measured as a function of increasing pH. Since zeta depends heavily on the ionic strength of the solution, we created SOP for Zetasizer for complex solvents, indicating concentrations of every constituent in the solution.
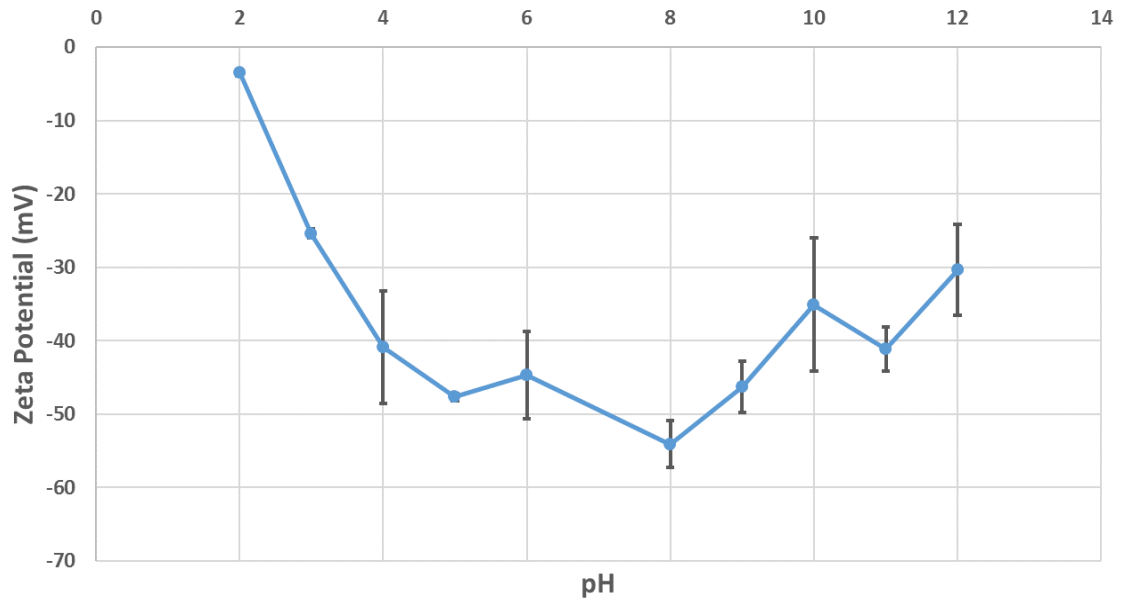
**Figure 49:** Zeta potential of P[FA:SA] nanoparticles as a function of increasing pH. Effective charge of P[FA:SA] (20:80) is less negative at acidic solutions, than in basic.

At low pH of 2 zeta potential is almost neutral, because all carboxylic end groups are in protonated state. With increasing pH, deprotonation of these groups takes place, decreasing the effective charge of the nanospheres.

Effect of pH on Hydrodynamic Diameter of PBMAD

PBMAD is a pH sensitive polymer. It is stable at lower pH, and is subjected to degradation at high pH. This property makes the polymer an ideal material for designing pH triggered controlled release delivery systems. A series of experiments at different pH were performed to outline its behavior in acidic and basic environments.

At low pH range (2 through 5) the polymer is stable over time (**Fig. 50**). The hydrodynamic diameter fluctuates from 200 to 600 nm with increasing ionic strength of the solution. At pH 11 and 12 the NP rapidly dissolve. It is interesting to note that at pH 6,8 and 9 the measurements were difficult to obtain, indicating dissolution of the nanoparticles. At pH 7 the size of the NP rapidly decrease from 300 nm to below 200 nm, then remains stable with time, signifying the disentanglement of the polymeric chains and their successful dissolution.
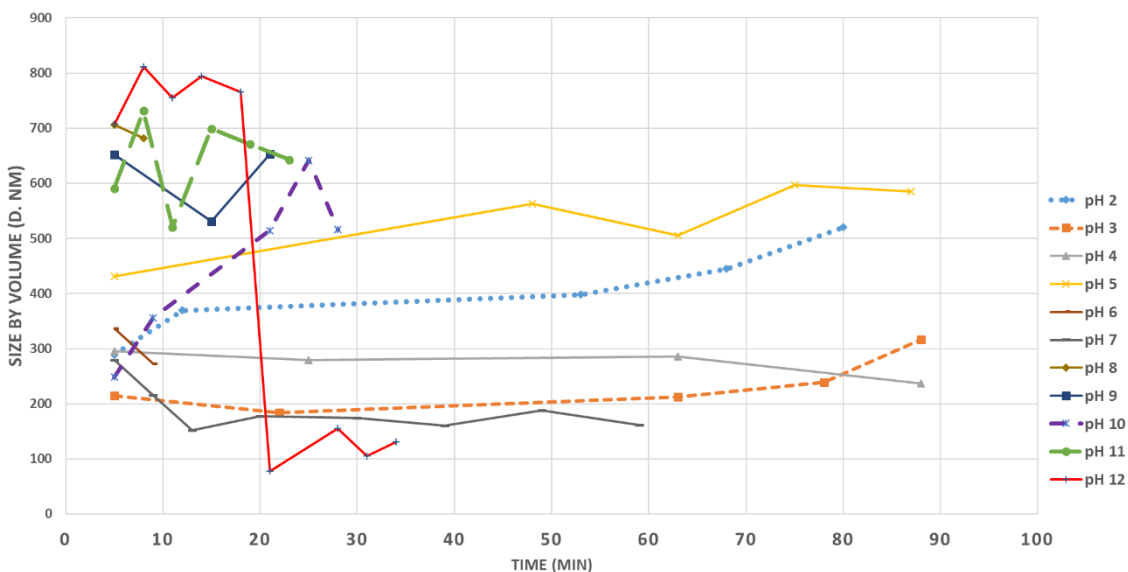
**Figure 50**: D(H) of PBMAD as a function of time at different pH solutions. Rapid dissolution is observed at high pH range. The NP were stable with time at low pH. At pH 10 the nanospheres rapidly increase in size, indicating certain degree of swelling, as the polymeric chains disentangle in the solution; manifesting as variation in thickness of electric diffusive layer around the spheres.

The average hydrodynamic diameter of PBMAD nanospheres was plotted as a function of increasing pH (**Fig. 51**). Size measurements appeared to be more stable at low pH range, while having large standard deviation at high pH. Effective size of the spheres in acidic environment was overall smaller, than the size in basic solutions.
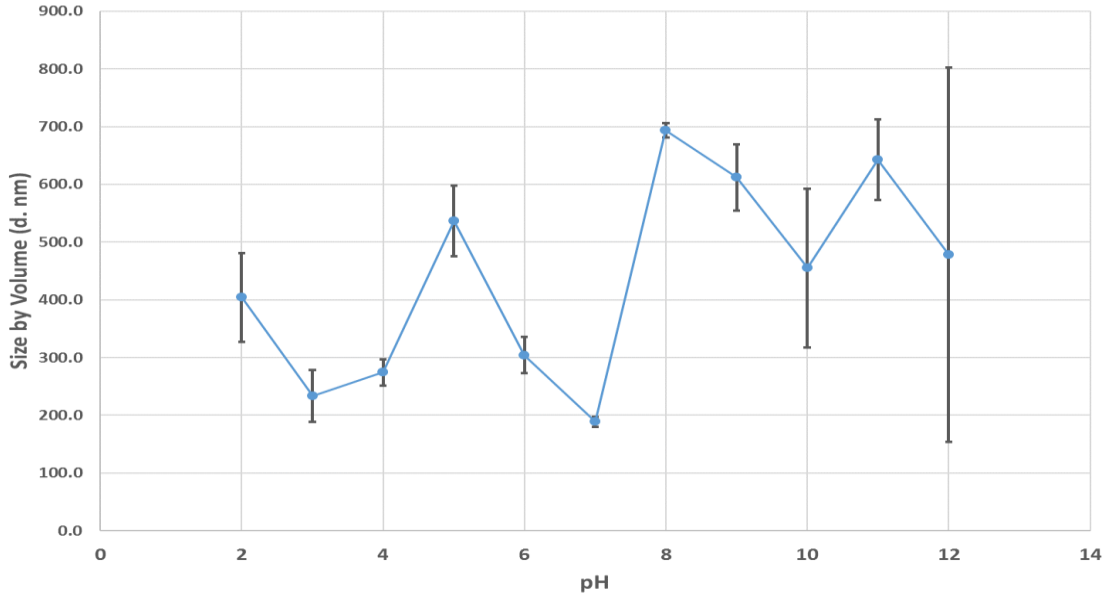
Figure 51: Effect of pH on hydrodynamic diameter of PBMAD nanospheres

Average d(H) of PBMAD was plotted against increasing pH. The measurements appeared to be more stable in acidic solutions, than in basic.
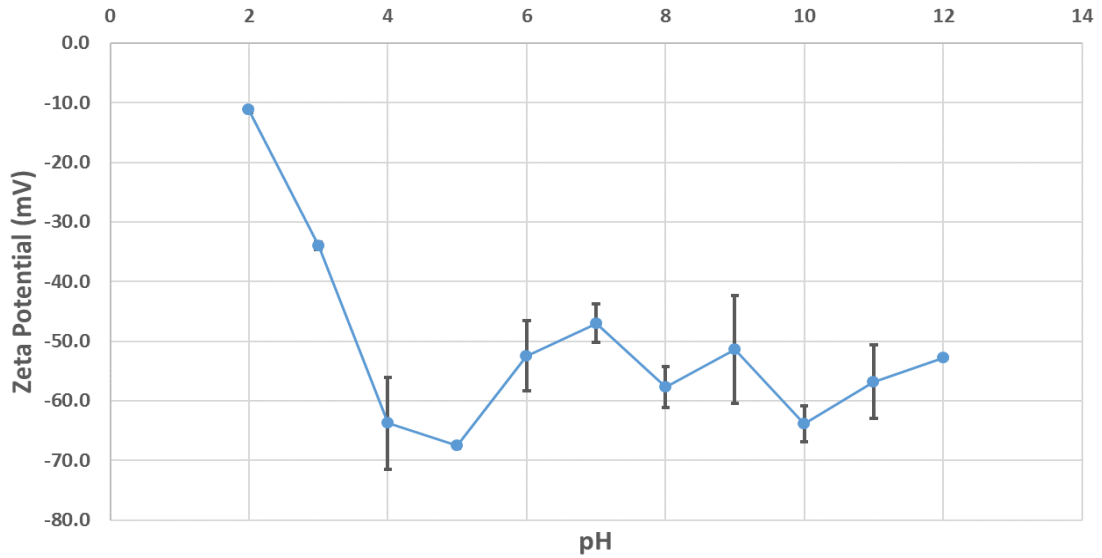
Figure 52:Effect of pH on zeta potential of PBMAD nanospheres.

Average zeta potential was plotted as a function of increasing pH of the solution.

Average zeta potential measurements at low pH of 2 and 3 was much less negative, compared to the effective charge measurements of PBMAD nanospheres at higher pH range (**Fig. 52**). Zeta potential measurements are in general very sensitive to pH of the solvent, therefore high concentration of H_3O^+ in the solution is most probably affecting the readings. Starting from pH 4 the effective charge of the NP is stable and consistent, ranging from -45 to -65 mV. PBMAD nanoparticles exhibit such high negative charge due to presence of carboxylic acid side groups in its composition.